Dissertation

submitted to the

Combined Faculty of Natural Sciences and Mathematics

of the Ruperto Carola University Heidelberg, Germany

for the degree of

Doctor of Natural Sciences

Presented by

Christine Ho (M.Sc)

Born in Paris, France

Oral examination: November 28th, 2019

Collective synchronization of coupled self-organizing mouse embryonic oscillators

Referees: Dr. Anne Ephrussi

Prof.Dr. Michael Brunner

Abstract

Synchronization abounds in nature at different scale and biological context: fireflies flash in sync, neurons fire together. Synchronization is the ability to coordinate events to operate in unison. It requires objects to sense and communicate with each other. This interaction is called coupling. How synchronization and coupling are achieved in nature are subject of intense studies.

One remarkable case of synchronization has been observed during the formation of the body axis in vertebrates. In vertebrates, the segmented vertebral column is established during somitogenesis at the embryonic stages. Somites form rhythmically, for example in mouse with a period of about 2 hours. This process is associated with the oscillatory activity of genes involved in Notch, Wnt and Fgf signalling pathways along the pre somitic mesoderm (PSM) tissue. Interestingly, in vitro randomization assays including tissue dissociation and re-aggregation, PSM cells spontaneously re-synchronize and self-organize into several miniature emergent PSM structures (ePSM). Thus, a randomized ensemble of genetic oscillators with different frequencies and phases establish synchrony and form ordered oscillating patterns. Although the requirement for Notch signalling pathway for synchronization is known, the general rules of coupling remain elusive.

To describe synchronization between coupled biological oscillators, Kuramoto in 1979 provided a model based on phase difference coupling. This model assumes that synchronization is continuous and driven by the phase difference between weakly coupled oscillators. This Kuramoto model is widely used to study synchronization phenomena, including PSM oscillations . However, theoretical predictions regarding the collective phase synchronization have not been tested experimentally yet. We developed a novel experimental strategy to quantitatively challenge the Kuramoto model, particularly in regard to its prediction of how the collective phase is determined. While the Kuramoto model predicts that the collective phase is equal to phase average of input oscillators, our results suggest that the collective phase is dictated by one phase of input oscillators. Combined with other results, our experimental findings do not match Kuramoto model predictions. I discuss future experimental strategies to test alternative models for PSM synchronization.

Zusammenfassung

Synchronisation ist in der Natur ein allgegenwärtiges Phänomen, von synchron blinkenden Glühwürmchen bis hin zum synchronen Feuern von Neuronen. Dabei wird die Synchronisation als die Erlangung der Fähigkeit des zeitlichen Ausgleichs von Vorgängen definiert. Um dies zu realisieren ist eine gegenseitige bi-direktionale Verbindung einzelner Kompartimente notwendig in der sowohl kommuniziert, als auch registriert werden kann - dies wird Kopplung genannt. Wie Synchronisation und Kopplung in der Natur reguliert werden ist von großen Interesse der Wissenschaft und Subjekt diverser Forschungsvorhaben.

Ein markantes Beispiel für Synchronisation in der Natur stellt die Entwicklung der Körperachse in Vertebraten dar. Während der Somitogenese, einem Schritt der Embryonalentwicklung, bilden sich periodisch Somiten, die Vorläufer der Wirbel. Dabei formt sich rhythmisch, mit einer Periode von ungefähr zwei Stunden, ein neues epitheliales Zellbündel (Somit) durch ein räumlich und zeitlich präzises Zusammenspiel von mehreren genetischen Oszillatoren verschiedener Signalwege. Gene der bedeutenden Delta-Notch, FGF und WNT Signalwege oszillieren und durch eine graduelle Phasenänderung entlang des PSM (presomitic mesoderm) bildet sich eine synchrone Gen-Expressionswelle von posterior in Richtung anterior des PSMs. Dieses Verhalten wird interessanterweise von dissoziierten und randomisierten PSM-Zellen in-vitro in sogenannten “emergent presomitic mesoderm” Zellkulturen (ePSM) rekapituliert. Kultivierte Zellen formen de-novo synchrone Oszillationszentren und zeigen selbstorganisierende Muster. Mit diesem experimentellen Ansatz konnte gezeigt werden, dass aus randomisierten Oszillatoren verschiedener Phasen und Frequenzen durch Kopplung erneut Synchronität erreicht wird. Durch vorangegangene Forschung ist die Rolle des Delta-Notch-Signalweges in die Kopplung dieser Oszillatoren bewiesen worden, jedoch sind die Regeln denen dies folgt nach wie vor spekulativ.

Kuramoto beschrieb 1979 mathematisch die Synchronisation zwischen zwei biologischen Oszillatoren aufgrund der Phasenunterschieds-Kopplung. Dieses Modell geht von der Annahme aus, dass die Synchronisation sukzessiv aufgrund eines Phasenunterschiedes zwischen zwei schwach gekoppelten Oszillatoren erreicht wird.

Kuramotos Modell wird bis heute genutzt, auch um den Segmentierungsprozess der Säugetiere zu beschreiben. Diese kollektive Phasensynchronisation konnte jedoch bis heute nicht experimentell bewiesen werden. Durch unsere neuen experimentellen Ansätze konnten wir Kuramotos theoretisches Modell während der Maus Segmentierung testen, insbesondere darauf wie die kollektive Phase bestimmt wird. Kuramotos Annahme, dass sich die kollektive Phase aus der arithmetisch gemittelten Phase aller Oszillatoren ergibt konnten wir falsifizieren. Unseren Experimenten nach entsprach die kollektive Phase stets der Anfangsphase einer der beiden Anfangs Oszillatoren anstatt deren Mittel. Die Synchronisation während der Somitogenese lässt sich somit nicht durch Kuramotos Annahmen beschreiben. Abschließend zeigt sich daher die Notwendigkeit für ein verfeinertes Kupplungsmodell.

Abbreviations and vocabulary

- **AP axis; Anterior-Posterior** Axis
- **ATAC-seq:** Assay for Transposase-Accessible Chromatin with high throughput Sequencing
- **Coupling**: interaction between two oscillators
- **DAPT**: =γ-secretase inhibitor, inhibitor of Notch signalling
- **ePSM**: emergent Pre-somitic Mesoderm, also termed “focus/foci”
- **FACS**: Fluorescence Activating Cell Sorting
- **FGF**: Fibroblast Growth Factor
- **Frequency**: the inverse of the period
- **Kuramoto model** mathematical synchronization model based on phase difference coupling of weakly interacting phase oscillators oscillators
- **Oscillations**: repetition of variation in time
- **Period**: The time for an oscillator to complete one cycle.
- **PSM**: Pre somitic Mesoderm
- **RAFL**: Randomization Assay for Low input
- **RA**: Retinoid Acid
- **Somites**: transitional embryonic structure originated from segmenting mesoderm
- **Synchronization**: adjustment of rhythms of oscillating objects due to their weak or strong interactions.
- **TB**: Tailbud
- **YFP**: Yellow Fluorescence Protein
- **Winfree model**: pulse coupling model in which each oscillator exerts a phase-dependent influence on all the other, the corresponding response of oscillator depends on its phase.

Preamble: Self-organization in cosmos

The universe tends to reach the total disorder. However, the concept of self-organization goes against this current. It is the emergence of natural order from chaos. As a biologist, think about how our 10 trillion living cells, work and collaborate and give rise to a human being. There seem to be conditions in the universe that engender novelty and complexity sprouts, mind emerges from matter. As humans, we are the sophisticated products of evolution. We are the results of the self-organized and emergent properties of matter. We are now able to do Science to understand the rules governing the universe. It seems that the universe wants to know itself through human beings! This is exactly one major purpose of doing Science: understanding and elucidating principles governing our universe in its complexity and its beauty.

To this end, Humans start to do mathematics: the language seemingly spoken by the Universe. (Some people would say: maths is the human language applied to Nature). So, we believe that nature and the universe can be understood by numbers, variables, and their relationships. Mastering this language allows us to understand the rules of non-living matters. We call it physics and chemistry. Then, certainly comes the time when this natural language is being used to understand life matters. We are now witnessing the age of quantitative biology, where we are trying to express and perceive Life by numbers and make sense of it.

This thesis will present one case study to understand self-organization principles using advanced quantitative methods applied to developmental biology, particularly during mouse somitogenesis.

Chapter I: Introduction

Part I: Self-organization and emergence properties in biological systems

"The moon spins in perfect resonance with its orbit around the Earth; millions of neurons fire together to control our breathing; every night along the tidal rivers of Malaysia, thousands of fireflies' flash in silent, hypnotic unison. All of these astonishing feats of synchrony occur spontaneously — as if the ***universe had an overwhelming desire for order".*** *Anonymous* Quote

"The tendency to synchronize may be the most mysterious and pervasive drive in all of nature. It has intrigued some of the greatest minds of the twentieth century, including Albert Einstein, Richard Feynman, Norbert Wiener, Brian Josephson, and Arthur Winfree. But only in the past decade have scientists from disparate disciplines come to the stunning realization that the study of synchrony could revolutionize our understanding of everything from the origin of life to certain types of human behaviour" (Strogatz, 2003).

1. Self-organization in biological systems

"But who is the architect who designs the plans which the workers execute… No reasonable person can imagine for one moment that every small worker is conscious of the purpose of its work, that is carried in its mind the plan, or even part of the plan of building operations". E. Marais, *The soul of the White Ant.*

a. Definition of self-organization and emergence

"Self-organization is a process in which pattern at the global level of a system emerges solely from numerous interactions among the lower-level components of the system. Moreover, the rules specifying interactions among the system's components are executed using only local information, without reference to the global system" (Camazine et al., 2001).

In brief, self-organization is the capability to establish ordered patterns without any external guidance. Self-organization system relies on local information shared between all the little parts that compose the great part. One feature of self-organized systems is the concept of emergence. Emergence refers to a process by which a system of interacting subunits acquires qualitatively new properties that cannot be understood as a simple addition of their individual contributions (Camazine et al., 2001). In other terms, emergence is the appearance of collective properties derived from the properties of parts. A system has emergent properties when the whole is greater than the sum of the parts.

In the context of embryonic development and pattern formation, there are several features of self-organization that needs to be considered (Camazine et al., 2001):

(1) Complex patterns can emerge based on a set of defined simple rules

(2) Strengthening the robustness of the system by minimizing mistakes during the development,: since every part of the great ensemble contains the information, if one-part crashes, other parts can take over.

(3) And more importantly, economizing energy and information that is needed to encode and achieve complex developmental program by the use of emergent properties.

2. Examples of synchronized biological systems

Nature provides many good examples of self-organized and self-synchronized systems such as pacemaker cells in our heart or neurons which can fire together in our brain(Yang and Wu, 2018). Even walkers on the London's Millennium Bridge show a spontaneous synchronized penguin-like march (Strogatz et al., 2005). Here we will discuss three examples of synchronized biological systems.

a. Birds flying in unison

Let's imagine thousands of birds, flying in unison without bumping into each other. They seem to be animated by one will and execute beautifully synchronized choreography in the sky. This phenomenon has been termed "Flocking birds" by the zoologist Wayne Potts in 1984 (Potts, 1984). His study showed that flocking birds don't just follow a leader or their neighbours. Instead, they anticipate sudden changes in the flock's direction of motion. And as he wrote, "a single bird may initiate a manoeuvre which spreads through the flock in a wave".

b. Dancing fireflies

Fireflies also known as 'lightning bugs" are little flies that carry in their abdomen luciferin. Each firefly is able to produce bioluminescence to attract prey and mates. Now imagine thousands of fireflies flashing up together in sync and forming wave patterns (BUCK and BUCK, n.d.; Mirollo and Strogatz, 1990; O'Keeffe et al., 2015). An interactive simulation of synchronized fireflies made by Nicky Case is available here

https://ncase.me/fireflies/. Please note than you can play with different parameters to obtain different kinds of patterns such as waves or pulses:

- Number of flies: number of individuals
- Fireflies' clock speed: period/frequency of the clock
- Nudge by neighbour: sort of "interaction strength" between the fireflies
- Bonus: if you click to "show clock" button: each firefly is represented as a clock. When the needle reaches "12 o'clock": this is a time when the firefly is flashing.

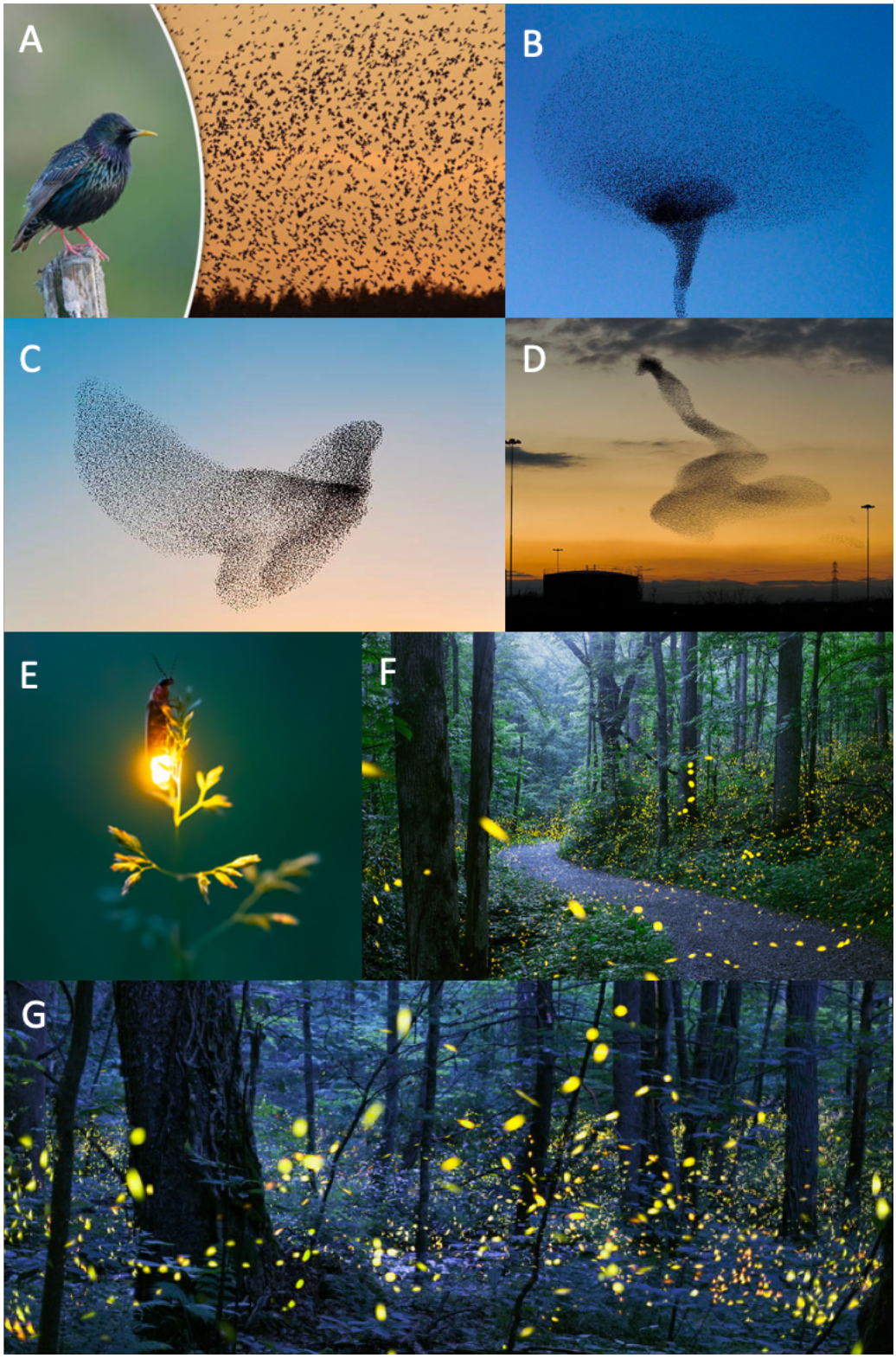

Figure 1 ***Synchronization abounds in nature*** *(A)One single bird and collective birds. (B) Tornado of starlings in Turkey (C) Starlings in bird formation Photo: Robert Wolstenholme/Solent News. (D)Starlings in the shape of a cobra in Swindon. Photo: Joe Wright. (E) Single Firefly illuminating grass. Fairfield, Iowa. (F)Synchronous fireflies from The Smoky Mountains National Park, Tennessee. Multiple 30s exposures, 2916. (G)Synchronous fireflies from Gatherine of Souls, 10m exposures, 2014.* [*https://www.fireflyexperience.org/photos*](https://www.fireflyexperience.org/photos)*.*

c. Mouse embryonic patterning

During mouse somitogenesis, embryonic tail elongates from the anterior to posterior direction. In tail, synchronized genetic oscillators create wave-like patterns (Tsiairis and Aulehla, 2016). When cells are randomized in vitro, wave patterns re-emerge. This thesis focuses on the mouse somitogenesis as a system for studying self-organization. as a model for studying complex self-organized model.

Part II. Somitogenesis, as a complex self-organized model

1. What is somitogenesis?

In vertebrates, segmentation takes place sequentially in the paraxial mesoderm from the anterior to posterior axis. The unsegmented mesoderm is called presomitic mesoderm (PSM) and it is situated at the posterior end of the embryo. PSM is the place where somitogenesis occurs: a morphological patterning process by which somites form. Somites are paired blocks of mesoderm that give rise to vertebra, skeletal muscle, cartilage, tendons, and skin at a later stage during development. Periodicity of somite formation varies between species. It ranges from 30 minutes in zebrafish to 90min in chicken and 120 minutes in mice (Gomez et al., 2008). In mice, somitogenesis starts on embryonic day 8 (E8.0) and ends to E13.5 (Tam and Tan, 1992).

2. "Clock and wavefront" model

The "Clock and Wavefront " model is widely used to, to explain how the number of repeated somites is controlled during animal morphogenesis (Cooke and Zeeman, 1976). This model involves a cellular oscillator in the PSM that cycles with a period that matches the rate of somite formation. Indeed, the PSM consists of cells expressing a network of genes oscillating in time. Genetic oscillations act like a "developmental clock" and a wavefront has been defined as "front of rapid cell change moving slowly down the long axis of the embryo". Below is how they initially described their theoretical model:

"*The model involves an interacting "clock" and "wavefront". The clock is a smooth cellular oscillator, for which cells throughout the embryo are assumed to be phase-linked. The*

wavefront is a front of rapid cell change moving slowly down the long axis of the embryo; cells enter a phase of rapid alteration in locomotory and/or adhesive properties at successively later times according to anterior-posterior body position. In the model, the smooth intracellular oscillator itself interacts with the possibility of the rapid primary change or its transmission within cells, thereby gating rhythmically the slow progress of the wavefront. Cells thus enter their rapid change of properties in a succession of separate populations, creating the pattern".

The Clock and Wavefront assumes the existence of positional information gradient (encoded by molecular gradients) along the PSM anterior-posterior axis. This gradient is interconnected with a smooth cellular oscillator ("the clock"). The clock instructs the timing at which a cell will undergo a "rapid change of state". For instance, a change of cell adhesion properties when they are becoming somites. The first experimental evidence of the genetic clock has been found in chicken embryos, *c-hairy1* (basic helix-loop-helix transcription factor that is a member of the Notch signalling pathway (Palmeirim et al., 1997). Subsequently, more oscillatory gene expression related to the Notch signalling pathway has been found in various vertebrates such as mammals, birds and reptiles (Kusumi et al., 2013). In addition to the Notch signalling pathway, it has been shown that target genes of Wnt signalling pathway display oscillatory expression in mouse PSM (Aulehla and Herrmann, 2004). Similarly, periodic fibroblast growth factor (FGF) signalling has been detected in PSM (Dale et al., 2006; Dequeant et al., 2006; Niwa et al., 2007).

3. Molecular "Clock and wavefront" model: signalling dynamics

It has been shown that vertebrate somitogenesis is associated with molecular oscillators that control the timing of somite formation (Palmeirim et al., 1997). This concept is called "segmentation clock". The clock is associated with the periodical expression of several cyclic genes including the Notch, (FGF), Wnt and retinoic acid (RA) signalling. These genes are expressed in a dynamic sequence. Let's imagine a football stadium where people execute Mexican waves. The crowds rise up and down from their seats in succession giving an impression of movement, creating waves. In analogy, gene expression goes "up and down" along the PSM, generating what we term "phase-shifted oscillations". As a

consequence, waves of FGF, Wnt and Notch signalling activity traverse the PSM tissue from the posterior end to the anterior (Aulehla et al., 2008; Pourquié, 2007). Every wave correlates with the formation of a pair of somites (Pourquié, 2007). This wave pattern of gene expression is achieved by the coordination of each PSM cell's activity, each cell functioning as an autonomous genetic oscillator (Masamizu et al., 2006; Webb et al., n.d.). (Dubrulle et al., 2001) suggested that 1) Dynamic expression of FGF8 in the presomitic mesoderm constitutes the wavefront of determination which sweeps along the body axis interacting with the segmentation clock to gate cells into somites 2) FGF signalling controls somite boundary position. This latest work has been theorized by (Baker et al., 2006). Two years after, (Goldbeter and Pourquié, 2008) put forward a theoretical model in which the segmentation clock is composed of a network of coupled oscillations involving FGF, Wnt, and Notch signalling components.

In summary, the segmentation clock can be seen as a population of cellular genetic oscillators that acts as a tissue-level rhythmic patterning system, regulating the timing of somite formation.

4. Molecular gradients in presomitic mesoderm tissue

In addition to oscillatory signalling activity of Notch, FGF and Wnt, signalling gradients have been found along the anterior-posterior axis of the PSM. Indeed, a Wnt signalling gradient is visible at the level of graded nuclear β-catenin protein levels, which has been shown to define the size of the oscillatory field and to control key aspects of PSM development and segment formation (Aulehla et al., 2008). From posterior to anterior PSM, FGF (Dubrulle et al., 2001; Dubrulle and Pourquié, 2004; Sawada et al., 2001) and Wnt/β-catenin (Aulehla et al., 2008, 2003) form a gradient, whereas the (Retinoic Acid) RA signalling pathway displays an opposing gradient of activity from anterior to posterior PSM(Diez del Corral et al., 2003; Moreno and Kintner, 2004; Vermot and Pourquié, 2005). This combination of morphogens and signalling are believed to control and maintain the undifferentiated states of cells in the posterior PSM. How these gradients of activity are established in the PSM is described in this review (Aulehla and Pourquie, 2010).

5. Interplay between signalling gradients and signalling oscillations

As explained above, the regulation of somite formation is underlay by a complex combination of signalling gradients and oscillations. On one hand, PSM is a place where two gradients are opposing: FGF/Wnt signalling gradients from posterior to anterior PSM and RA signalling originating from somites. On the other hand, PSM expresses cyclic genes including target genes of Notch, Wnt and FGF signalling pathways. In addition to Wnt3a gradient in posterior PSM, *Axin2* (a negative regulator of Wnt pathways and also a direct target of Wnt3a) shows an oscillatory expression in mouse PSM (Aulehla et al., 2003) In this work, Aulehla et al., 2003 proposed a model for the molecular control of segmentation where Wnt3a is a molecular pivot between the gradient and oscillations. As they explained (Aulehla and Herrmann, 2004) nicely: "*Cells exposed to higher-than-threshold levels of Wnt3a go on oscillating (clock on), whereas neighbouring (more anterior) cells exposed to lower levels stop the clock because of insufficient Wnt signalling activity (clock off). This novel link between the morphogen gradient and the clock provides a plausible explanation for how the gradient is translated into the stepwise formation of segments: Activation of the "Wnt on" phase of the clock cycle creates at the threshold position an interface between neighbouring "clock on" and "clock off" states, setting the boundary position. The periodicity of the clock cycle in combination with continuous posterior "moving" of the threshold ensures setting of the boundary position at regular intervals*".

As we have seen above, FGF, Wnt and Notch signalling pathways are playing central roles in somitogenesis. However, several perturbation studies emphasize the role of Notch signalling in synchronization in somitogenesis (Delaune et al., 2012; Horikawa et al., 2006; Jiang et al., 2000; Lewis, 2003; Riedel-Kruse et al., 2007). However, the molecular details of this cell-cell communication are still elusive. In this regard, we will focus on the role of Notch signalling in PSM tissue.

6. Coupling and lateral inhibition mediated by notch signalling

A. Canonical Notch signalling pathway

Notch signalling is one of the major signalling pathways studied in molecular biology and frequently reviewed (Guruharsha et al., 2012; Hori et al., 2013; Penton et al., 2012). In brief, Notch signalling involves ligands of the DSL (Delta/Serrate/lag-2) family on the

surface of the signal-sending cell binding to Notch receptors on the receiving cell's surface. Notch receptors consist of two distinct domains: Notch Extracellular Domain (NECD) and the Transmembrane Domain-Notch Intracellular Domain (TM-NICD). Ligand proteins binding to the extracellular domain induce proteolytic cleavage and release of the intracellular domain into the cytoplasm (Brou et al., 2000; Struhl and Greenwald, 1999). Then, the NICD is translocated into the cell nucleus and triggers the activation of downstream Notch targets (Bray and Bernard, 2010; Kopan and Ilagan, 2009). This mode of signalling, mediated by cell-cell contact, is termed **trans-activation**.

Another remarkable mechanism regarding Notch signalling communication is **cis-inhibition** (De and Bray, 1997; Micchelli et al., 1997). Cis-inhibition occurs when an interaction between Delta-Notch takes place within the same cell, leading to the neutralization of Notch receptors. As a consequence, cells with high Delta levels turn into signal cells and cannot receive signals via Notch (Sprinzak et al., 2010). This gives rises to a unidirectional signalling mode of communication termed "walkie-talkie" (Sprinzak et al., 2011, 2010). Heterogenous expression of Notch ligands can result in pathway suppression in the signal-sending cell, a process known as **lateral inhibition**. This process has been first described in *Drosophila* during neurogenesis (Cabrera, 1990) and embryonic development (Fehon et al., 1991).

B. Notch signalling in somitogenesis in brief

Notch signalling component genes have been detected during mouse segmentation (Bettenhausen et al., 1995) and it has been shown that Notch1 receptor plays an important role in segmentation coordination (Conlon et al., 1995). In zebrafish, Notch signalling is responsible for the synchronization of oscillatory expression of *her1* and *her7*. Genetic perturbation of those genes leads to disruption of normal segmentation in fish (Giudicelli et al., 2007; Henry et al., 2002; Holley et al., 2002). Loss of Notch signalling in zebrafish leads to a "salt-pepper" pattern of her gene expression, suggesting that Notch signalling is acting to synchronize the oscillations of adjacent cells, rather than driving these oscillations (Jiang et al., 2000).

In mouse and chick embryos, cyclic activity of the Lunatic fringe protein (LFNG), a member of the Notch signalling coordinates oscillatory clock expression. *Lfng* expression

in the posterior PSM is cyclic, and either loss or stable overexpression of *Lfng* perturbs clock activity and normal segmentation (Dale et al., 2003; Evrard et al., 1998; Serth et al., 2003; Zhang and Gridley, 1998). More recently, (Okubo et al., 2012) has suggested that LFNG plays a role in synchronizing oscillation in the mouse PSM by periodically preventing Delta-like ligand (DLL1) in the signal-sending cell from activating signalling in adjacent signal-receiving cells.

Various roles of Notch signalling during vertebrate somitogenesis is recapitulated and detailed nicely in this review (Wahi et al., 2016):

- In the segmentation clock, Notch synchronizes oscillations in neighbouring cells.
- Notch signalling is required for clock activity in some species.
- Notch signalling functions during somite patterning and boundary positioning.

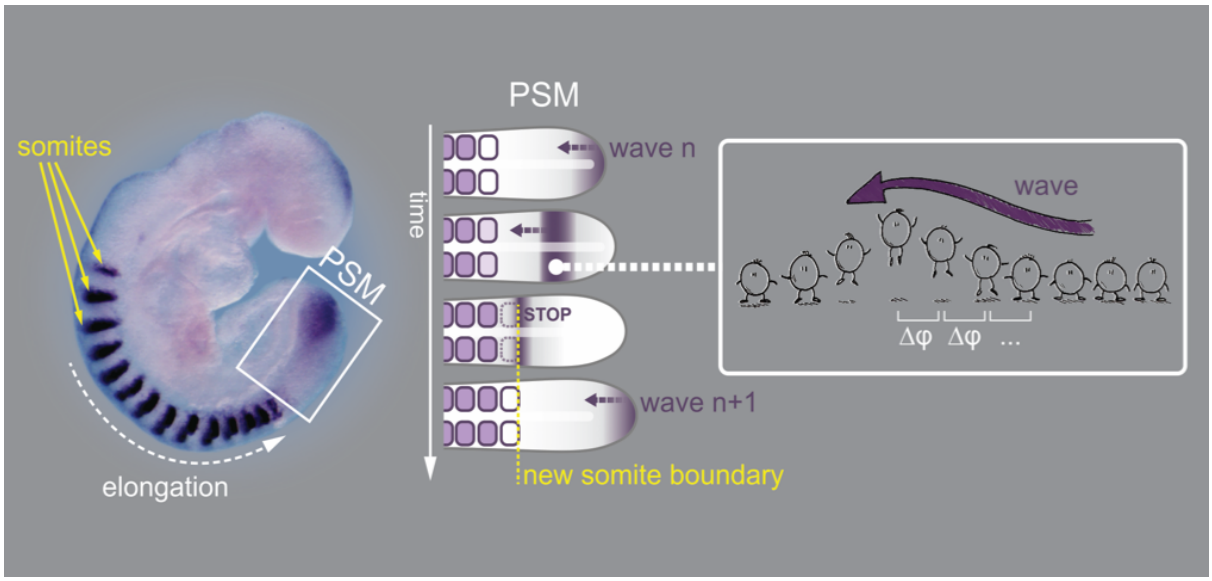

Figure 2 ***Scheme of mouse somitogenesis at E9.5 day of development.*** *Mesoderm segmentation is giving rise to one pair of somites every 120min.*

Part III: Summary of previous investigations from the lab: methods and findings

Somitogenesis is a periodic event consisting of coordinated activity of a population of cells. Each cell works as an autonomous oscillator. To visualize this oscillatory dynamic, previously the lab has established quantitative real-time imaging methods and experimental assays.

1. Characterization of segmentation clock dynamics in vitro

a. Tail culture experiment

To quantify segmentation clock activity in time and space, we combine dynamic signalling reporter systems with real-time imaging and embryo/explant culture. To do so, we culture tails from LuVeLu mouse embryos at E10.5 stage of development.
A Notch-signalling reporter we use throughout this study is *LuVeLu.* The LuVeLu mouse line expresses Venus100, a YFP derivative, under the control of a 2kb enhancer/promoter fragment of the cyclic Notch-target gene pathway Lfng26Lfng promoter101,102. To enable visualization of dynamic events, mRNA coding for the reporter was destabilized by the 3' UTR of the endogenous Lfng transcript*31*. Additionally, the fluorophore was destabilized on protein level by fusion to a modified PEST domain103. Using quantitative real-time two-photon microscopy, tail culture experiment reveals waves of activity sweeping through the presomitic mesoderm (PSM) in posterior to anterior direction. Each wave's arrival at the anterior end of the PSM precedes the formation of one new somite (Lauschke et al., 2013).

Periodic waves have been quantified and characterized along the anterior-posterior axis. At the posterior region, cells oscillate at 130min, while at the half-posterior PSM, they oscillate at 150min and finally in the anterior region, they oscillate at 170min. (Figure 3). Period measurements revealed a Notch oscillation frequency gradient (Lauschke et al., 2013; Tsiairis and Aulehla, 2016) from the posterior to the anterior direction. More recently, Dr. Gregor Mönke, a current postdoc in our lab established a sophisticated quantitative analysis method. This novel tool enables the visualisation of

the phase and period dynamics at the PSM tissue level in space and time. Recent analysis of tail "wavelet movies" have confirmed previous findings in the lab. (Figure 3).

To sum up, Notch signalling transcriptional waves slow down and stop when they are approaching the region where somites are newly forming.

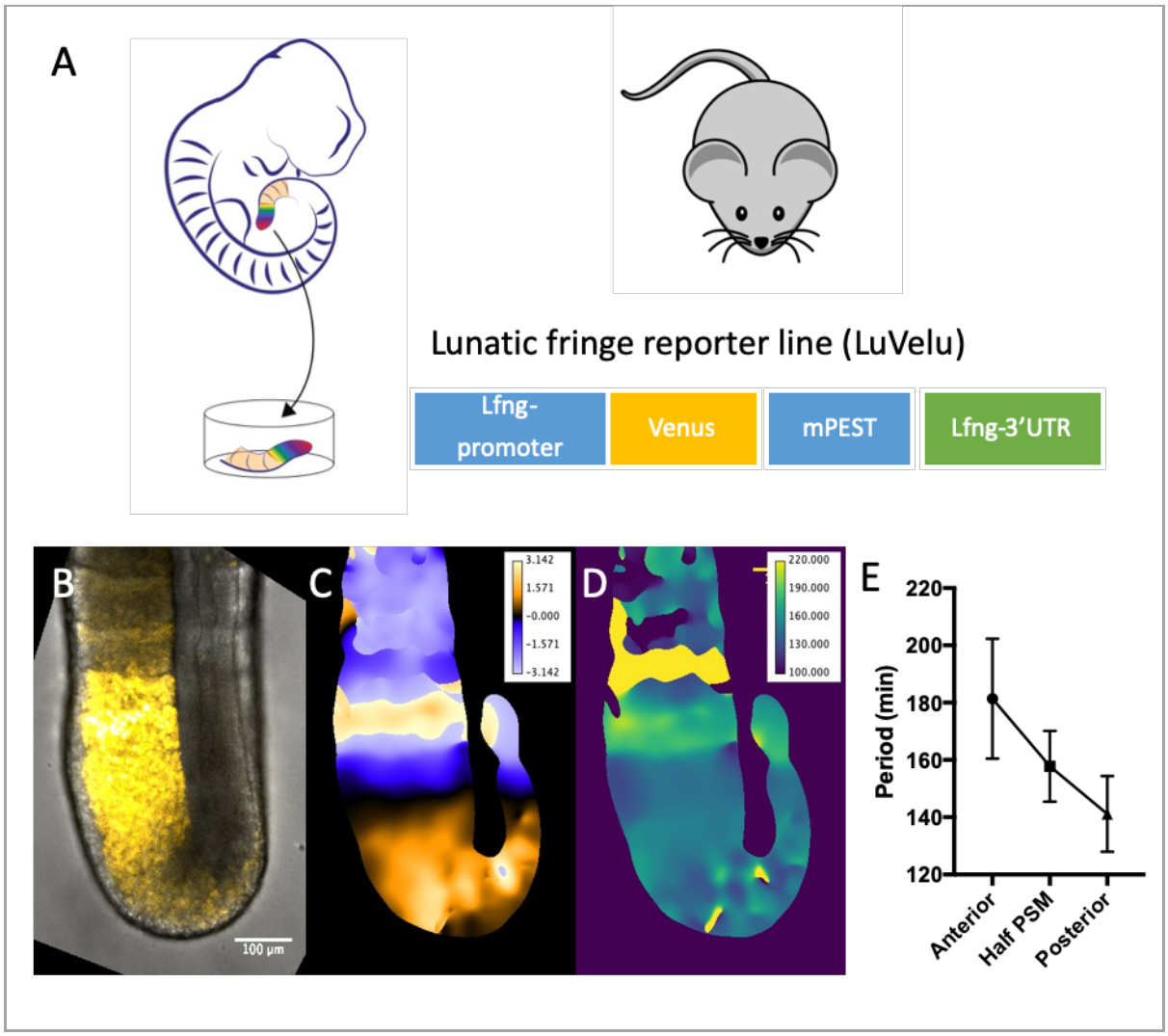

Figure 3 ***Real-time visualization of Notch signaling oscillation during mesodermal patterning****. (A) Lfng Venus transgene construct. (B) Snapshot of a representative LuVeLu in vivo real-time imaging experiment after 455min of culture (C) Snapshot of phase movie. (D) Snapshot of period movie. (E) Quantification of Notch oscillation period gradient within PSM and standard deviation for N=19 tails.*

b. *Two-dimensional segmentation assay aka "Spread-Out"*

To examine the nature of these signalling activity waves, a previous PhD student Volker Lauschke has established a 2-D segmentation assay also known as "Spread out" assay.

This assay consists of physically excising the posterior region of the PSM, i.e. the tailbud. The tailbud is placed with the transverse cut facing downwards on a fibronectin-coated dish. After the tailbud is placed on the dish, cells spread almost concentrically on the dish and shows gene activity oscillations with a period similar to what has been measured tail explants (Lauschke et al., 2013).

Wavelet movies applied on "Spread Out" cultures, reveals a Notch oscillation frequency gradient from the centre to the periphery of the spreading tissue (Figure 4). Waves emerge from a central cellular population that does not display LuVeLu signal. These waves concentrically transverse the tissue and stops at the outer boundary when a new segment is forming.

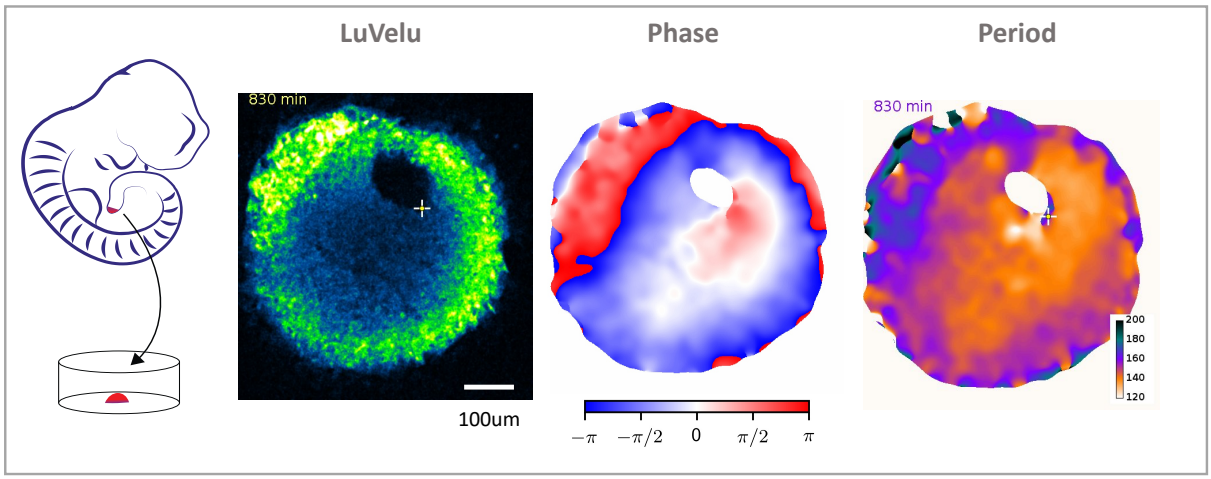

Figure 4 ***Real-time visualization of Notch signaling oscillations in 2dimentional.*** *From left to right: Scheme of the experiment. Snapshot of a representative ex vivo LuVeLu report cell culture assay after 830min of culture. Snapshot of phase and period movie of the same experiment.*

2. Randomized PSM cells self-organize into mini emergent PSM

a. Reaggregation assays with multiple inputs

Previously, using real-time imaging of a dynamic Notch signalling reporter, LuVelu (Lfng-Venus-Lfng) in mouse (Aulehla et al., 2008), our group observed that genetic oscillators from PSM cells display periodic waves in a two-dimensional culture system (Lauschke et al., 2013). However, little is known about the origin of spatiotemporal wave patterns. To address this problem, an in vitro approach has been established (Tsiairis and Aulehla, 2016). To this end, Charisios Tsiairis (former postdoc in our lab) has pioneered the self-organization assay. This assay consists of mechanical cell dissociation and re-

aggregation: he pooled PSM tissue from at least 6 embryos, dissociated them into single cells and re-aggregated them by centrifugation. The pellet of re-aggregated PSM cells was cut into small pieces. Each piece of the reaggregate is seeded in a plate coated with fibronectin. Surprisingly, after randomization, PSM cells can self-organize into several miniature PSM structures. They termed it "ePSM" for "emergent PSM".

b. Notch frequency gradient, β-catenin gradient forms de novo within ePSMs

Interestingly, ePSM recapitulates some features found *in vivo* PSM (Tsiairis and Aulehla, 2016):

(1) *In vivo* PSM signaling activity wave patterns sweep through the PSM in posterior to anterior direction. In these wave patterns, we observed simultaneously a frequency gradient and subsequently a phase gradient. Cells in the posterior PSM oscillate faster than cells located in the anterior PSM. Similarly, inside each ePSM, the cells located in the centre oscillate faster than those at the periphery. In other terms, a **Notch oscillation frequency gradient emerges spontaneously after randomization within ePSM**.

(2) Additionally, *in vivo* PSM displays a Wnt signalling/β-catenin protein gradient from the posterior to the anterior part (Aulehla et al., 2008). Similarly, after randomization, we also found a **gradient of β-catenin protein** from the centre to the periphery within each ePSM.

How these two gradients are re-established after cell randomization is unknown and not studied yet. An overview of different techniques of investigation previously developed in the lab is presented in Figure 5.

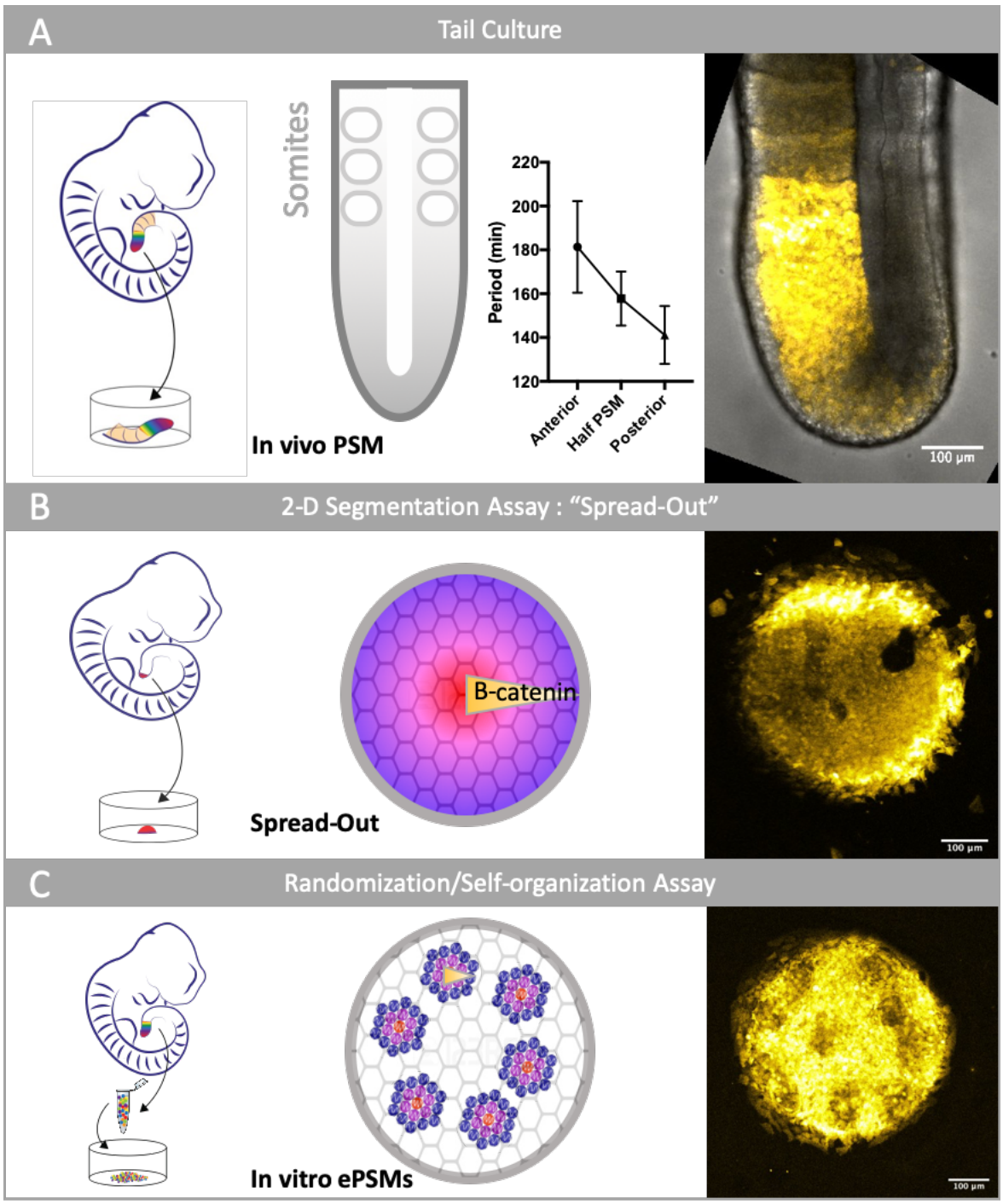

Figure 5 ***Methods for studying Notch signaling oscillations during mesodermal patterning.*** *(A) Tail Culture assays (B) 2-D segmentation assay, also known as "spread-out" (C) Self Organization assay.*

Part IV: Oscillations in somitogenesis

In PSM tissue, we observe, oscillatory wave patterns linked to a tight synchronization of genetic oscillators can be visualized using real-time imaging experiments.

In this thesis, we will mainly represent oscillations in two manners (Figure 6):

1) **Time-series**: Intensity is depicted in x-axis over time.
2) **Polar Plot**: phase representation of an oscillation

We will use the following terms:

- **Oscillations**: regular and repetitive process in time.
- **Period**: time to complete one oscillation cycle (inverse of frequency).
- **Phase**: a particular state of an oscillation, for instance "peak" or "trough".

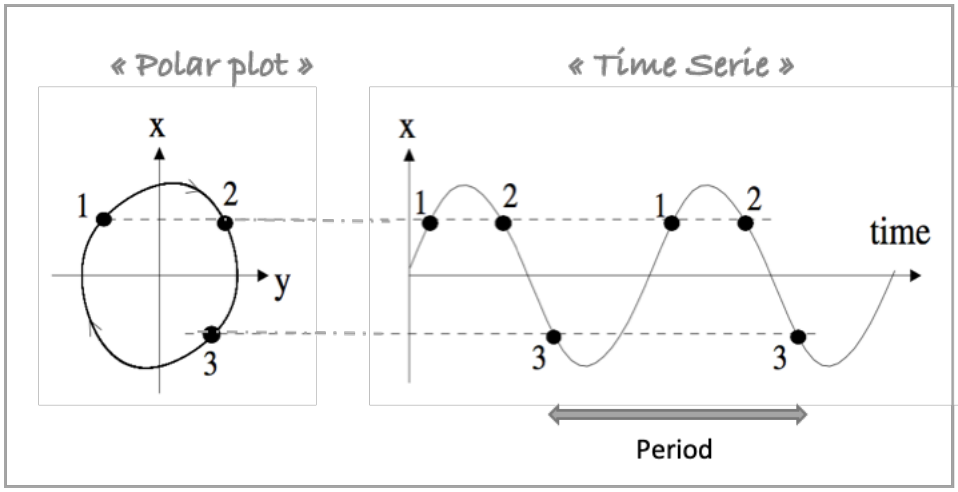

Figure 6 ***Representations of oscillations*** *from (Pikovsky et al., n.d.).*

1. Synchronization and Coupling

In the 17th century, Christian Huygens, a Dutch physicist was sick in his bed for a couple of days. In his room, two pendulum clocks were hanging on the wall. After some time,

from his bed, he noticed that two clocks started to swing in synchrony. To confirm this observation, he hanged two pendulum clocks on the common wooden beam placed at the top of two chairs. He observed that two clocks were synchronized in anti-phase. (Figure 7) He reported this phenomenon on his mail to his father in 1665 and then to the Royal Society of London. Christian wrote about "*Le phénomène de la sympathie, sympathie des horloges*". "*Sympathy of two clocks* in 1665. In this dissertation, he was the first one to describe the phenomenon of clock synchronization that he termed "sympathy". He intuitively understood that the conformity of the rhythms of two clocks had been caused by the motion of the beam. In modern terminology, this would mean that the clocks were synchronized in anti-phase due to the coupling through the beam (Peña Ramirez et al., 2016; Willms Allan R. et al., n.d.).

Figure 7 ***Christian Huygens and sympathy of clocks****. In 1656, a Dutch physicist and mathematician Christiaan Huygens completed the world's first pendulum clock. A lifelong bachelor, Huygens built clocks of many shapes and sizes and collected his clocks in a single room. In Huygens's day, most people would have attributed this odd behaviour either to God or to Satan, but as a rationalist, Huygens went searching for another reason. (Top right) Portrait of Christian Huygens by Caspar Netscher (Gemeentemuseum Den Haag). (Bottom left) Example of Huygens Original's clock. (Bottom right) Original drawing of Christiaan Huygens illustrating his experiments with two pendulum clocks placed on a common support.*

Huygens has introduced two important concepts for this thesis: the concept of **synchrony** and the concept of **coupling**. **Synchronization** is an adjustment of rhythms of oscillating objects due to their weak interactions. These interactions between oscillators are termed: **coupling**. Two coupled clocks are synchronized if: 1) Their phase difference remains constant over time and 2) Their frequencies match (Pikovsky et al., n.d.).

2. Kuramoto model: Phase difference coupling models

In the segmentation clock field, numerous studies tried to understand and theorize the coupling rules governing synchronization in PSM tissue (Morelli et al., 2009; Murray et al., 2013; Okubo et al., 2012; Shimojo et al., 2016). A well-studied theoretical approach to describe synchronization computationally is applied by Gregor Mönke. To describe how coupling between non-linear oscillators is achieved, theoretical physics proposes two distinct classes of coupling models 1) phase difference coupling (Kuramoto, 1984) and 2) pulse coupling models (Winfree, 1967). Importantly, for its simplicity and mathematical convenience, Kuramoto model (Kuramoto, 1984) is the commonly used model to provide a theoretical framework to describe synchronization between genetic oscillators in PSM tissue (Morelli et al., 2009; Murray et al., 2013; Okubo et al., 2012; Shimojo et al., 2016).

In the general Kuramoto coupling model, (later one we will term it "phase difference coupling model"), if phase oscillators "A" and "B" are identical, we can write the model equations (Order Differential Equation ODE) as below:

$$\delta_t \varphi_A = \omega_A + cH(\varphi_B - \varphi_A)$$
$$\delta_t \varphi_B = \omega_B + cH(\varphi_A - \varphi_B)$$
$$\theta = \varphi_B - \varphi_A$$
$$H = sin(\theta)$$

Oscillator A	**Oscillator B**
Phase A φ_A	Phase B φ_B
Frequency A ω_A	Frequency B ω_B
How phase A is changing overtime (left hand of ODE) $\delta_t \varphi_A$	How phase B is changing over time (left hand of ODE) $\delta_t \varphi_B$
"c" coupling strength, here constant	
"H" is a coupling function (Ermentrout, 1985)	
θ is the phase difference between two oscillators A and B, the main feature of oscillator interactions	

In the presence of identical phase oscillators, phase difference coupling models assume:

(1) Synchronization is driven by the phase differences between oscillators.

(2) Synchronization between two oscillations occurs throughout the entire oscillations cycle, i.e. oscillators "feel" the presence of the neighbouring oscillator continuously.

(3) Synchronization is a continuous and mutual process.

The interaction between Kuramoto coupled oscillators (*i* and *j*) can be described by a coupling function as shown (Figure 8). It is generally defined as a function of phase differences. The dynamics of the phase depends on:

(1) Natural frequency of the oscillators: "phase velocity of the oscillators"

(2) The coupling strength: "interaction forces between the oscillators"

(3) And importantly (the very definition), the phase difference between the two oscillators

Pure Kuramoto coupling model predicts that after synchronization, two oscillators reach **both collective phase and frequency averaging**. These are the two main features and predictions of the Kuramoto model.

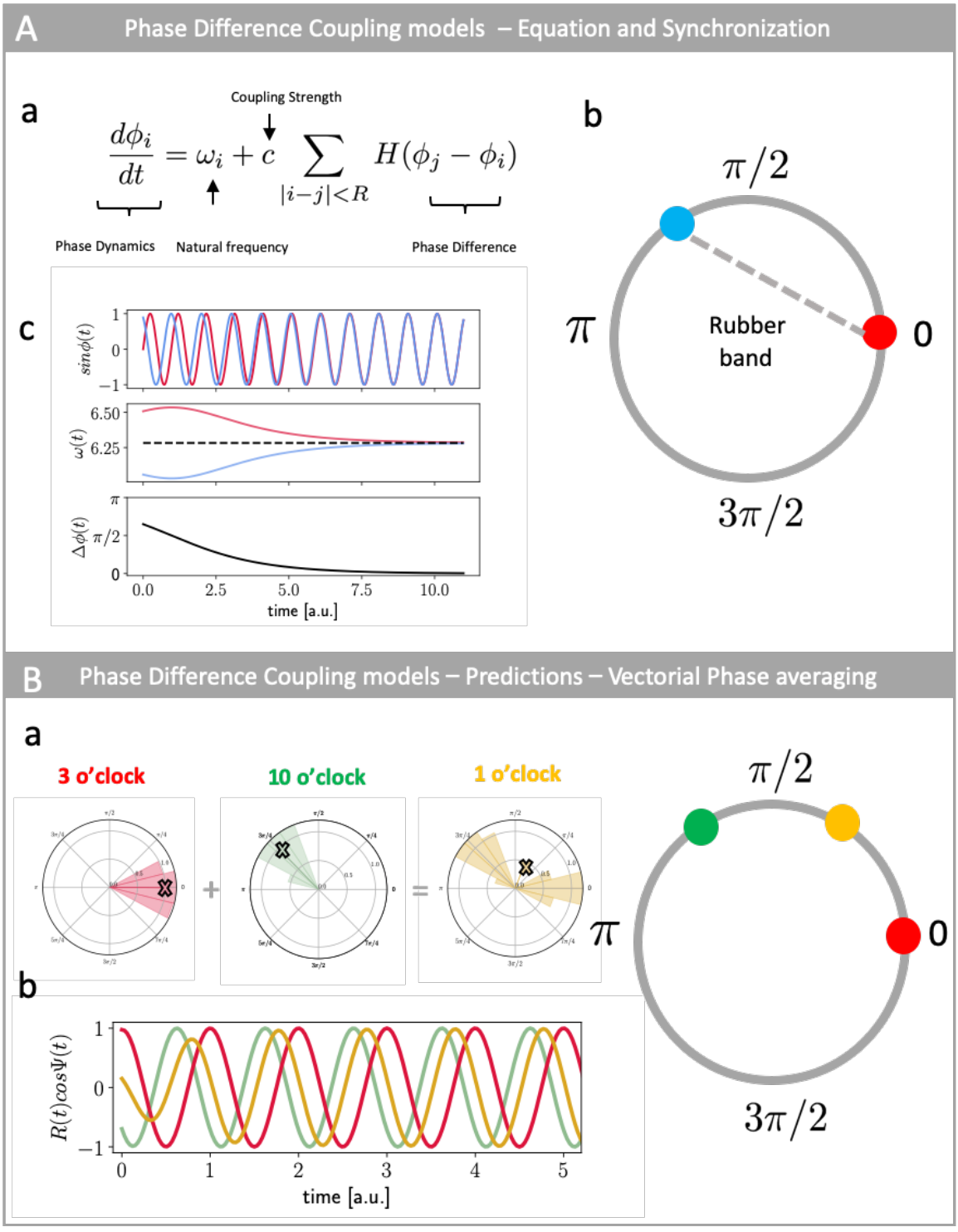

Figure 8 ***(A) Phase Difference coupling models: equation and predictions****. (Aa) General Coupling function describing the interaction between two phase oscillators. (Ab) Scheme representing two oscillators at different phase on a polar plane. Two oscillators are linked by their phase difference similar to a "rubber band". The phase difference drives the synchronization. (Ac) Numerical simulations showing synchronization between two oscillators (top) two oscillatory traces by sinusoidal functions (red and blue) reaching the synchrony. (Middle), natural frequencies of two oscillators. The" Red oscillator is slowing down" while the "blue oscillator is speeding up" thus leading to the synchrony. (Bottom) Graph showing the phase difference between two oscillators. The phase difference is reaching zero when the synchronization is achieved.* ***(B) Phase difference coupling model predicts a vectorial phase average*** *(Ba) Initial phase distribution of two populations of oscillators A and B. Each population of oscillators shows a different initial phase distribution on the polar plane. The model predicts that the average of A and B (yellow) is between their initial phase distribution (yellow cross). (Bb). Simultaneous observation of all three populations reveals phase conservation.*

Chapter II: Aims of the thesis

PSM cells can self-organize into several miniature emergent PSM structures (ePSM) after being randomized and reaggregated. Randomized PSM cells (with mixed phases and frequencies) can synchronize de novo, leading to the formation of ordered patterns oscillating in sync. From numerous perturbations studies (Delaune et al., 2012; Horikawa et al., 2006; Jiang et al., 2000; Lewis, 2003; Riedel-Kruse et al., 2007), it is well known that the Notch signalling pathway is involved in synchronizing PSM oscillations. Despite knowledge of the molecular machinery at work, the general rules of coupling remain elusive.

To explain synchronization in PSM cells, main theoretical studies in our field(Morelli et al., 2009; Murray et al., 2013; Okubo et al., 2012; Shimojo et al., 2016) used a theoretical model developed by Kuramoto in 1979. In the Kuramoto model, the phase difference is the main feature that drives synchronization continuously and mutually between oscillators. For this reason, this model can be termed “phase difference coupling model”. Besides, numerical simulations performed by Gregor Mönke (postdoc in the lab) show that this model makes distinct predictions regarding collective phase and frequency, which both represent averages of the input oscillators.

To drive phase difference coupling models, phases are assumed to be equal to each other. However, Notch and Delta protein expression is highly dynamic in PSM (Bone et al., 2014). On one hand, there is a heterogeneity of protein level expression during Notch oscillation cycle - and on the other hand, all phases are equivalent as described in theory. Because of this discrepancy, the use of Kuramoto model to describe synchronization in PSM remains questionable. Moreover, theoretical predictions regarding collective phase have never been tested experimentally. For these reasons, we want to challenge experimentally the Kuramoto model. Previously, for technical reasons, predictions made in phase coupling model couldn't be tested with the conventional methods available. This highlights the importance to find a new experimental method to address this problem. Therefore, in this thesis, we have to achieve three major tasks:

1. Establishing a new experimental strategy enabling to investigate the phase synchronization at the quantitative level.

2. Quantitative testing of theoretical model predictions regarding the collective phase dynamics.

3. Determining the coupling rules governing the empirically observed synchronized oscillations in PSM tissue

Chapter III: Results

Part I: Developing a novel experimental strategy and assays

1. Experimental design

To address how phase synchronization is established, we take two populations of oscillators with distinct phases and mix them. Then, we compare the collective phase with the two original phases of the input oscillators.

To this end, we use PSM cells from two different embryos, which naturally oscillate in different phases even within one litter. Using these two PSM tissues, we then perform three independent randomization cultures: We take one cell population oscillating in a specific phase (eg: Phase A, culture 1) and a second cell population oscillating in another specific phase (eg: Phase B, culture 2). Finally, we combine cells from each PSM and determine the phase of the mixed population (Phase AB, culture 3). The common phase of the mixed population (culture 3) will be compared to the two original phases without mixing (cultures 1 and 2) (Figure 9). To this end, we took only the very posterior part of the PSM (tailbud), where the cells oscillate in phase (Lauschke et al., 2013). Therefore, we need to be able to culture a very low number of cells. However, previously in the lab, no suitable methods were available.

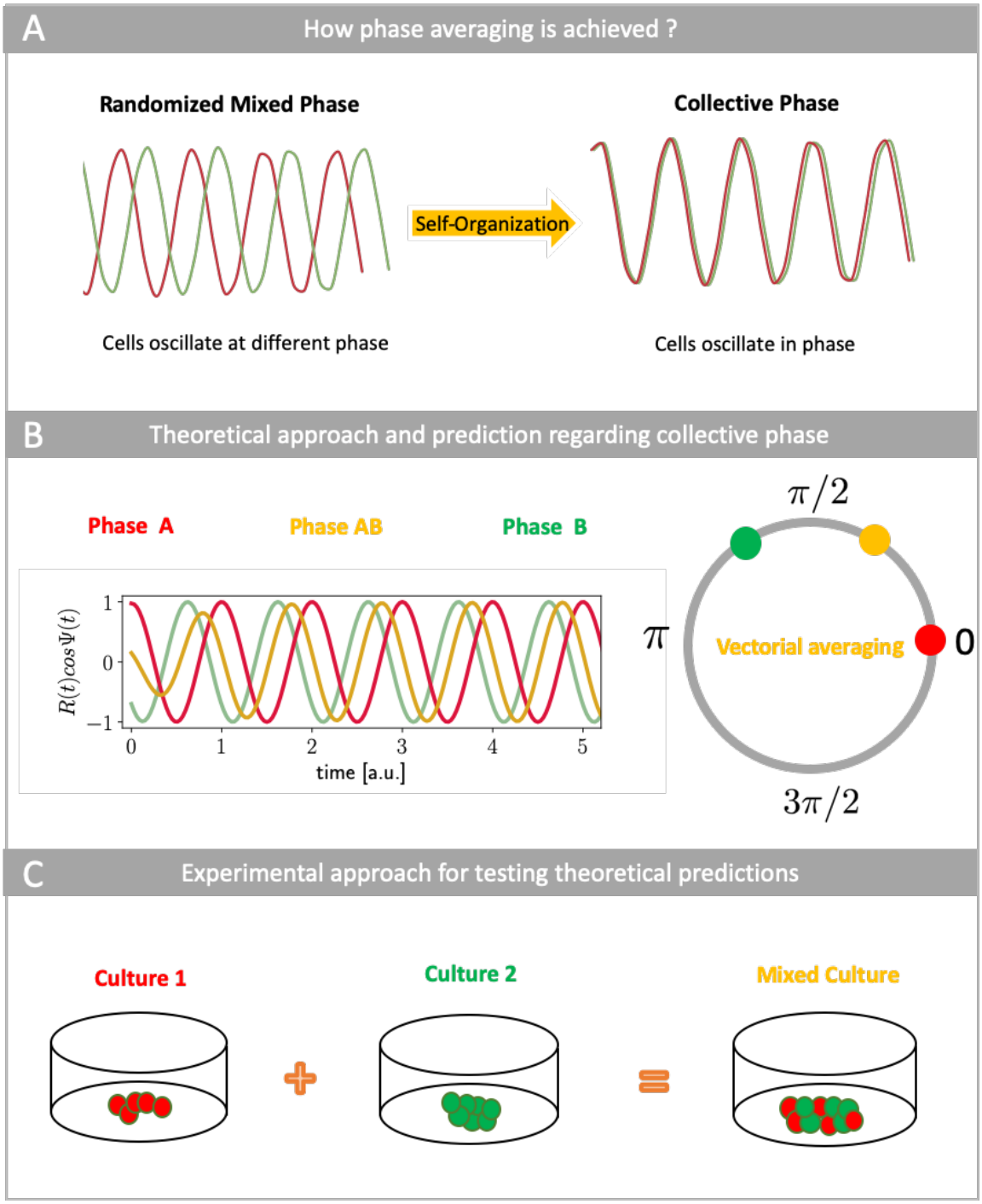

Figure 9 ***General problem and experimental strategy****. (A) How phase averaging is achieved? After randomization, cells oscillating at different phase are mixed, then after self-organization, cells established collective synchrony. (B) Theoretical predictions show collective phase is equal to the phase average of input oscillators. (C) Experimental strategy for testing theoretical predictions regarding collective phase.*

2. Limitations of reaggregation assays

Previously in the lab, the randomization assay (also known as "self-organization assay") was developed by Charisios, a former postdoc in the lab and presents several features (Tsiairis and Aulehla, 2016):

- **Multiple embryos input**

The principle of this method is based on the mechanical dissociation of the cells and their reaggregation by centrifugation to obtain a visible pellet of cells. This technique demands a critical number of cells obtained by pooling approximately six PSM tissues or even more. So, the input consists of a mix of multiple PSM tissues coming from different mouse embryos. Samples coming from different embryos do not constitute a clean configuration to determine the collective phase.

- **Multiple frequencies and phases mixed**

Each PSM tissue is a mix of cell populations oscillating at different frequencies and phases. Indeed, PSM displays the frequency gradient from the posterior to the anterior axis and cells are phase-shifted along that axis (Lauschke et al., 2013). Since reaggregation assay requires a mix of several PSM from different embryos (with unknown original phases and frequencies), it would be difficult to test phase averaging if the phase input is not determined at the onset of the experiment.

To conclude, previous reaggregation assay isn't a suitable method to study phase synchronization in PSM tissue. This highlights the importance to establish a novel experimental method.

3. Development of RAFL method

a. Randomization Assay for Low input (RAFL)

I developed a novel randomization assay method which aimed at correcting the limitations of the previous randomization experimental protocol. The principle is based on the randomization of only few cells using a micro culture insert (500um size of diameter). The mechanical dissociation is directly performed inside of the micro insert under the stereoscope to monitor the cells and seeded them on the spot. Because of the low input of the cells required, only one PSM tissue is necessary to perform this assay while at least 6 PSM tissue were required before. We can aim to a smaller part of the PSM, choosing only the posterior part of the tissue. Therefore, only a restricted region with a narrow frequency and phase distribution is kept for initial cell input. Comparison between randomization assay using multiple PSM input and RAFL is recapitulated in (Figure10).

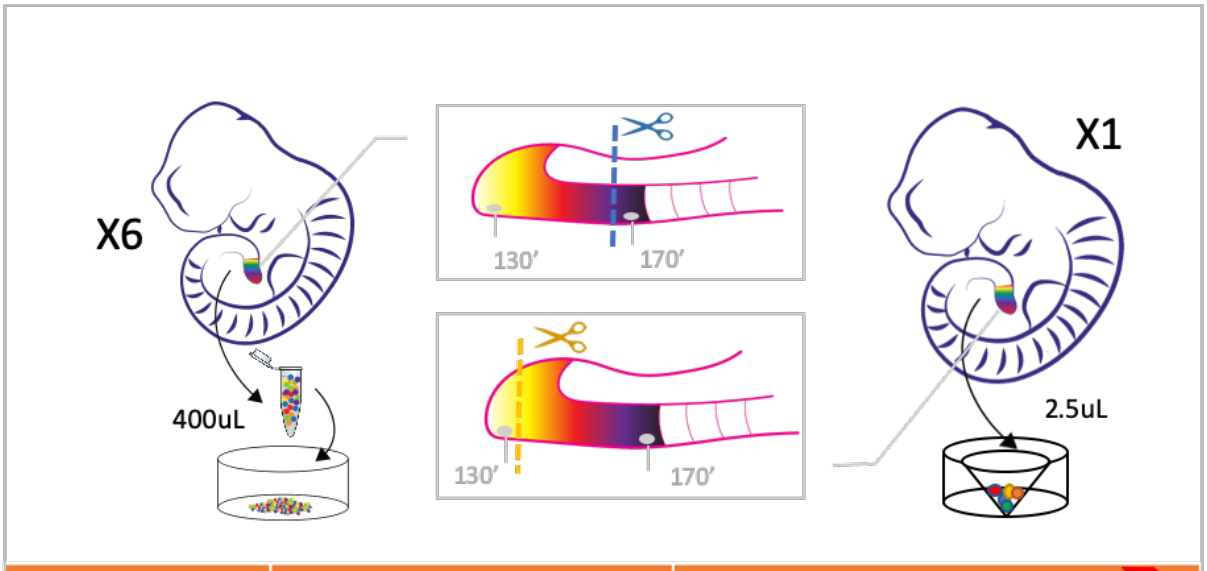

	Randomization Assay with Multiple Input (Tsiairis et Aulehla., 2016)	Randomization Assay for Low input (RAFL) NEW
Principle	Dissociated PSMs cells are re-aggregated by centrifugation in 400uL	PSM cells from single embryo are dissociated in tiny volume 2.5uL
Input	> 6 PSM	Only 1
Phase Distribution	Large	Narrow
Frequency Distribution	Large	Narrow
Duration of the experiment	Between 1h30 and 3h	< 30min in average
Difficulties Critical points	• Need a high number of cells for making a pellet • Scratching the pellet can damage cells	• Small volume pipetting
Benefits	• Works	• Define single embryo input • Convenient for using rare mutants

Figure 10 ***Comparison between previous established randomized assay (Tsiaris et Aulehla., 2016) versus newly established Randomization Assay for Low input (RAFL)***

b. *Recapitulation of ePSM features*

In order to validate this method, we randomized PSM cells using RAFL method and checked whether the results are consistent with previous findings (Tsiairis and Aulehla, 2016).

Unlike the previous randomization protocol which requires at least 6 PSM tissues, we used one single PSM tissue. After their randomization, cells self-organized into small emergent PSM structure (ePSM) (Figure 11). The number of formed ePSM was usually around 6. This depends on the cell confluency. Curiously, when two ePSMs formed very close, they fused together and formed one bigger ePSM. For each region where an ePSM is formed, we drew one Region Of Interest (ROI) (Figure 11**)** and quantified the LuVeLu intensity using FIJI software (Schindelin et al., 2012). Then, we extracted the phases and frequencies using Wavelet analysis developed by Gregor Mönke (Mönke et al., in preparation). We observed that all ePSMs display oscillations that are synchronized with each other (Figure 11). Spatial visualization of wavelet analysis method showed period gradient within each PSM (Figure 11). These results are consistent with what it has been found previously but using multiple PSM as input (Tsiairis and Aulehla, 2016).

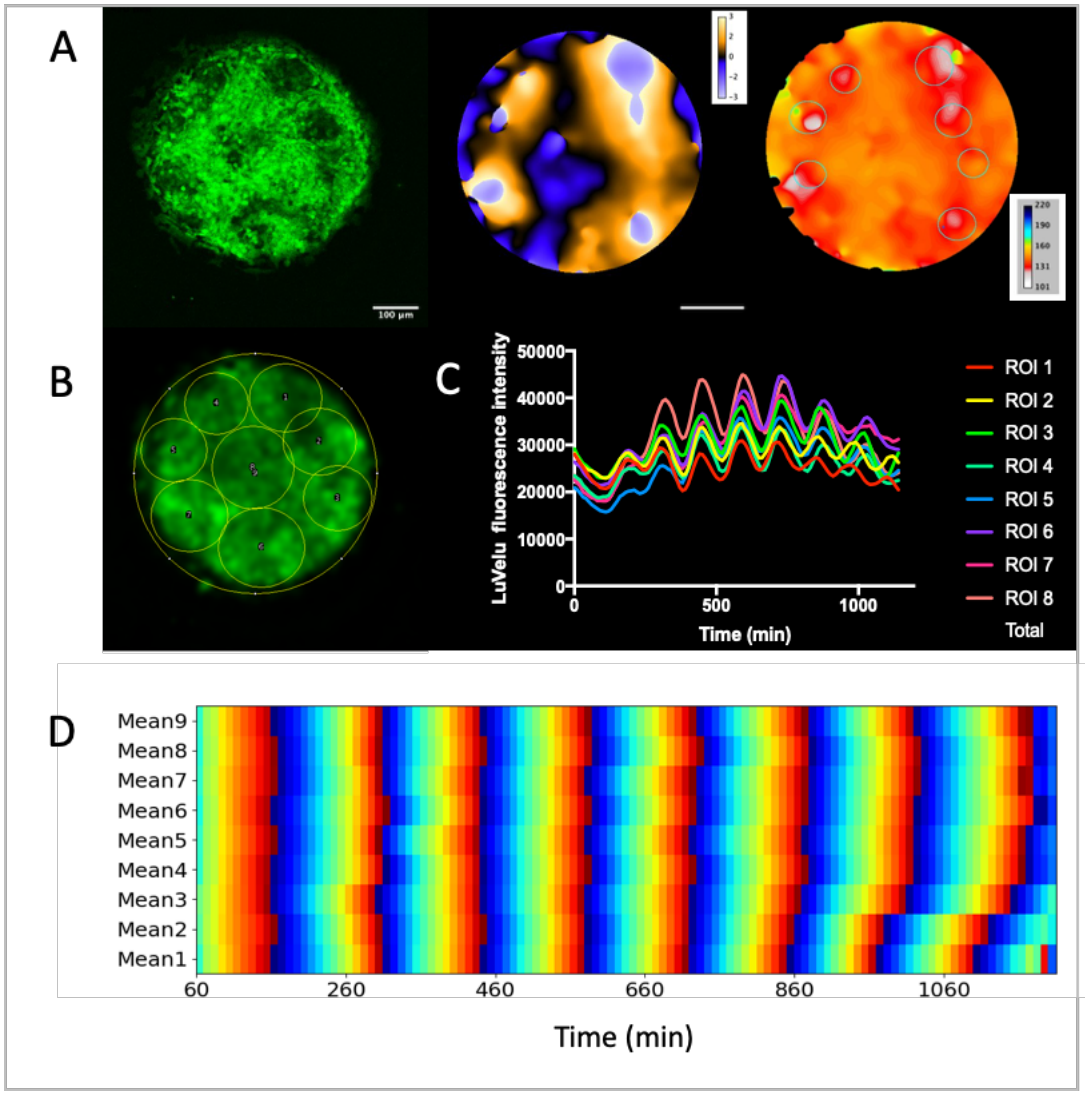

Figure 11 ***Randomization assay using single PSM tissue.*** *(A)From left to right: Snapshot of a representative in vitro LuVelu reporter cell randomization assay. Visualization of Notch oscillation phases and frequencies. Snapshots are taken after 480min of cell culture. (B) Snapshot of randomization assay taken after 15hours of cell culture. Every ROI correspond to a region where a mini PSM emerges (C) Quantification of LuVelu oscillations from randomized single PSM cells over time. (D) Oscillation phase representation of each ePSM (eg ROI) displayed.*

In addition, we randomized cells originated from different regions of PSM tissue and compared their oscillations. Randomized cells from:

- Single entire PSM tissue: cells oscillate with an average period of 145min.
- Single posterior PSM tissue: cells oscillate with a period close to 130min
- Single anterior PSM tissue: cells oscillate at 160min with a premature arrest of oscillations due to imminent cell differentiation to somites (Figure 12).

These results are consistent with previous findings in the lab (Lauschke et al., 2013; Tsiairis and Aulehla, 2016).

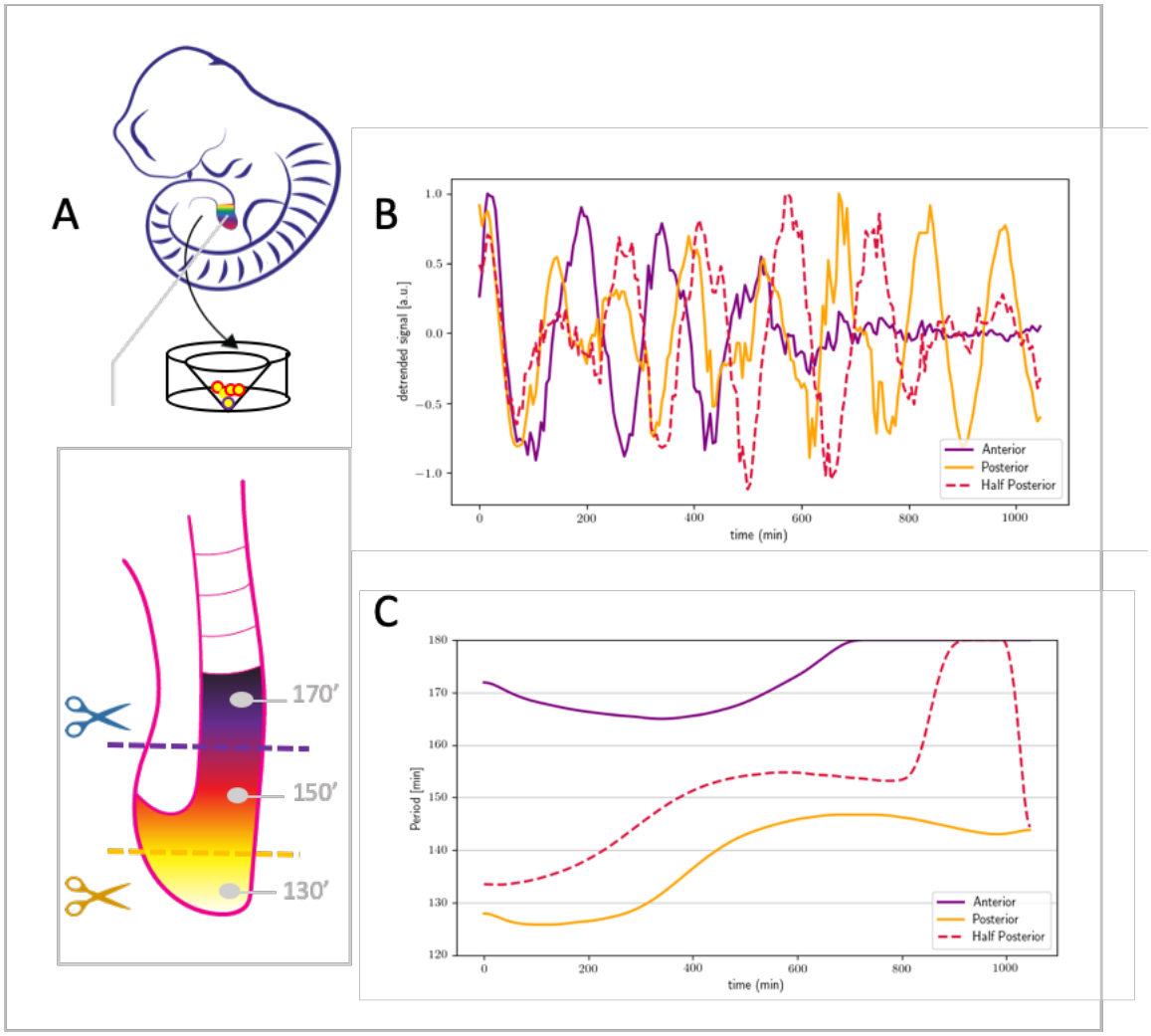

Figure 12 ***Randomized PSM cells oscillate at different period according to their initial position along the anterior-posterior axis.*** *(A) Scheme of PSM tissue along the anterior-posterior axis showing gradient of Notch oscillation frequency (B) Detrended signals for LuVelu intensity over time of randomized cells from anterior, posterior and half posterior of PSM tissue. (C) Period quantification of measured oscillations presented in (B).*

Wavelet analysis in space showed a frequency gradient going from centre to periphery of each ePSM (Figure 13). Moreover, β-catenin immuno-staining snapshot after 24hours of cultured PSM cells shows a high level of β-catenin protein inside of each ePSM (Figure 13). These two findings are consistent with previous results found in the lab (Tsiairis and Aulehla, 2016).

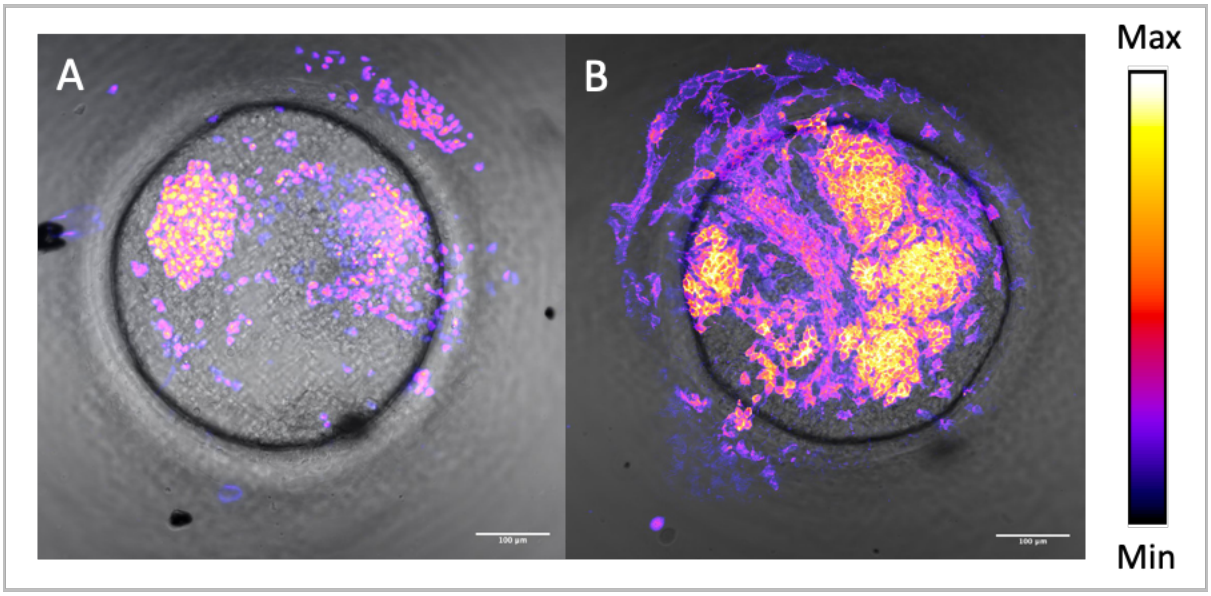

Figure 13 ***Immunostaining for ß-catenin protein for randomized PSM samples.*** *(A-B) Snapshots of ß -catenin protein immunostaining after 24h of culture.*

To conclude, RAFL method enables to reproduce previous findings using Charisios's protocol (Tsiairis and Aulehla, 2016) using one single PSM tissue.

4. RAFL method: little game-changer in the lab

In addition to the experimental outcome generated by RAFL, we can mention a couple of interesting facts that explain why RAFL is a successful and fruitful method for the lab.

A. RAFL: toward MORE "3R" S principles

The principles of "3R" (Replacement, Reduction, and Refinement) are framing the way how we conduct animal research in the lab. They are defining as following:

- **Replacement**: methods which avoid or replace the use of animals.
- **Reduction**: methods which minimise the numbers of animals used per experiment.
- **Refinement**: methods which minimise animal pain and improve welfare.

Previously, experiments performed using reaggregation method required often the sacrifice of 3 mice and more per assay. In contrast, now only one single embryo is enough.

Therefore, RAFL method has reduced considerably the number of mice used per experiment, which is more in agreement with the reduction principle.

B. Randomization assay using rare mutant mouse PSM cells

Requirement of low cell number is the main feature that allows the use of other mouse strains. Indeed, our lab possesses numerous rare mutant mouse lines in use for other research projects running by my labmates. Moreover, certain mouse females from those mutant mouse lines give a poor number of available living embryos. For this reason, certain questions requiring genetic perturbations in self-organization context are not addressable. RAFL has corrected these limitations and offers now new possibilities to progress in other research projects in self-organization context.

In summary, I established a novel *in vitro* approach to address phase synchronization problem during mouse somitogenesis. This method entitles Randomization Assay for Low input (RAFL), enables to culture a very low number of cells coming from a specific part of PSM tissue. RAFL method produces results and findings similar to what Charisios found during his postdoc research. As a bonus, RAFL offers new possibilities to conduct research in self-organization context using precious mouse lines, more in agreement with good ethics in animal research.

Part II: Unmasking the coupling rules in mouse PSM tissue

1. The "AB experiment" design

The phase difference coupling framework is commonly used to model segmentation clock synchronization in PSM (Morelli et al., 2009; Murray et al., 2013; Okubo et al., 2012; Shimojo et al., 2016). To experimentally test the predictions based on phase difference coupling, we used the following approach: we used PSM cells from two different embryos, which naturally oscillate in different phases. To have a defined phase input, we took only the most posterior part of the PSM (tailbud or "TB"), where the cells oscillate in phase (Lauschke et al., 2013).

Using these two PSM tissues, we then performed three independent randomization cultures: we took TB "A" oscillating in a specific phase (eg: Phase A, culture 1) and a second TB "B" oscillating in another specific phase (eg, Phase B, culture 2). Finally, we combined cells from each TB and determined the phase of the mixed population (phase AB, culture 3). The common phase of the mixed population (culture 3) was compared to the two original phases without mixing (cultures 1 and 2) (Figure 14A). To determine the origin of the cells in the mixing, the first input (TB "A") is labelled with an H2B-mCherry marker in addition to the LuVeLu reporter, while the second input (TB "B") only carries the LuVelu label.

2. "Winner takes it all" scenario

Using the newly established RAFL, we then performed the experiment described above (Figure 14A) using LuVeLu fluorescence intensity as a readout. For each cell population, we then quantified oscillations of LuVeLu signal for several Regions of Interest (ROIs). Each ROI corresponds to one region, where a miniature emergent PSM formed *de novo* after randomization (Figure 14B). We then extracted the phases for each ROI (eg: Phase A cells, Phase B cells; phase AB cells). Within the same cell population, all ROIs displayed very robust oscillations and oscillations of all ROIs were synchronized to each other. While cell populations A and B oscillated with distinct phases (Figure 14C), the mixed population showed a phase profile similar to one of the two populations (for instance B), although the cell populations had initially been mixed at equal volumes. Since

phase difference between oscillators is the central marker in Kuramoto model (aka phase difference coupling model), we calculated the phase difference between these three populations. In agreement, the phase difference between cell population B and the mixed population AB was close to 0 (Figure 14D), while the phase difference between A/B and A/AB were similarly different from 0 rad. Moreover, phase oscillator representation (Figure 14F) A/B and A/AB looks similar. Remarkably, phase oscillators of population B and population AB overlaps together. Moreover, in this case, the average frequencies of both populations are very close, approximately 130min. In other words, mixed population AB synchronize according to the population B (Figure 14E).

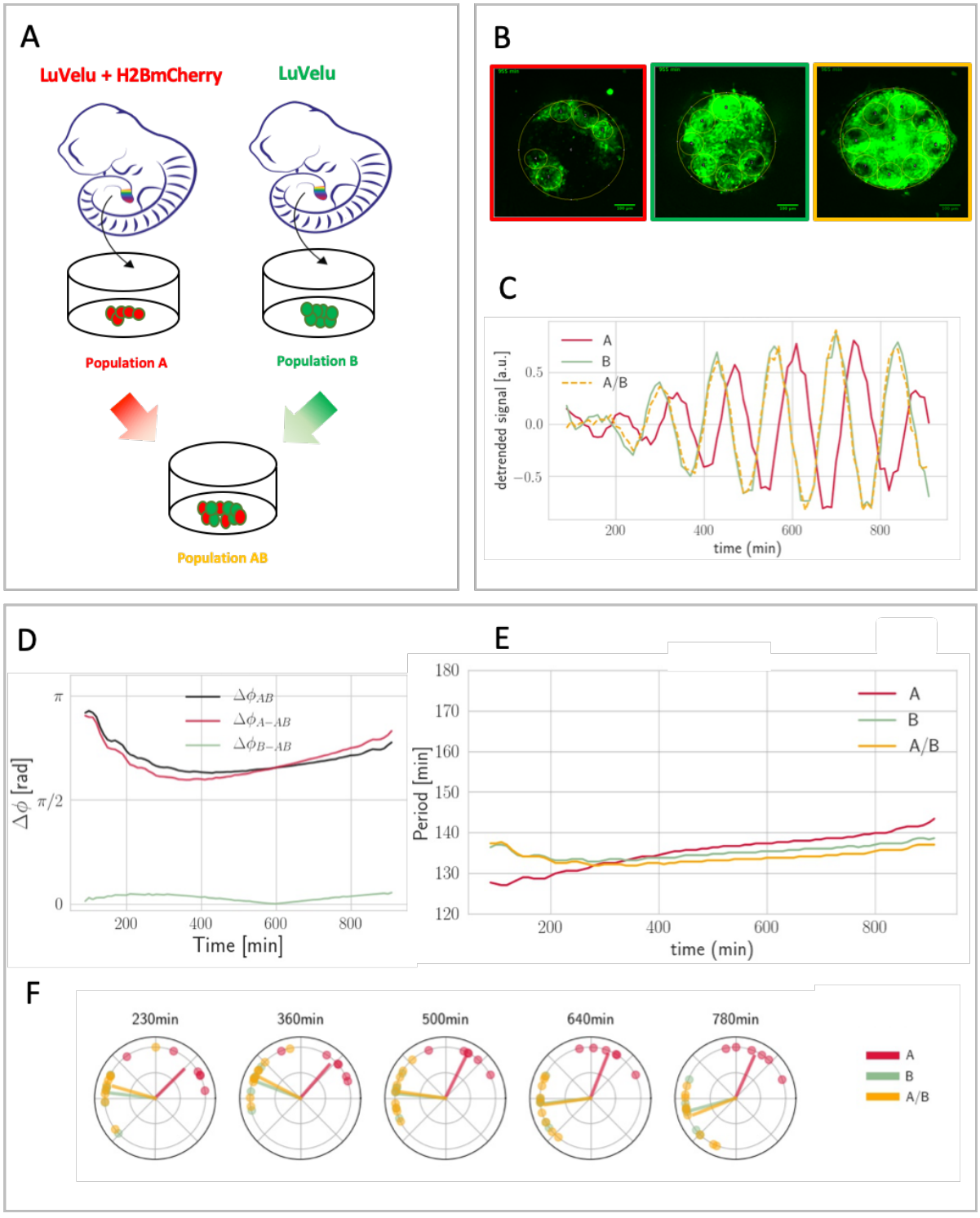

Figure 14 ***Testing experimentally the collective phase (N=17/24).*** *(A) Overview of the experimental design: We randomized two posterior PSM slices (tailbud) from different independent embryos. Afterwards, for cultivation, half of each cell population was mixed seeded and the other half as seeded separately serving as a reference. Then with each cell population, we performed real-time imaging to extract oscillations from the LuVelu fluorescence signal. (B) Snapshots taken at the end of the culture for each population; Red: cell population A; Green cell population B and Yellow: mixed population from A and B. (C) Time series: detrended signals of LuVelu intensity for each cell population. (D) Phase difference between each cell population. (E) Period quantification for each population over time. (F) Snapshots of representations of phase oscillators for each population at different time points.*

3. After mixing, “losing population” oscillates in phase with the “winning population”

In the previous experimental example, we have declared B population as winning population. Indeed, mix population “AB” display oscillations that resemble oscillations from pure population “B”, while pure “cells A” oscillate in a different phase than “pure cells B” (Figure 15A). This suggests that after mixing, “cells A” changed its original phase to synchronize in phase with B cells. To check this suggestion, we measured inside of the mix AB sample, oscillations of only “cells A”. To this end, we extracted LuVeLu signals that overlap with H2BmCherry signals (H2BmCherry is exclusively expressed in cells A). Then, we compared oscillations of “cells A” before and after the mixing with “cells B”. We found that inside the mix, “cells A” oscillates in different phase compared to the unmixed pure “cells A” (Figure 15B). We also compared oscillations from “cells A” in the mix and pure “cells B” and we found that they are synchronized in-phase (Figure 15C). Thus, after mixing “cells A” changed its original phase to synchronize in phase with “cells B”.

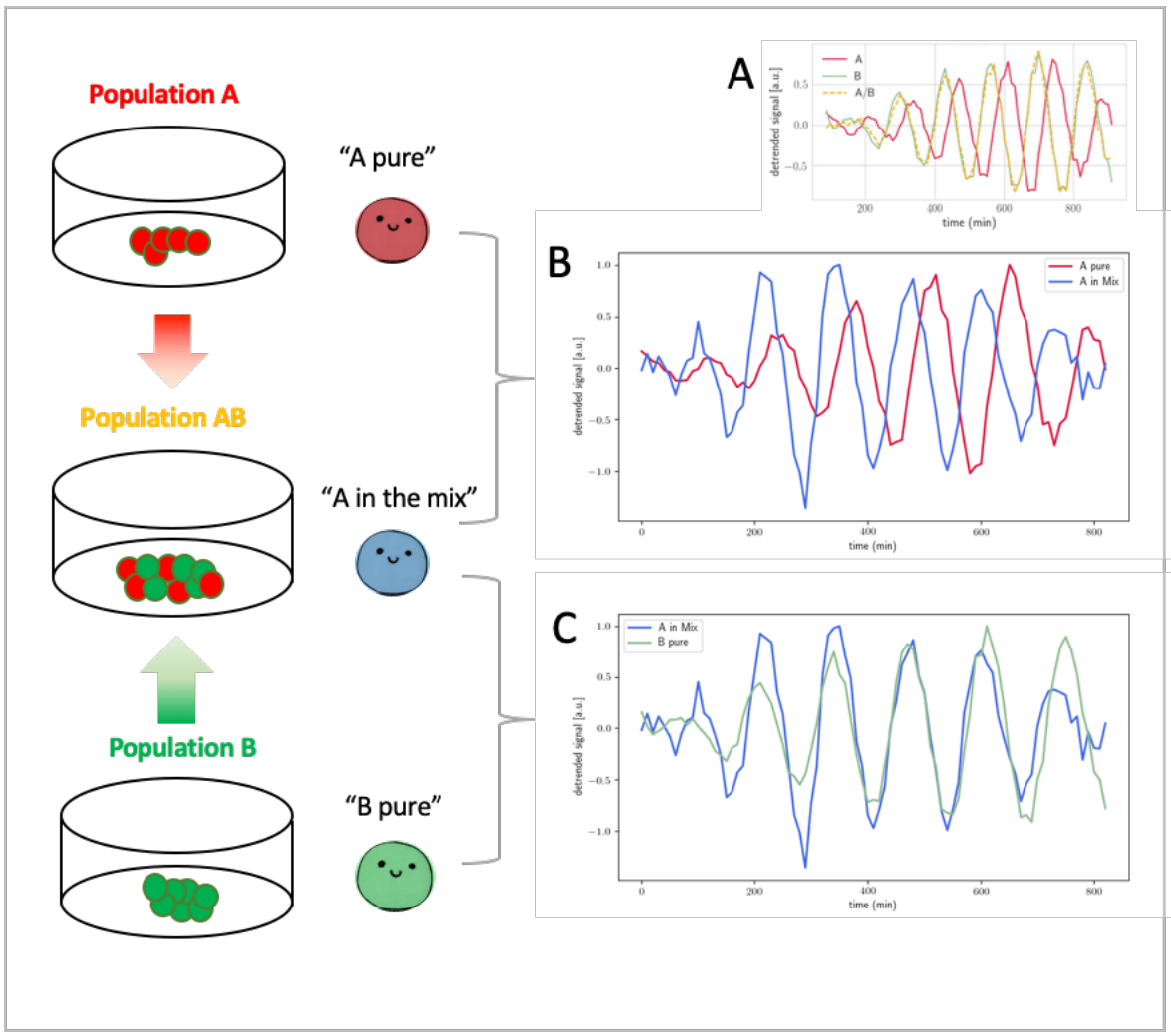

Figure 15 ***Measuring Notch signaling oscillations inside of the mix population (N=1).*** *(A) Time series: detrended signals of LuVelu intensity for each cell population (Figure14C). (B) Detrended signals for LuVelu intensity of pure cell A and cells A in the mix. (C) Detrended signals for LuVelu intensity of pure cell B and cells A in the mix.*

4. Hallmarks of the "winning population "

In most cases, 0 to 200min of imaging is the time when cells are recovering from the mechanical stress induced by cell dissociation. Not many oscillations can be extracted during this time since the signal is usually noisy. After 200min, first collective robust oscillations can be observed and measured. After 500min, PSM cells start to make waves and re-establish the frequency gradient within each ePSM. This might introduce some variations for phase and period calculation. Therefore, to determine the winning population, the optimal temporal windows is often situated between 200min to 500min of culture. Experimentally, the winning population can be characterised by three quantitative criteria:

- **Analysis of time series**: winning population oscillate in phase with mixed population AB. Their time series are overlapped.

- **Analysis of Frequency/period**: the frequency/period of winning population and mixed population are very similar.

- **Phase difference:** winning population and mixed population are synchronized in phase, so their phase difference is close to 0.

Among 24 experiments performed in similar conditions, 17 out of 24 assays display a clear winner population: either A or B population (Table 1 and Table2, Supplementary data). This suggests that most of the time, the collective phase is not equal to the phase average of input oscillators. Thus, if two PSM cell populations (oscillating in different phases) are mixed, the mixed population will synchronize in phase to one of the original cell populations. Using a metaphor to illustrate this finding: if we mix a red drink and a blue drink, we will not get a purple drink, but either blue or red.

Which initial population (A or B) determine the collective phase and frequency ?		
Date of the experiment	**Collective Phase (Phase A or B)**	**Collective Frequency (Frequency A or B)**
170720	Phase B	Frequency averaging A is slower than B (2min difference)
170731	Phase A	Frequency A A is slower than B (5min difference)
170802	Synchronous	Synchronous
170808	Phase B	Frequency B B is faster than A (10min difference)
170810	Phase A	Frequency A A is faster than B (5min difference)
170815II	Phase B	Same frequency for A and B
170824	Phase B (then drift)	Frequency averaging A is slower than B (10min difference)
180501	Phase B (then drift)	Frequency B (then drift)
180503I	Phase B (then drift)	Frequency B (then drift)
180503II	Phase A (very noisy)	Frequency A A is faster than B (5min difference)
180514	Phase A	Frequency A A is faster than B (5min difference)
180606	Synchronous	Synchronous
190408	Phase B	Frequency averaging
190814	Phase B	Frequency B (then drift)

Table 1: Summary of AB experiment results

5. Winner population can win twice

To check whether a same input population can win twice, we performed similar AB experiment but this time, we generated a second mixed population AB. We called it "AB prime". As previous experiment showed, while cell populations A and B oscillated with

distinct phases, the mixed population showed a phase profile similar to one of the two populations, here population B. Moreover, “AB prime” population also shows a similar profile to population B. This result suggests that the winner population can win twice (Figure 16).

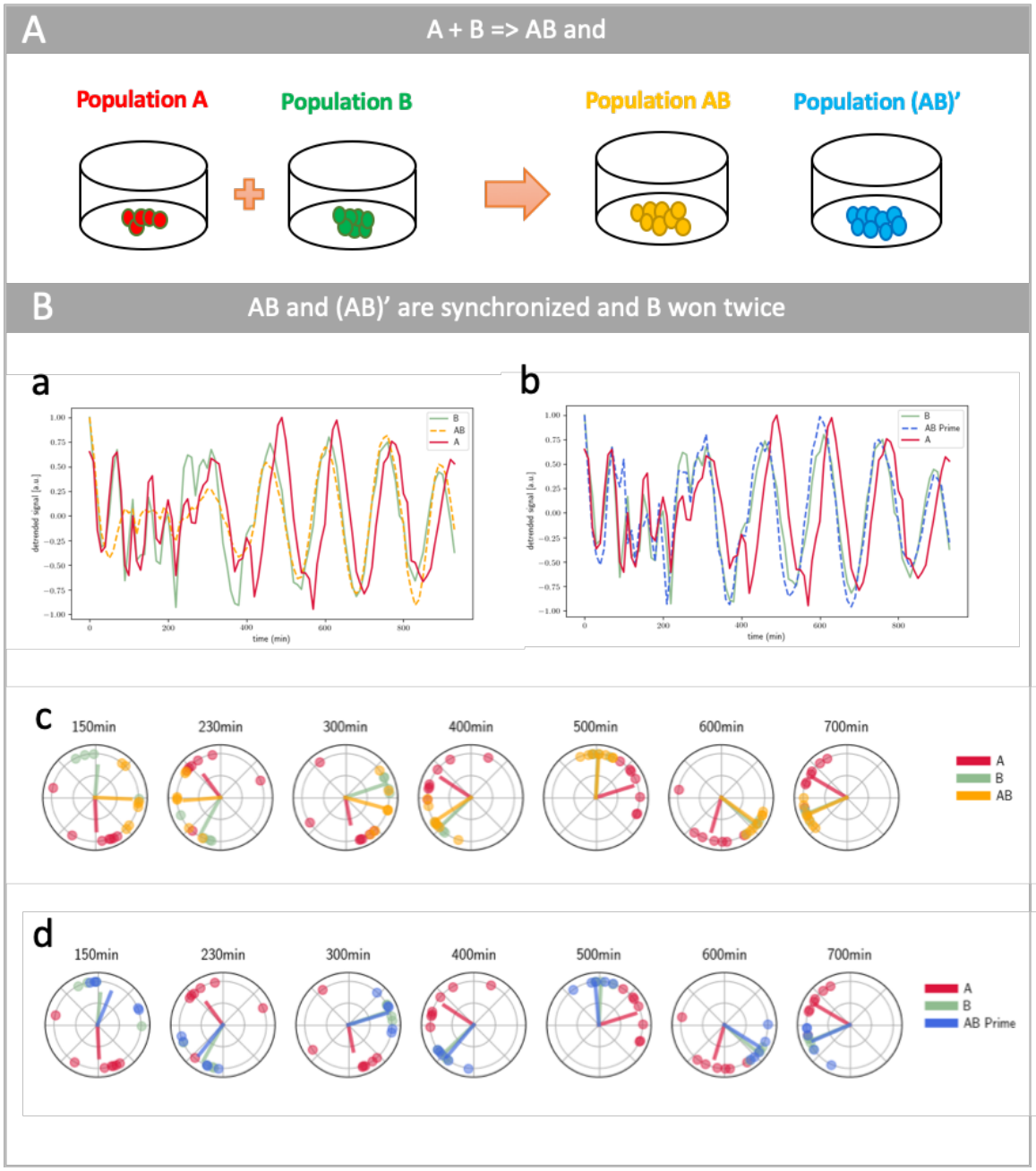

Figure 16 ***Double “AB experiment” (N=1)*** *(A)Overview of the experimental design: We randomized two posterior PSM slices (tailbud) from different independent embryos. Afterwards, for cultivation, half of each cell population was mixed and seeded and the other half as seeded separately serving as a reference A, B and AB (mixed population). A second, AB population is generated, we called it “AB prime”. (B) Then with each cell population, we performed real-time imaging to extract oscillations from the LuVelu fluorescence signal. (Ba-b) Detrended signal of LuVeLu intensity for each cell population. (B c-d) Snapshots of representation of phase oscillators for each population at different times.*

6. "Minority can win"

Importantly, in the phase difference coupling model, the phase average is sensitive to input ratios. Numerical simulations show that the unequal input of cells can drastically influence the phase averaging. Indeed, if Population A represents 90% of the cells in the mixture AB, the phase average of mixture AB is close to the Phase A. In other terms, the model predicts that the phase average must be close to the phase of the cells present in the majority (Numerical data not shown). We wanted to test this prediction. Since only population A carries the H2B-mCherry marker, we used FACS to calculate the ratio between Cells A and Cells B in the mixed population. In this experiment (Figure 17Ba), FACS analysis revealed that the mixed AB consisted of 20% of A cells and 80% of B cells. By checking the oscillatory phase of each population, A, B and AB (Figure 17Bb-e), we observed that the mixture AB phase matches with the phase A. To confirm it, calculation of the phase difference between A and AB population is close to 0 (Figure 17Bc). Similarly, mixed population AB and population A share the same period (Figure 17Bd). So, population A can dictate the collective phase and frequency in the mixed population even though they are in minority. This result suggests that collective phase determination is not dependent on the ratio of input populations.

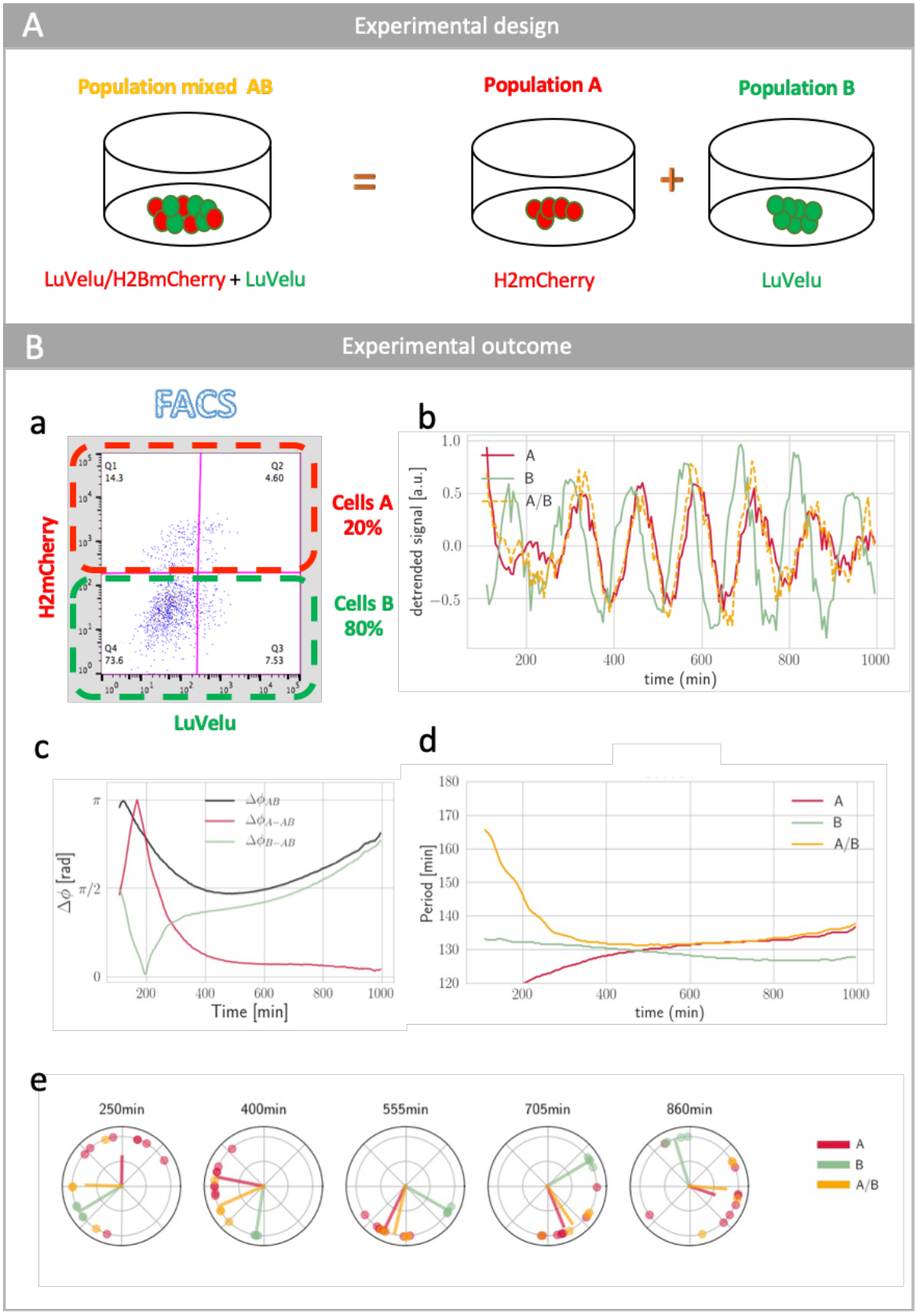

Figure 17 ***Testing the influence of the initial population ratio on the collective phase (N=4)*** *(A) Scheme of three independent randomization assays. (Ba) FACS results showing the ratio of two input cell populations A and B in the mixed population AB. (Bb) Detrended signals for each cell population. (Bc) Phase difference between each cell population: A-B (black) A-AB (green) and B-AB (red). (Bd) Period quantification of each population over time. (Be). Snapshots of representation of phase oscillators for each population at different time points.*

We performed 10 similar experimental assays where we counted cells in the mixed population AB. By 3 times, both populations are already synchronous. One case, the majority wins with 52% of cells in the mixture. Four times, the winning population was in minority: 20%, 30%, 33% and 44%. Finally, we recorded two cases where collective phase is equal to the phase average of input populations.

Which initial population (A or B) determine the collective phase and frequency ?		
Date	**Collective Phase With winning ratio**	**Collective frequency**
180328	Phase B (44%) Phase A and B very close	Frequency B B is slower than A (5min difference)
180425_2	Phase A (51%) Phase A and B very close	Frequency A A faster than B 10min difference
180425_1	Phase averaging	Frequency averaging
180510	Synchronous	Synchronous
180514	Phase A (20%)	Frequency A
180527	Synchronous	Synchronous
180620	Phase A (33%)	Similar Frequency A and B
180628	Phase averaging	Frequency averaging
180701	Phase A (30%)	Frequency A A slower than B (10min difference)
180707	Synchronous	Synchronous

Table 2: ***Summary of AB experiment results including initial ratio of input populations.***

7. “Phase averaging” scenario

Among 24 experimental assays performed, we recorded only 2 rare experimental cases where the collective phase is equal to phase average of input populations. (Figure 18 Table1, Table2). In this rare example, both populations display a different average frequency (Figure 18). Indeed, Frequency A is close to 142min while frequency B is around 150min. The frequency difference between them is approximately about 8 min. Interestingly, the mixed population AB shows a frequency which is the average frequency from both input population A and B (Figure 18). This result matches with theoretical predictions made in the phase difference coupling model framework.

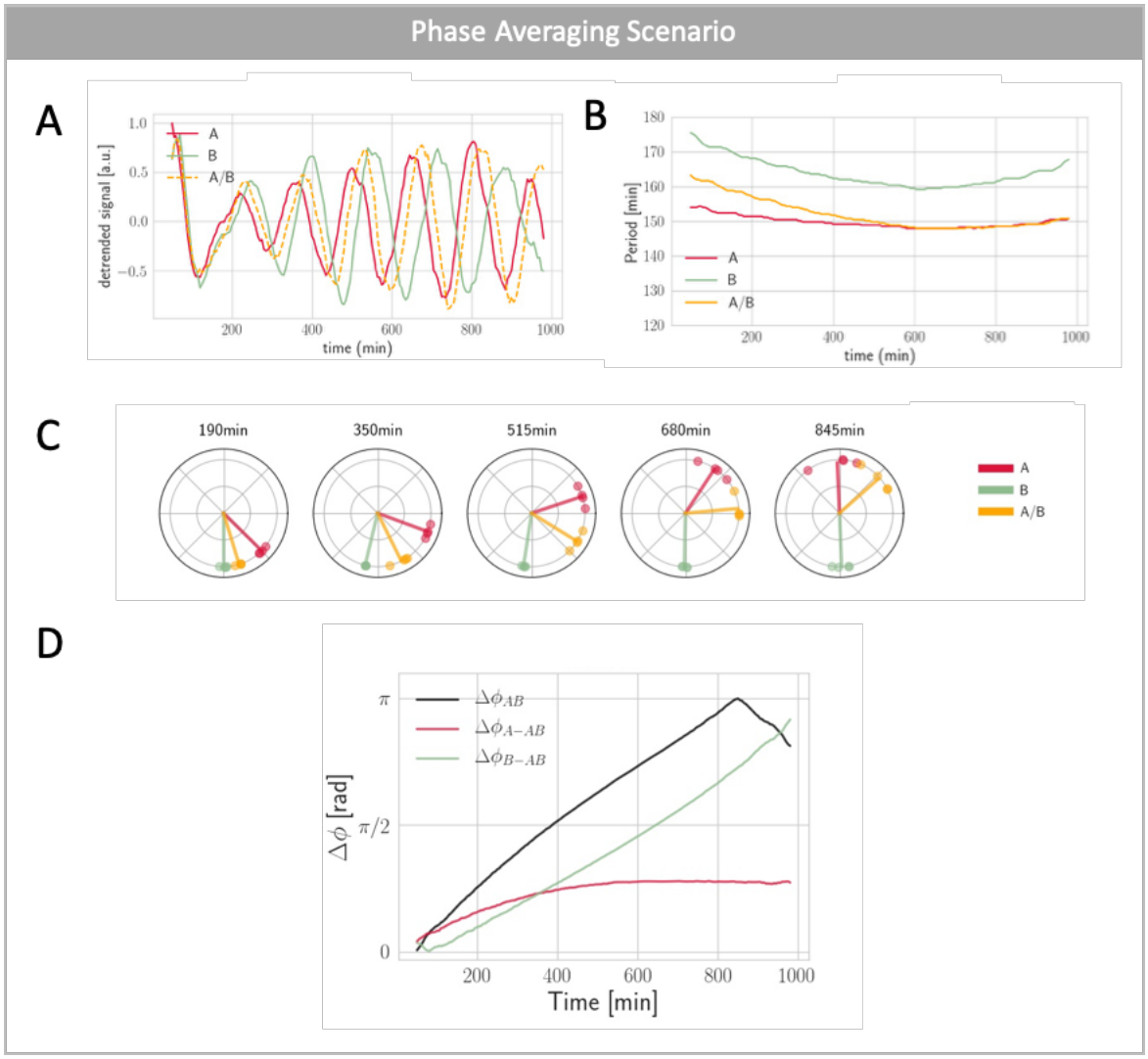

Figure 18 ***Example of phase averaging outcome(N=2/24).*** *(A) Time series: detrended signals of LuVelu intensity for each cell population. (B) Period quantification over time for each cell population. (C) Representation of phase oscillators*

for each population over time. (D) Phase difference between A-B (black) A-AB (green) and B-AB (red) populations.

8. "A and B population are initially synchronous" scenario

We also noted 4 remarkable examples where A and B populations were synchronous since the onset of the assay. In this particular configuration, phase A and phase B are identical as shown in (Figure 19). Similarly, both populations have the same frequency (Figure 19). Therefore, we can't declare any winning population which determine the collective phase and frequency.

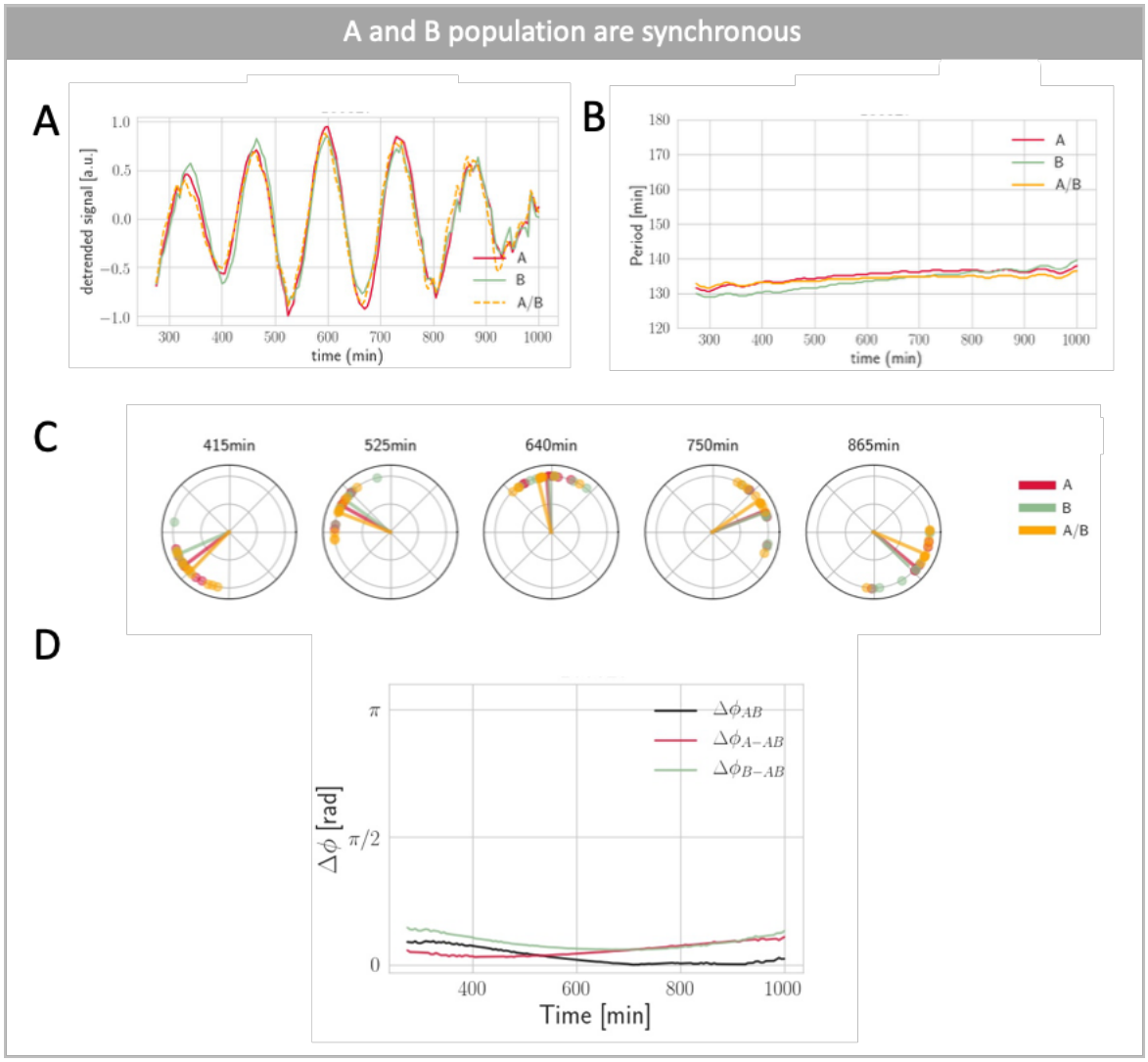

Figure 19 ***Example where both populations are synchronous (N=4).*** *(A) Time series: detrended signals for LuVelu intensity for each cell population. (B) Period quantification of each population over time. (C) Snapshots of representation of phase oscillators for each population at different time point (D) Phase differences between A-B (black) A-AB (green) and B-AB (red) population.*

In summary, we showed:

- **In the large majority of cases, the collective phase matches with the phase of one input population.**
- **This winning population is not dependent on its initial population ratio.**
- **The winning population can win twice.**

Part III: Comparing theoretical predictions and experimental outcome

Presented by Kuramoto, phase difference coupling model makes clear predictions regarding the collective phase and frequency:

- **Phase averaging**: Numerical simulations suggest that the collective phase is equal to the average of input.

- **Frequency averaging**: in the phase difference coupling framework, frequencies of two coupled oscillators reach the average.

- **Input Number**: unequal input of cells can drastically influence the phase averaging. The model predicts that the phase average must be close to the phase of the cells present in majority.

However, Figure 20, A, C compare theoretical and experimental collective phase and more importantly, Figure 20 B D show theoretical and experimental phase difference. Overall results are plotted in Figure 20E. Clearly, there is a mismatch between theoretical predictions made in Kuramoto model and our experimental findings.

In summary (1) Most of the cases, the collective phase and frequency match the phase and frequency of one input population, (2) The phase determination is independent of the ratio of input cells. Because of (1) and (2), **phase difference coupling model is experimentally falsified and thus, has failed to explain synchronization occurring in PSM tissue.**

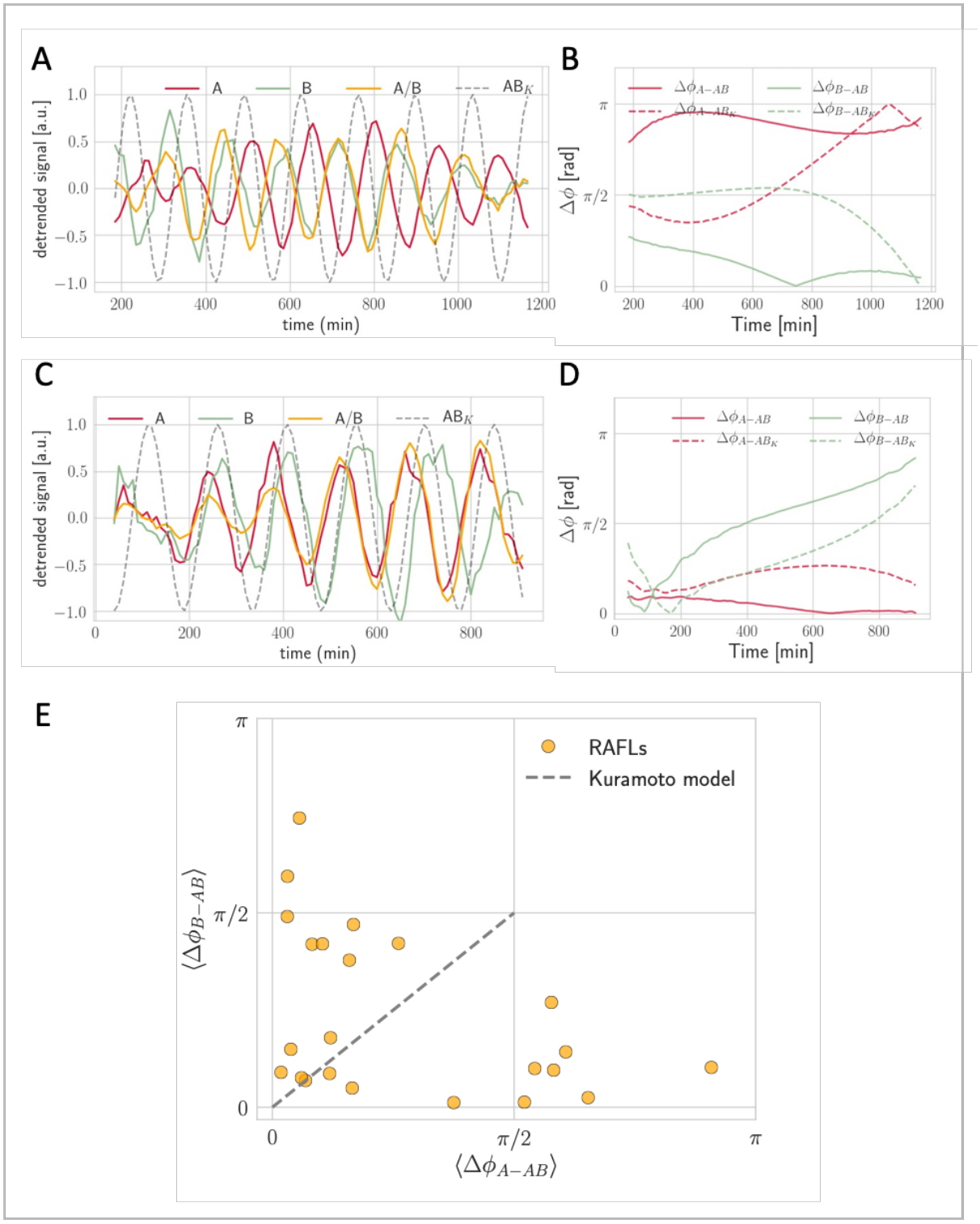

Figure 20 ***Comparison between theoretical predictions and experiment outcomes. N=24.*** *(A-C) Time series: detrended signals for each cell population. Dash line represents theoretical phase averaging according to Kuramoto's model (ABk). (B-D) Phase differences between cell population. Dash lines represent the theoretical phase difference between cells. (E) Summary of phase differences of each experiment. Theoretical prediction is drawn in dash line (Kuramoto model).*

Chapter IV: Discussion

Part I: Falsification of Kuramoto model and alternative model suggestion

Segmentation of the vertebrate body axis in space and time is linked to coordinated genetic oscillations. .From numerous perturbation studies it is well known that the Notch signalling pathway is involved in synchronizing the oscillations on a tissue level(Delaune et al., 2012; Horikawa et al., 2006; Jiang et al., 2000; Lewis, 2003; Riedel-Kruse et al., 2007). However, despite knowledge of the molecular machinery at work, the general rules of coupling remain elusive.

Theoretical approaches to explain the phenomenon of collective synchronization were pioneered by Arthur Winfree in 1967. Winfree used the scalar product of two different period functions, namely the phase-dependent influence function and the sensitivity function. Unfortunately, the product of coupling functions constituted a major obstacle for mathematical analysis. Later on, Yoshiki Kuramoto was working on the phase transition in magnetic spins. In this research field, the coupling function is given by sinusoidal functions and the phase difference. Kuramoto was interested in using Winfree's work to explain the collective synchronization phenomenon. His main motivation was to overcome the mathematical analysis problem and thus to find a solvable theoretical model. Kuramoto simplified Winfree ‘s model and provided a new analytic framework to theorize the phase dynamics of coupled oscillators. In his model, the interaction between oscillators is captured by a phase coupling function and the phase difference is the main feature driving continuous and mutual synchronization between oscillators(Kuramoto, 1984). For this reason, this model is termed “phase difference coupling model”. This model makes clear predictions regarding the collective phase and collective frequency, which represent averages of input oscillators. Most theoretical studies in the segmentation clock field are based on this model (Morelli et al., 2009; Murray et al., 2013; Okubo et al., 2012; Shimojo et al., 2016). However, it is unclear whether the assumption of a continuous and mutual synchronization driven mechanism described above is valid from molecular point of view.

On one hand, Notch and Delta proteins are dynamically expressed (Bone et al., 2014)and on the other hand, the Kuramoto model uses an abstract approach replacing

molecular dynamics with phase dynamics. For instance, if Notch-Delta proteins are present at a low level (or high level), how can we be sure that phases (used in the Kuramoto model) are reflecting in vivo protein levels? Does “trough” in phase mean “zero” in terms of protein level? While Kuramoto model assumes equal phases (to drive continuous and mutual synchronization), the correspondence might not be so straightforward from biochemistry point of view, since protein levels can be discontinuous and inequality expressed over time. Because of this mismatch, the use of Kuramoto model to describe synchronization in PSM tissue remains questionable.

The goal of this thesis is to reveal the fundamental rules of synchronization and to experimentally challenge the Kuramoto model. To this end, we developed a novel experimental strategy to quantitatively test model predictions of phase synchronization in embryonic PSM cells. We find that the experimental results don’t match with Kuramoto model predictions. This leads us to falsify the Kuramoto model and show that this model fails to explain synchronization in PSM tissue, using in vitro assays. We hence have to consider other alternative theoretical models, such as Winfree’s pulse-coupled models, and discuss whether these are in agreement with features observed experimentally.

1. Pulse Coupling models applied in somitogenesis

Based on numerous perturbations studies in segmentation clock field (Delaune et al., 2012; Horikawa et al., 2006; Jiang et al., 2000; Lewis, 2003; Riedel-Kruse et al., 2007). synchronization between PSM cells is supported by Notch and Delta-ligand interactions. Indeed, in our biological system, we can assimilate the Notch Receptor "the Receiver" and Delta, the "Sender of the signal".

Interestingly, Kuramoto model consists of model Notch Delta protein dynamics into phase dynamics. Moreover, it has been shown that Delta ligand levels oscillate (Bone et al., 2014)and hence it is possible that the signal is sent only in a specific part of the Notch oscillation cycle. This suggests that phase are not equivalents and therefore synchronization doesn't occur in a continuous fashion as assumed in the Kuramoto model

As Kuramoto himself explained during the conference ("Dynamics of Coupled oscillators" in 2015), Winfree's model is probably more realistic and natural to picture the dynamics of biological coupled oscillators. Indeed, in 1967 (before Kuramoto), Arthur Winfree used two complex functions to mathematically approach the collective synchronization phenomenon. He introduced the pulse coupling model in which each oscillator exerts a phase-dependent influence on all the other, the corresponding response of oscillator depends on its phase. Unlike others in the Kuramoto model, in pulse-coupled models, synchronization is triggered by a specific signal which occurs only in a particular part of the cycle (which is independent of the phase difference) (Goel and Ermentrout, 2002). The synchronization is therefore discontinuous and depends on two important factors (Figure 21Aa):

(1) Factor "S" for "Stimulus" corresponds to a signal, a kick or pulse that hits the system to force the synchronization.

(2) Factor "R" for "Response" refers to the "Phase response". Indeed, some phases can be more sensitive or responsive to perturbations. In other terms, synchronization always occurs in phase dependent-manner".

In Figure 21Ab, let's say a stimulus is sent at 3 o'clock". Green oscillator is kicked to synchronize. In our biological system, Delta plays the role of the "Stimulus" and Notch signalling is the "Response". Thus, from this biochemical point of view, discontinuous coupling models, such as pulse coupling models, might appear more realistic in our biological system. Moreover, in the framework of pulse coupling models, Winfree described two sub-classes of pulse coupling models: **weak pulse coupling** and **strong pulse coupling models**. Numerical simulations done by Gregor Mönke revealed different predictions according to the coupling strength:

- **Weak pulse coupling models**

Upon weak pulse coupling, the collective phase is equal to phase average of the input oscillators. This prediction is similar to what would be predicted by phase difference coupling models (Figure 21) (as described in the introduction) (Goel and Ermentrout, 2002).

- **Strong pulse coupling models**

Interestingly, a different outcome is seen upon strong pulse coupling: the collective phase is determined by one of the input phases (Figure 22Be). Figure 22A shows two pulse-coupled oscillators displaying different phases. The yellow line shows the theoretical collective phase after the pulse coupling. As shown in Figure 22B after the pulse, synchronization between two pulse-coupled oscillators occurs very rapidly. More interestingly, Figure 22C shows a fast acceleration of oscillators when it reaches the pulse. Subsequently, phase difference is reaching 0 overtime in a discontinuous manner.

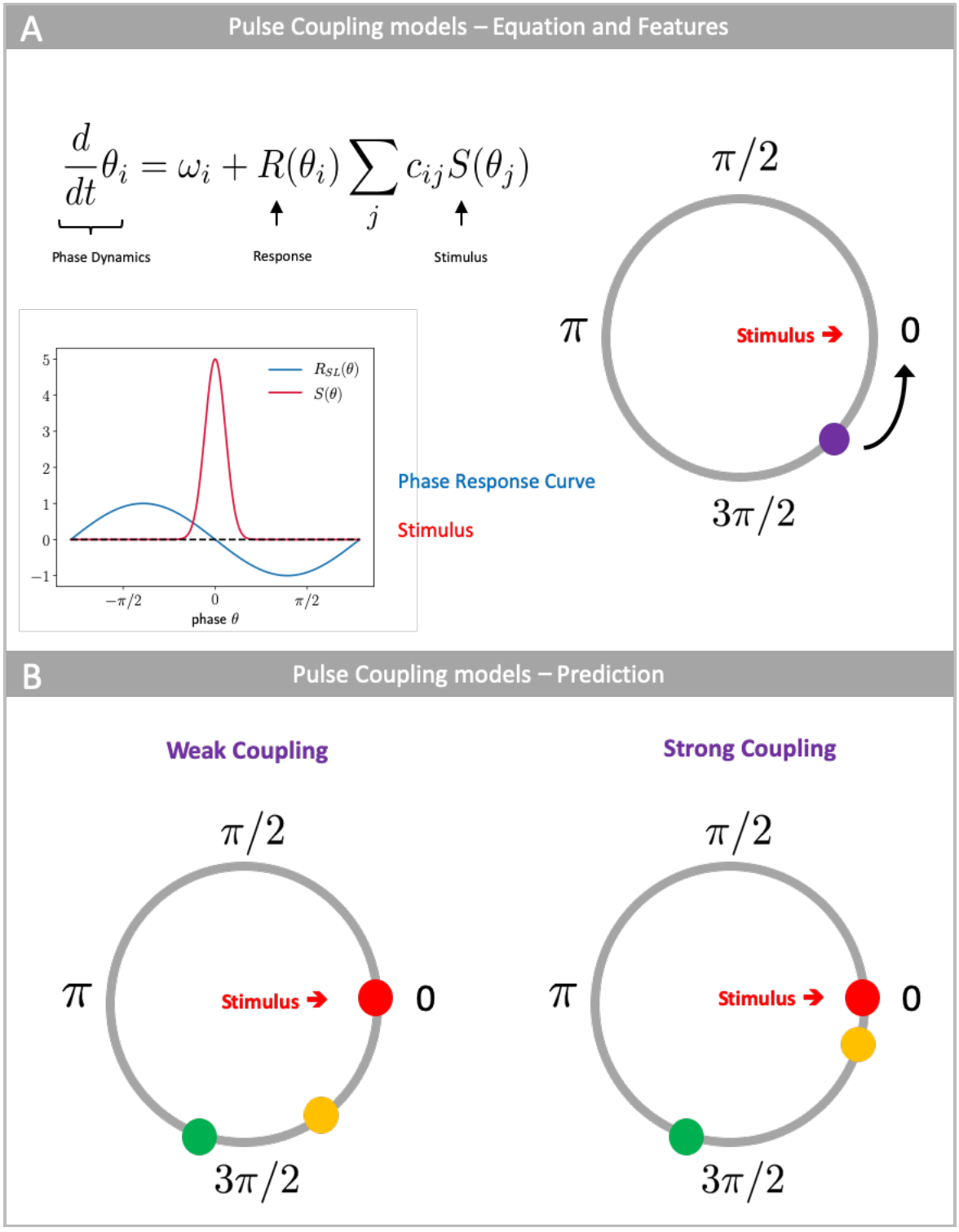

Figure 21 ***(A) Pulse Coupling Models, equation and features.*** *(Aa) General equation and coupling functions of phase dynamics. (Ab) Scheme representing two oscillators at different phase on a polar plane. When a stimulus hit "3 o'clock", the purple oscillator is pushed toward 3 "o'clock". This is the mechanism that drives the synchronization. (Ac) This model depends on the Phase response (R) and the Stimulus (S).* ***(B) Pulse coupling model and collective phase predictions.*** *(Bb)Weakly coupled oscillators achieve phase averaging whereas (Be) strongly coupled oscillators determine their collective phase according to one input populations.*

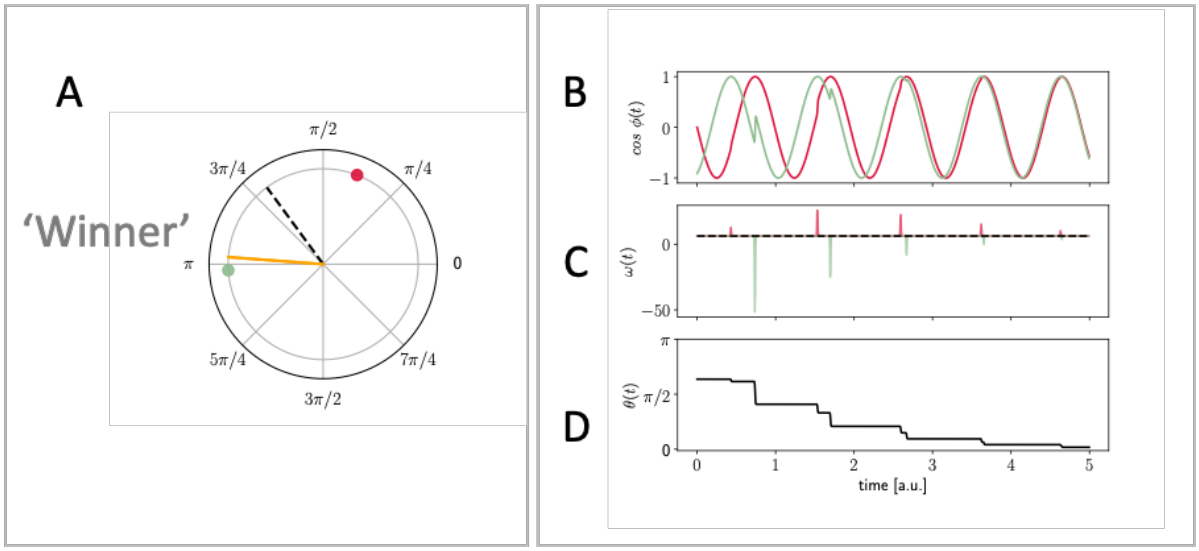

Figure 22 ***Numerical simulations showing synchronization for pulse-coupled oscillators.*** *(A) Red and Green are strongly pulse-coupled oscillators and oscillate at different phase. Dash line shows collective phase when oscillators are weakly coupled. Yellow line shows collective phase when oscillators are strongly coupled. (B) Virtual time series for two strongly coupled oscillators (C) Frequencies and (D) Phase Difference between two strongly coupled oscillators.*

In brief, strong pulse coupling models make the following predictions:

(1) No phase averaging: collective phase resembles one input phase

(2) Pulse-dependent: to trigger the phase synchronization, the system needs a "kick".

(3) Synchronization is not dependent on the ratio of input cells: i.e the minority of oscillators can dictate the collective phase

Interestingly, given (1) (2) and (3), our experimental results appear to be in agreement with these predictions. Therefore, unlike previous studies (Morelli et al., 2009; Murray et al., 2013; Okubo et al., 2012; Shimojo et al., 2016), we experimentally falsify Kuramoto model and its predictions in embryonic PSM. We present evidence arguing for pulse coupling models developed by Arthur Winfree in 1967. Indeed, this model can recapitulate features observed experimentally, more in agreement with Notch/Delta interaction dynamics. While so far, we have only indirect experimental evidence supporting a pulse-coupling model, this theoretical framework makes clear predictions that stimulate future experiments. The next session will present the scope for testing pulse coupling models in the context of somitogenesis.

Part II: Strategies to reveal evidence supporting pulse coupling models

1. Modulating the coupling strength

Coupling strength can be defined as a constant describing the "interaction forces between coupled oscillators". Little is known about what coupling strength means in biology. Various parameters in biology might play a role in coupling strength, such as affinity between Notch receptor and its ligand Delta, or adhesive junctions between PSM cells (Shaya et al., 2017). In the pulse coupling model framework, Kuramoto model made clear predictions regarding the collective phase. The collective phase is determined by the coupling strength. Indeed, if oscillators are weakly coupled, then the collective phase is determined by averaging the two input oscillators. If oscillators are strongly coupled, then the collective phase is determined by "the phase-winner" oscillator. Our experimental findings are in agreement with the strong pulse coupling. If pulse coupling is the correct model, so modulation of coupling strength in randomized cells PSM should change the collective phase outcome (as the theory predicts). For instance, decreasing the coupling strength between cells in our assays, should lead to collective phase averaging. To this end, we imagine randomization assays combined with different experimental strategies:

- A titration of DAPT (Notch signalling inhibitor) to decrease chemically the coupling strength in dose dependent fashion.

- Similarly, we can titrate N-cadherin antibodies to prevent intercellular contacts and thus decrease the coupling strength.

- A use of mouse mutant of Notch receptor to disrupt genetically the interaction between Notch receptor and Delta ligand.

2. Measuring single cell oscillations in multicellular context

One way to test the pulse coupling is to identify the "pulse" and when it occurs during Notch signalling oscillation cycles. To do so, we want to use single-cell approach to observe a sudden phase change to reach a collective phase triggered by the pulse (similarly to what numerical simulations Figure 22). To this end, we established single-cell tracking and quantification of signalling oscillations. We performed randomization assays associated with a mosaic cell labelling. Indeed, in addition to the LuVeLu marker, we incorporated a low number of cells that carry both H2BmCherry (a nuclear marker) and LuVelu markers. For analysis, we trained "Ilastik" software (Sommer et al., 2011) to segment cells expressing H2BmCherry marker.

After a successful segmentation, segmented cells were tracked over time. Then, we extracted signals from LuVelu channel to run the phase extraction pipeline. We found that single cells can oscillate robustly and display frequencies than can vary between 130 to 150 min. Interestingly, cells situated at the periphery of ePSM show a decreasing frequency over time (Figure 22 A, B, E). The next step will be to run single cell analysis on phase synchronization experiments and track "the looser population" of cells carrying H2BmCherry and LuVelu markers. We will then compare single-cell oscillations to the oscillations of the winning population that dictates the collective phase. We hope that in the near future, we will be able to experimentally visualize the pulse.

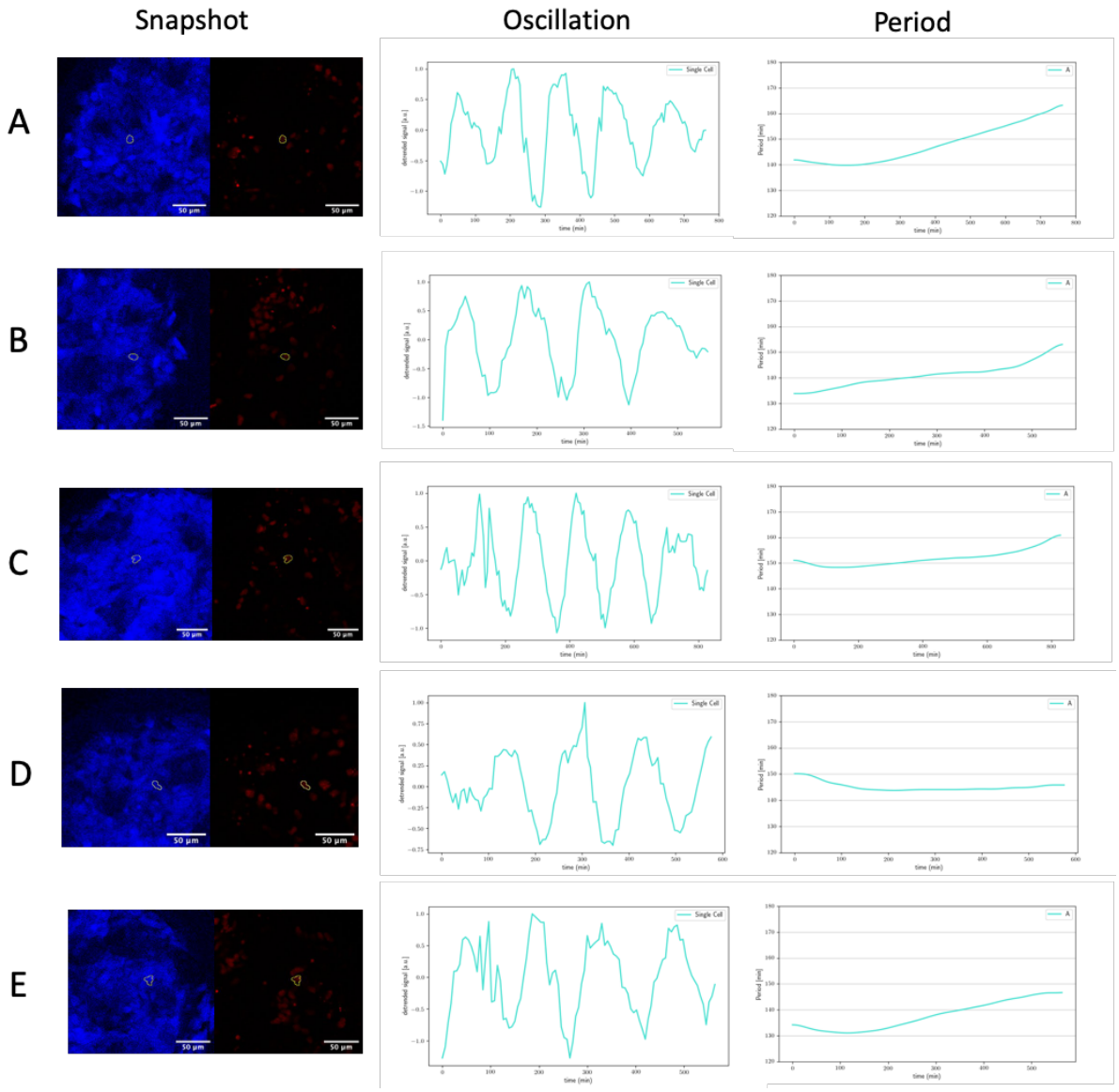

Figure 23 ***Single-cell oscillations and their respective period in randomization assays.*** *(Left panel) Snapshots of randomization assays after 300min of cell culture. LuVelu channel in blue and H2BmCherry channel in red. (Middle panel) detrend signals of LuVelu intensity for single cell oscillations (Right Panel) Temporal evolution of period for each associated single cell. Scale bar= 50um.*

3. "Selective AB" experiment

In the framework of a strong pulse coupling mechanism, initial phases of input population A and B have a predictive value for the collective phase determination. In this case, phase at the onset of the experiment would indicate in which part of the oscillation cycle a pulse occurs. Hence, our goal is to determine the initial phase of populations A and B prior to their randomization (Figure 24). Initial phases are accessible by quantifying the oscillations in tails before their dissociation.

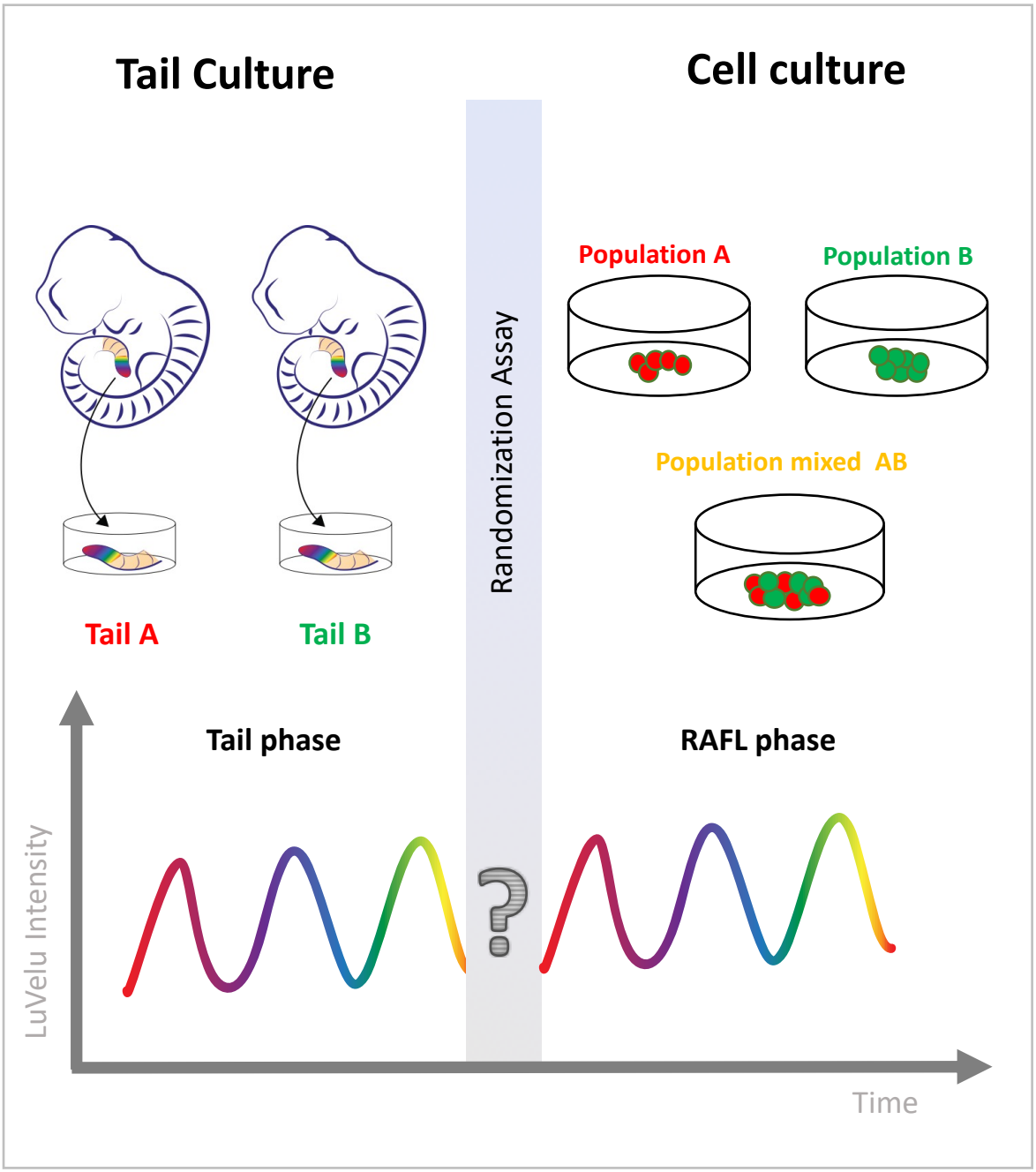

*Figure 24 "**Selective AB" experiment design.** Phases from tails will be extracted and compared to extracted phases from RAFL.*

To examine whether the initial phase is predictive to determine the collective phase, we quantified oscillations in tails A and B and compared them with their respective oscillations obtained after cell randomization. To this end, we first cultured and imaged tails A and B for 8 hours. After 8 hours of imaging, only the posterior part of tails A and B

were randomized and mixed. After this process, we obtained: population A, population B and the mixed population AB. We represented tail and RAFL oscillations as well as their respective period (blue line) Figure 25A-B. We used actual tails traces oscillating with a period of 139min and propagated them virtually (dash line). We then compared the phases obtained from tails (propagation) and RAFL. As shown in Figure 25A, when tails are dissociated during their ascending phase, randomized cells oscillate in anti-phase compared to the propagated tail oscillations. In contrast, when tails are dissociated during their descending phase Figure 25B, randomized cells oscillate in phase compared to the propagated tail oscillations. This observation suggests that dissociation can induce an important phase shift between initial and post-randomization phases. We did this experiment for 24 independent tails and drew a phase map showing initial phases in tails before and after cell dissociation. Phases were extracted at time points as indicated by red stars and black dots shown in Figure 25A and B. Unexpectedly, this phase mapping exhibits a (type 0) phase resetting (Gray and Chattipakorn, 2005). This indicates that the dissociation process per se might induce a strong shock in cells (Figure 24C). We are currently trying to understand how this can influence the outcome of the collective phase in the mixed population. This experiment reveals another layer of complexity of our biological systems.

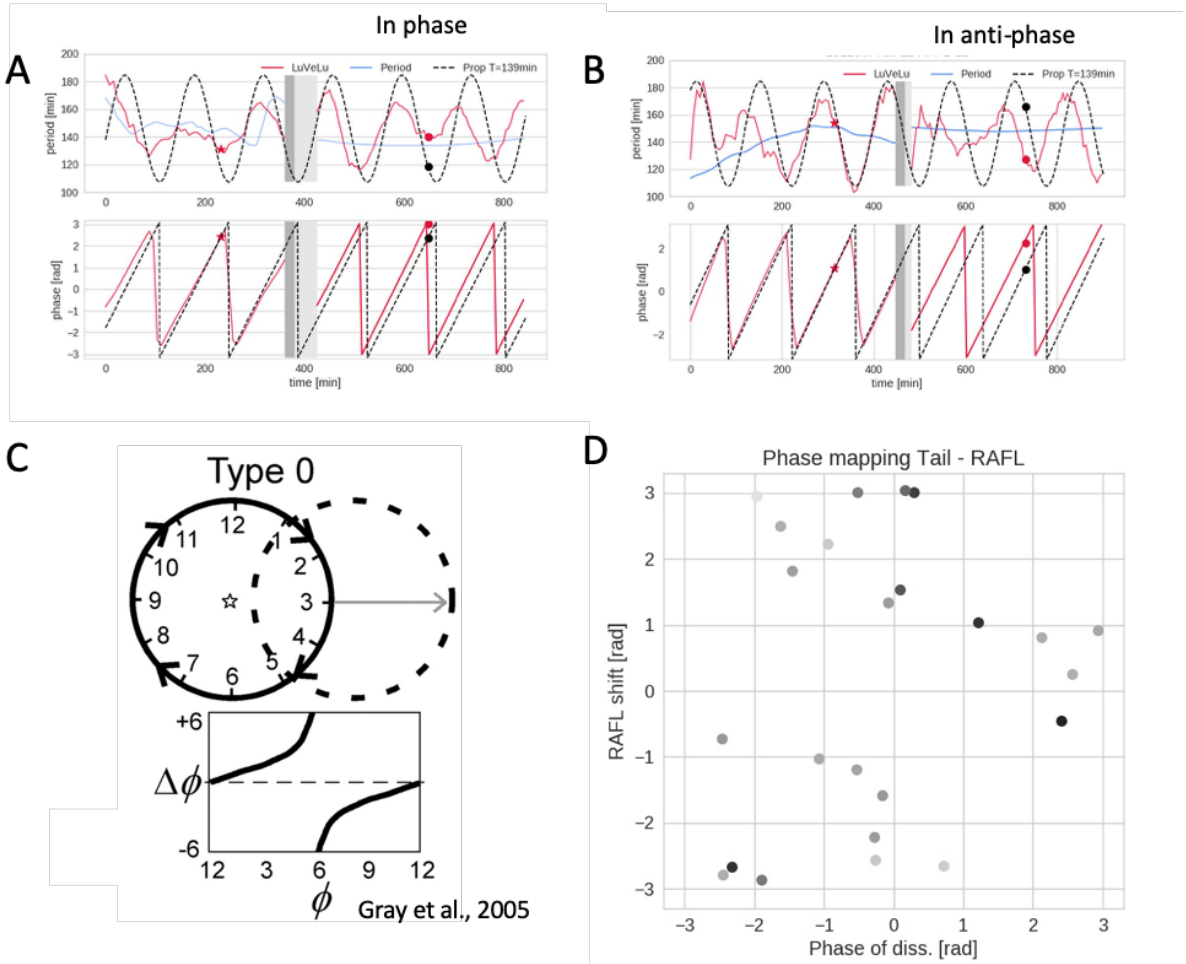

Figure 25 ***Results of Selective AB experiments*** *(N=24) (A)Tail Dissociation during their descending phase. (B) Tail Dissociation during their ascending phase. Red line shows actual LuVelu signals. Dash line shows propagated tail signals for 139min period. (C) Scheme for the "Type 0" phase resetting, showing how phase is shifted after the shock. (Gray et al., 2005). (D) Phase Response Curve (PRC), phase comparison between pre and post dissociation. X axis: Phase - tail before dissociation (phase of dissociation x axis in radian) and phase after randomization (RAFL – shift in rad).*

4. The "Wall Clock" experiment

As described by Winfree, pulse coupling model involves oscillators which exert a **phase-dependent influence** on all the others. The corresponding **response** of oscillator **depends on its phase**. Therefore, to apply the pulse coupling model in somitogenesis context, we need to characterize the impact of the dissociation on the phase.

To address this question, we designed an experiment that allows us to study the impact of cell dissociation of the phase. The idea was to compare two groups of cells: one in which cells are dissociated and one in which they are not. To do so, we pooled a group of 3 to 4 tailbuds. Those tailbuds were randomized and split into two dishes - "Alpha" and "Alpha

prime". As "Alpha" and "Alpha prime" groups were identical (they both came from the same pool of cells), they continued to oscillate independently in sync throughout the 10 hours of culture. The Alpha population was our reference group, or the "**Wall Clock**". After 10 hours of culture, only PSM cells from the "Alpha prime" group were dissociated for a second time and placed back in the culture for imaging. Meanwhile, PSM cells from the "Alpha" group were left intact in the incubator (as they are the reference clock). Using the phase extraction method, we compared oscillations between Alpha and Alpha prime cells (Figure 26A).

Preliminary results suggest that the phase at which cells are shuffled influences the outcome of randomization:

(1) If PSM cells are shuffled during their "Ascending phase" or the peak (n=2)

Randomized PSM cells oscillate in **anti-phase** compared to cells that did not get shuffled. The results show that randomization at ascending or peak phases or peak induces a phase- shift compared to the original phase.

(2) If PSM cells are shuffled during their "descending phase" or the trough (n=1)

Randomized PSM cells oscillate **in phase** compared to the control. It seems that descending and trough phases can be conserved after randomization. Although preliminary, these results are consistent with our findings from the "selective AB experiment" and strengthen the idea that initial phase prior to cell randomization affects the phase recorded after randomization.

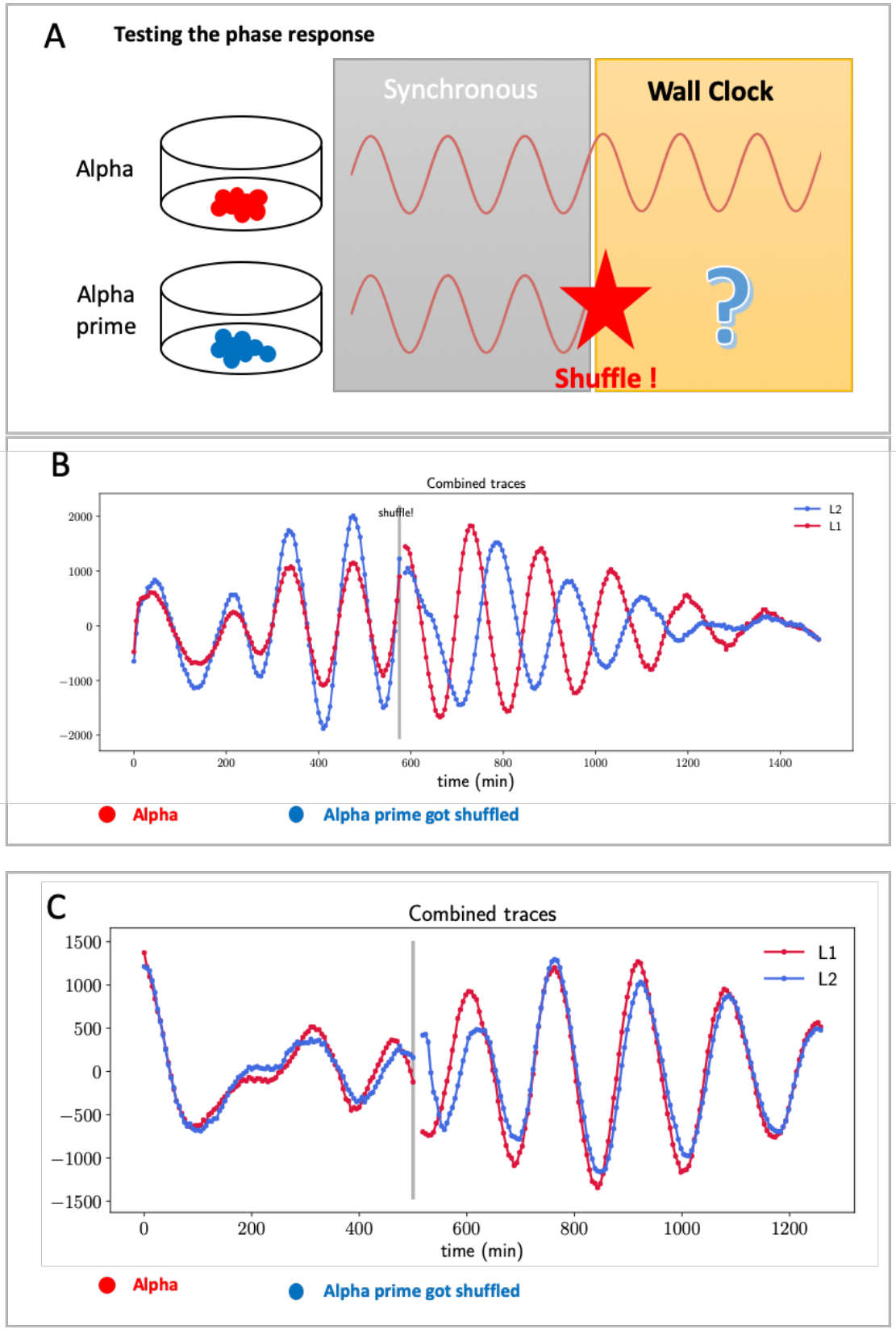

Figure 26 ***Principle of the Wall Clock experiment to test the phase response (N=3).*** *(A) Scheme depicting the design of the Wall Clock experiment. Alpha oscillating cells is a reference of the Alpha prime cells who got shuffled. (B-C) Detrended signals for LuVeLu intensity for each group of cells.*

Part III: From in vitro to in vivo, what do the results imply for PSM waves?

In the results part, we demonstrated how after randomization, PSM cells acquired their new collective phase. This is determined by the phase of one of the input oscillators whereas the Kuramoto model has predicted phase averaging. From these results, what can we infer about the collective oscillations seen in embryonic PSM tissue in vivo?

In vivo, we observe waves of Notch signalling activity sweeping from the posterior PSM to the anterior PSM. Similarly, after reaching their collective phase, randomized PSM cells start to form waves within ePSM from centre to periphery. In the embryonic PSM, the generation of waves can be explained by the (Notch signalling oscillation) frequency gradient from posterior to anterior axis (Lauschke et al., 2013). Similarly, within each ePSM (Notch signalling oscillation) a frequency gradient emerges from centre to periphery. How this frequency gradient is re-established remains unknown. However, to generate a frequency gradient and subsequent waves of Notch signalling activity, symmetry breaking must happen in the system.

One possible cause (or consequence) of this symmetry breaking is the existence of molecular gradient such as Wnt/β-catenin (Aulehla et al., 2008, 2003). Indeed, β-catenin molecular expression is graded from posterior to anterior in the embryonic PSM. Similarly, after randomization, a β-catenin protein gradient was found ranging from the centre to the periphery of each ePSM (Tsiairis and Aulehla, 2016). In order to address the role of this gradient in symmetry breaking, we used a gain of function approach. We used mutant embryos carrying the daBC gene, for dominant active β-catenin (Harada et al., 1999), which present an accumulation of the β-catenin protein throughout the PSM tissue (Aulehla et al., 2008). We randomized PSM cells which carry the daBC mutation and also positive for LuVelu. Surprisingly, preliminary results (data not shown) show that mutant cells fail to establish collective synchronization, suggesting that the β-catenin molecular gradient might play a role in synchronizing Notch signalling oscillations.

In the framework of pulse coupling models, the coupling strength plays an important role regarding the collective phase outcome. Indeed, if oscillators are strongly coupled, the

"winner takes it all" scenario happens. In contrast, if the oscillators are weakly coupled, the collective phase is predicted to the be close to the average of input cell phases. Using only the posterior PSM (tailbud) as cell input, we observe mainly the "winner takes it all" scenario. Based on the pulse coupling model, this indicated that posterior PSM is that posterior PSM is composed of oscillators which are strongly coupled. However, somitogenesis is a dynamic process where cell properties evolve over time along the anterior-posterior (AP) axis. This might suggest that coupling strength can be changed as well along the AP axis. This hypothesis can be supported by the existence of a gradient of N-cadherin-dependent adhesion molecules making the interface of the future somite boundary in the anterior PSM (Chal et al., 2015).

If this hypothesis is correct, this suggests that coupling strength is graded from posterior to anterior region. In brief, if the pulse coupling model is valid, posterior PSM cells are strongly coupled whereas anterior PSM cells are weakly coupled.

One important finding regarding the self-organization assay is that after cell randomization, the β-catenin protein gradient can be formed de novo from the centre to the periphery within each ePSM. Therefore, we wanted to investigate whether the Wnt signalling pathway can play a role in the formation of ePSM.

Previous members in the lab have studied (Lauschke et al., 2013; Sonnen et al., 2018) the activity of endogenous Wnt signalling in the 2D-segmentation assay context. To do so, a previous PhD student in the lab, Volker Lauschke, generated knock-in real-time reporter mouse lines for *Axin2*, a bona fide direct Wnt signalling target gene (Aulehla et al., 2008; Jho et al., 2002; Lustig et al., 2002). This was done by inserting sequences encoding a destabilized reporter, Venus-PEST into the endogenous Axin2 locus separated by a 2A-site (Szymczak et al., 2004).

In vivo fluorescence imaging of the Axin2-T2A-VenusPEST reporter mouse line, hereafter termed Axin2T2A, revealed gene activity oscillations within the PSM, with a period of 142.8 ± 14.4 SD min (Sonnen et al., 2018). Furthermore, *2D* segmentation assays

(Lauschke et al., 2013) Axin2T2A oscillations with a period comparable to *in vivo* oscillations.

To study Wnt signalling dynamics in RAFL, I used a novel reporter line developed by Nobuko-Tsuchida-Straeten, a research technician in our lab. Nobuko has generated a novel knockin real-time reporter mouse line for *Axin2:* Axin2 stop GSAGS Achilles.

Achilles is a new YFP (Yellow Fluorescence Protein) developed by Miyawaki Lab in RIKEN in Japan. They reported that Achilles protein is a brighter fluorophore than Venus. Achilles is a rapidly folding YFP variant which matures faster than Venus, giving a stronger signal when visualizing highly dynamic processes like somitogenesis (Diaz-Cuadros et al., 2018). Nobuko has characterized the Axin 2 stop GSAGS Achilles line and showed that it recapitulates the results found previously with the AxinT2A line in 2D segmentation assays. We then used the Axin2 stop GSAGS Achilles to check whether Wnt signalling can oscillate after cell randomization. So, we randomized a single whole PSM tissue from the Axin2 stop GSAGS Achilles line. We saw distinct "onion ring" patterns corresponding to regions where ePSMs form. The fluorescence signal was very bright at the periphery and darker at the centre within each ePSM. (Figure 27) Moreover, we detected synchronized Wnt signalling oscillations after 8 hours of cell culture. However, the amplitude was lower and noisier than that of Notch signalling oscillations. (Figure 27).

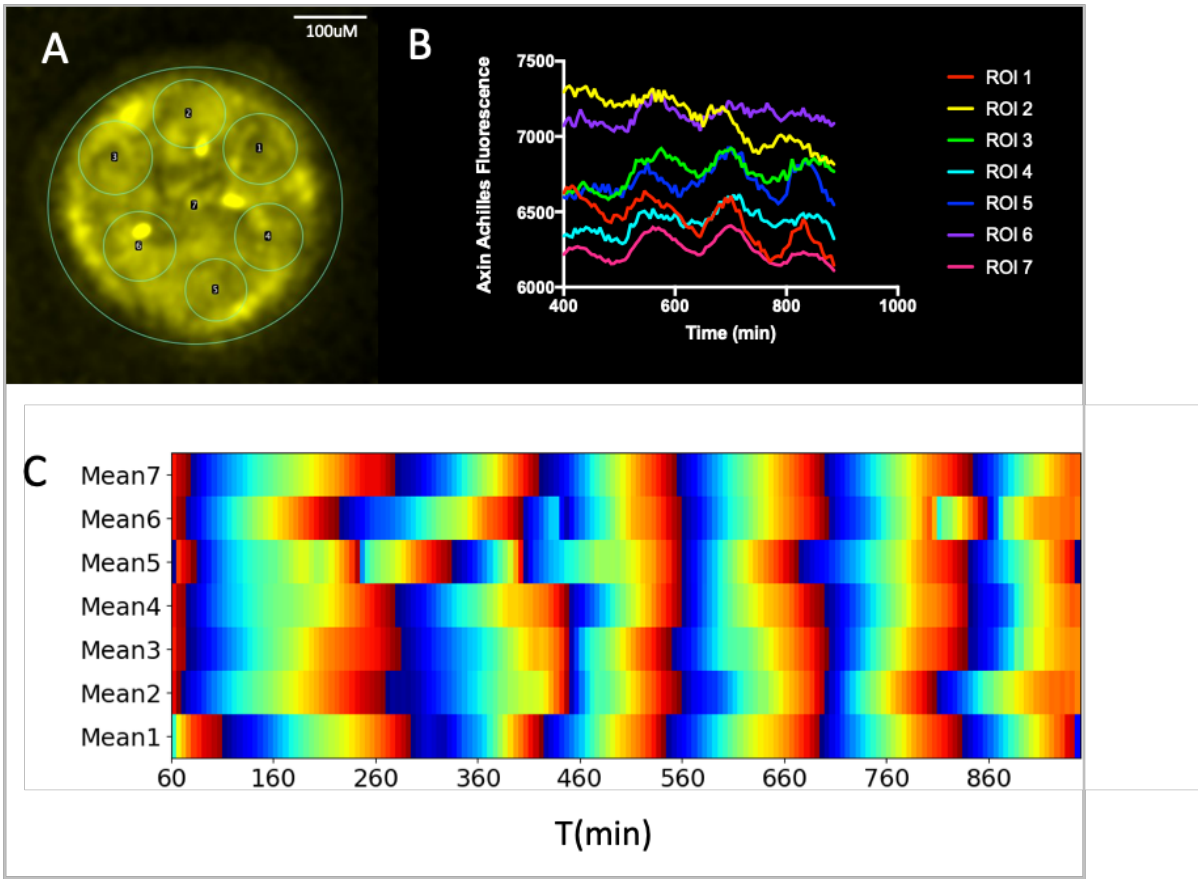

Figure 27 ***Real-time visualization of Wnt signaling oscillations in self-organization assay using single PSM tissue****. (A) Snapshot taken at the end of the culture using Axin 2 stop GSAGS Achilles (B) Quantification of Axin 2 Achilles signals from randomized over time. (C) Oscillation phase representation for each foci (eg ROI).*

Part IV: Outlook of the study

Despite a deep molecular knowledge regarding Notch signalling pathways and its roles in synchronization in PSM tissue level, little is known about the real rules that governing the coupling between embryonic oscillators. Exclusive molecular approach fails to explain fully the functioning of our biological system and depict its complexity. Therefore, my doctoral research includes theoretical approach to abstract the system taking advantage of the mathematical formalisms. This allows us to make predictions and challenge them in order to validate, test or falsity current model presented in the field of segmentation clock. To this end, I collaborated closely with Gregor Mönke, a theoretical physicist to complement the experimental approach and overcome its limitations.

The key milestones of this research topic are represented in the timeline below. The story starts with the basic observations made in Huygens's room and is prolongating

till today in Aulehla lab. This thesis focuses on intercellular coupling mediated by Notch signalling pathways. However, Notch signalling are not the only clock present in PSM tissue. Indeed, Wnt signalling activity also oscillate. Recent studies showed that Notch and Wnt signalling are coupled at both cellular and tissue level (Lauschke et al., 2013; Sonnen et al., 2018). On one hand, cells are coupled with each other, and on the other hand, Notch and Wnt signalling pathways are coupled inside of cells. It would be interesting in the near future to broaden the coupling phenomenon and reconcile the intercellular and intracellular coupling.

$$\dot{\theta}_i = \omega_i + \left(\sum_{j=1}^{N} X(\theta_j)\right) Z(\theta_i), \qquad i = 1, \ldots, N,$$

Pulse Coupling Models

Winfree et al., 1967 pioneering theoretical approaches to explain collective synchronization. He has introduced pulse coupling models and its equations.

$$\dot{\theta}_i = \omega_i + \sum_{j=1}^{N} \Gamma_{ij}(\theta_j - \theta_i), \quad i = 1, \ldots, N.$$

Phase Difference Coupling Models

Kuramoto simplified Winfree's work. Interaction between oscillations are then captured by phase coupling function (Kuramoto 1984). In K-model, the phase difference is the main feature that drives synchronization continuously and mutually between oscillators.

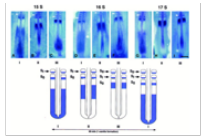

Segmentation Clock

Palmeirim et al., 1997 provides the first experimental evidence of the genetic clock. It has been found in chicken embryos, c-hairy1 (basic helix-loop-helix transcription factor that is a member of the Notch signalling pathways

$$\dot{\varphi}_j(t) = \omega_j + \nu[\varphi_{j+1}(t) - \varphi_j(t)] + \frac{\varepsilon}{2a^2} \sum_{k=j+p\pm1} \sin[\varphi_k(t-\tau) - \varphi_j(t)].$$

K-model Applied in Segmentation Clock

To explain synchronization in PSM cells, main studies in our field used the phase difference coupling framework (Kuramoto model) (Morelli et al., 2009; Murray et al., 2013; Okubo et al., 2012; Shimojo et al., 2016).

1665 — **1967** — **1976** — **1984** — **1985** — **1997** — **2000-2012** — **2009-2016** — **2019**

Sympathy of two clocks

Christian Huygens observed that two clocks placed next to each other can swing in sync. He was the first one who described the sympathy between two clocks. Sympathy is the ancient terminology for "coupling".

Clock & Wavefront model

Cooke and Zeeman (1976) proposed a theoretical model to to explain how the number of repeated somites is controlled during animal morphogenesis

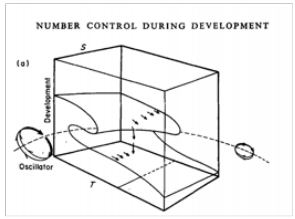

Notch Signalling Discovered

Wharton et al., 1985 presented the primary structure of Notch. For the first time, it has been speculated that Notch in involved in cell–cell interaction mechanism.

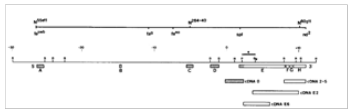

Notch & Synchronization in PSM

From numerous perturbations studies (Delaune et al., 2012; Horikawa et al., 2006; Jiang et al., 2000; Lewis, 2003; Riedel-Kruse et al., 2007), it is well known that the Notch signalling pathway is involved in synchronizing PSM oscillations on the tissue level

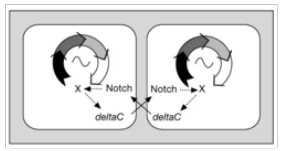

Falsification of K-model

This thesis presents several experimental evidences that don't match with theoretical predictions made in Kuramoto Model but rather with Pulse coupling model. Future research aims providing an experimental validation of the pulse coupling mechanism.

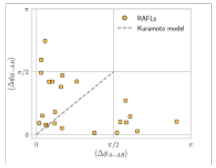

Chapter V: Material and methods

1. Mouse lines

The LuVeLu transgenic and R26-H2Bm Cherry LuVelu mouse reporter lines are previously described (Aulehla et al., 2008). Axin2stop GSAGS Achilles mouse reporter line developed in Aulehla lab (data not published).

2. Ex vivo culture and randomization/Self organization assays

a. Medium preparation and reagents

Working with mouse embryos requires two different media: one used for dissection and one is used for culture. Reagents and their concentration used for respective media are presented below:

	Dissection Medium	Culture Medium
DMEM/F12 without Glucose, Pyruvate, Phenol red	50mL	10mL
Penicillin/Streptomycin		10%
Bovine Serum Albumin (BSA)	1%	1%
Glucose	2mM	2mM
Glutamine	2mM	2mM
HEPES	10mM	

b. In vivo tail explant culture

E10.5 embryos of LuVeLu het x CD1 crosses were dissected in embryo culture medium (DMEM-F12 [Cell Culture Technologies] with 1% BSA, 2mM glucose and 2mM glutamine) with 10mM HEPES (pH7, Gibco). Embryonic tails including the PSM and three somites were isolated and cultured in 300µl embryo culture medium without HEPES in 4-well chamber slides (Lab-Tek, 155583). Culture conditions were 37°C, 5% CO2 60% O2.

c. Ex vivo cell culture assay for mesodermal patterning

4-well chamber slides were coated with fibronectin (50µg/ml [Sigma. F1141] in 100mM NaCl) for 2h at room temperature or overnight at 4°C. Subsequently, the wells were desiccated for 5 minutes and washed with embryo culture medium (DMEM-F12 [Cell Culture Technologies] with 1% BSA, 2mM glucose and 2mM glutamine) for at least 10 minutes.

Tailbud mesoderm was isolated by cutting the embryonic tail transversely behind the neuropore. Isolated tailbuds were placed with this transverse cut facing down into

fibronectin-coated dishes and cultured in 270µl embryo culture medium. Culture conditions were 37°C, 5% CO_2 and ambient or 60% O_2 as indicated.

d. Randomization assays by reaggregation

This assay is described in (Tsiairis and Aulehla, 2016). For randomization assays, entire PSM were isolated and pooled in groups of six. Pooled PSM were gently pipetted to achieve mechanical dissociation of cells. The cells were then filtered through a 10 mm filter (ParTec). To obtain randomized PSM cell populations, dissociated cells were centrifuged at 400 rcf for 4 min, and hereby, a cell pellet was formed. Subsequently, this cell pellet was cut into four to five smaller pieces that were plated on fibronectin-coated slides (50ug/mL in PBS) containing culture medium. They were cultured up to 24 hr at 37C and 5% CO2.

3. Randomization Assay for Low input (RAFL)

A. Randomization of one single mouse PSM or Tailbud

To realise RAFL, Ibidi microwell Fultrac plate is coated with fibronectin (50ug/mL in PBS) for at least 2 hours in the cold room. Then, single PSM was isolated and cut at different regions according to the purpose of the study: only tailbud, half posterior PSM or anterior PSM. After the cut, PSM tissue was collected inside of the microwell insert in 1.75uL of volume. Then, PSM tissue was gently pipetted to achieve mechanical dissociation of cells inside microwell inserts. Suspended cells of 1.75uL were then filtered through a 40mm filter (ParTec) and plated on the fibronectin-coated microwell. After seeding, cells were centrifuged quickly at 400 rcf for 30secondes to spin them down. Finally, randomized PSM cells were cultured in the culture medium for 15hours at 37C and 5% CO2.

B. Testing experimentally Phase synchronization “AB experiment”

To test theoretical prediction regarding phase synchronization, we performed multiple classic “AB experiments”. To do so, we used two different mouse embryos at 10.5 development. One LuVelu embryo is carrying H2mCherry Marker (population A) and the second embryo is only positive for LuVelu (population B). We firstly dissociated PSM

tailbud A in 1.8uL of dissection medium and secondly, we dissociated the PSM tailbud B. The cell dissociation is made mechanically using a 2.5 pipetman. Dissociated cells A and B have been filtered through a 40mm filter (ParTec) as well. Then, we took 0.7uL from each population to get the mixed population AB. Finally, A, B and mix AB cells are quickly centrifuged for 30 seconds at 400rcf. Samples are finally filled with culture medium and imaged overnight.

4. Quantitative real-time imaging

a. Confocal imaging

Imaging was performed on an LSM780 laser-scanning microscope (Zeiss). mVenus was excited using a 514nm and mCherry at 561nm. An Argon laser (Lasos LGK 7812 ML5) was used for excitation of both fluorophores. The following settings were used for all confocal imaging experiments: 20x Plan-Apochromat objective (NA 0.8); Z-stack with 4 planes with a spacing of 3µm; 4x line averaging; 5 minutes temporal resolution, 512x512.

b. Two photons imaging

Tail imaging was obtained with Two-photon imaging. Imaging was performed on an LSM780 laser-scanning microscope (Zeiss). A Ti: Sapphire laser (Chameleon-Ultra, Coherent) was used for sample excitation at a wavelength of 960nm. All samples were imaged through a 20x Plan-Apochromat objective (NA 0.8) using the following settings: Z-stack with 6- planes with a spacing of 6µm; resolution; 4x line averaging; 5 minutes temporal resolution.

5. Data analysis

a. Wavelet analysis in time

To quantify oscillations, regions of interest (ROIs) were defined region (ePSM) within the samples and the signal was processed using Fiji software (Schindelin et al., 2012). The extracted phase of the oscillations was used to calculate the instantaneous period and amplitude of the signal. Phase extraction and period of the signals were performed with "Wavelet analysis script" in with Python. This script was written and developed by Dr Gregor Mönke (Manuscript in preparation). Signal analysis toolkit can be found here: https://git.embl.de/moenke/TFApy

b. Visualizing oscillations

To visualize oscillations, period, phase and wavelet power on tissue imaging (RAFL, tail explants), wavelet analysis was applied on the imaging via Galaxy (EMBL) (method not published).

6. Cell counting via FACS

For cell counting according to the fluorescence intensity, the dissociated cells were sorted using a MoFlo Legacy High-Speed cell sorter (Beckman Coulter Inc.) equipped with a 100um nozzle. BD FACS Flow sheath (Becton Dickinson GmbH), filtered in-line thought a PALL Fluorodyine II filter 0.2uM (Pall GmbH), was used a sheath in the acquisition of the samples. Acquisition was triggered on FSC using a 512/15 bandpass (BP) filter and the same filter was used for SSC measurements. Venus fluorescence intensity was measured after filtering through a 545/35nm bandpass filter, while a second detector measured cellular autofluorescence through a 630/40nm BP filter. Data was acquired using MoFlo Summit software (Beckman Coulter), while post-acquisition analysis was done with FlowJo9.2 software (Tree Star, Inc). The sorting was completed within 30 min and the sorted cells were processed as previously described to form aggregates.

7. Mosaic cell labelling and single-cell oscillations

A. Sample preparation

To perform this experiment, we used R26-H2Bm Cherry-LuVelu mouse reporter lines as previously described (Aulehla et al., 2008). To perform mosaic cell labelling, we dissociated one single PSM tissue positive for LuVelu marker and mixed with 1/3 of another PSM tailbud containing a nuclear marker: H2BmCherry in addition to LuVelu reporter. In fine, we obtained reaggregated of LuVelu PSM cells with less per cent of cells which is tagged in red.

B. imaging settings for cell tracking

Imaging was performed on an LSM780 laser-scanning microscope (Zeiss). mVenus was excited using a 514nm and mCherry at 561nm. An Argon laser (Lasos LGK 7812 ML5) was used for excitation of both fluorophores. The following settings were used for all confocal imaging experiments: 20x Plan-Apochromat objective (NA 0.8); Z-stack with 8 planes with a spacing of 3µm; 4x line averaging; 5 minutes temporal resolution, 1024x1024.

C. Data analysis

Cell Segmentation, tracking and single-cell oscillations has been performed with Ilastik (Sommer et al., 2011) on H2BmCherry channel. To validate the quality and visualized the tracked cells we used FIJI plugin MaMut (Wolff et al., 2018). Single-cell oscillations from LuVelu channel has been extracted using a homemade FIJI plugin.

Reagent or Resource	Source	Identifier
Chemicals, Peptides, and Recombinant Proteins		
DMEM/F12 without Glucose, Pyruvate, Phenol Red	Cell Culture Technologies	N/A
Penicillin/Streptomycin	Thermo Fisher Scientific	Cat# 15140122
Fibronectin	Sigma-Aldrich	Cat#F1141
DAPT	Sigma-Aldrich	Cat#D5942
B-catenin protein	BD Transduction Laboratories	Cat#610153
D-(+) Glucose Solution	Sigma	G8769-100ML
BSA	Equitech-Bio, Inc.	Cat#BAC62
L-Glutamine Solution	Sigma	G7513-100ML
HEPES Buffer Solution	Gibco	15630-106
Experimental Models : Organisms/strains		
Mouse: LuVeLu:CD1-Tg(Lfng-YFP/PEST)OP	Aulehla et al., 2008	
Mouse: Axin2: Axi,2 stop GSAGS Achilles	Not published	Aulehla Lab
Software and Algorithms		
Fiji	Schindelin et al., 2012	https://fiji.sc/
MaMut plugin (Fiji)	Wolff et al., 2018	https://imagej.net/MaMuT
Python/Spyder Anaconda		https://www.spyder-ide.org/
Ilastik	Sommer et al., 2011	https://www.ilastik.org/index.html
Wavelet Analysis	Monke et al., in preparation	
Other		
LSM 780 laser-scanning microscope (Objective Plan-Apochromat 20x/0.8)	Zeiss	N/A
MZ16F stereo microscope with DFC420C digital camera	Leica	N/A
micro-Insert 4 Well FulTrac in µ-Dish 35 mm, high	Ibidi	Cat#80486

Appendix - Supplementary data

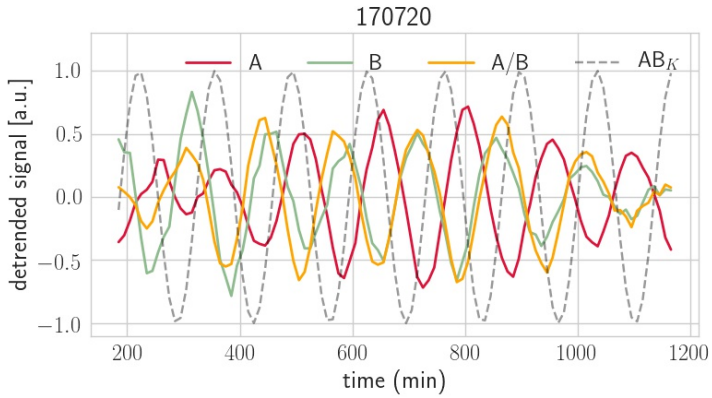

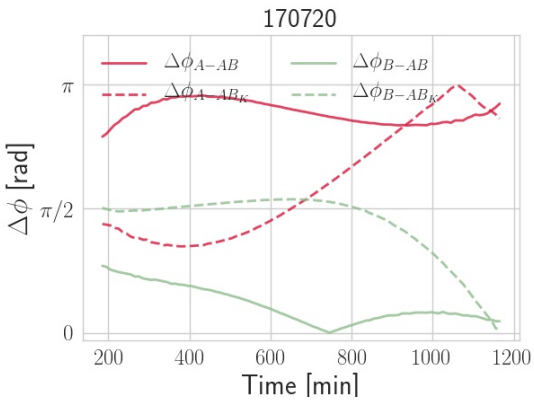

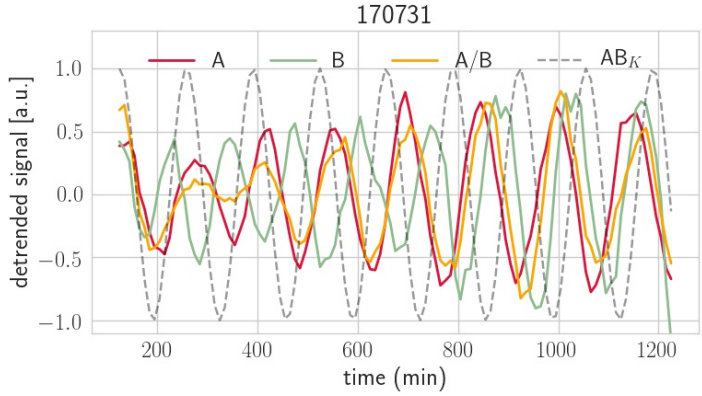

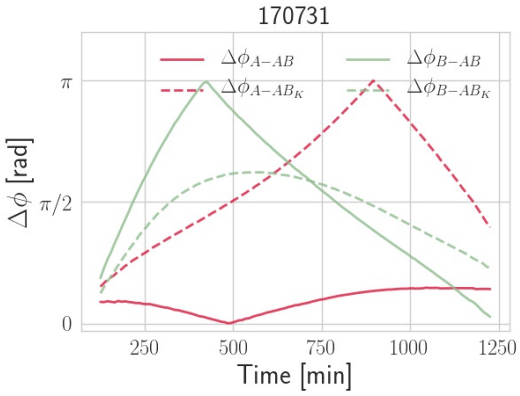

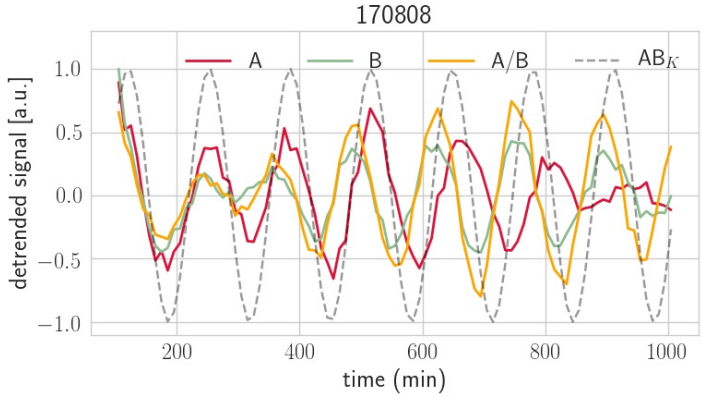

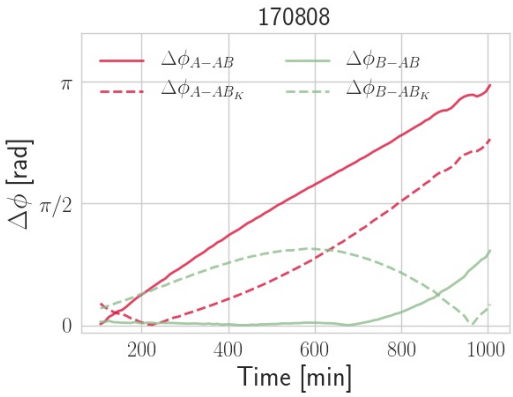

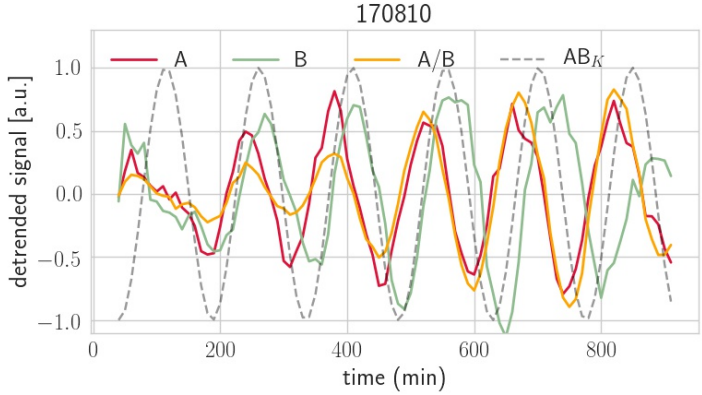

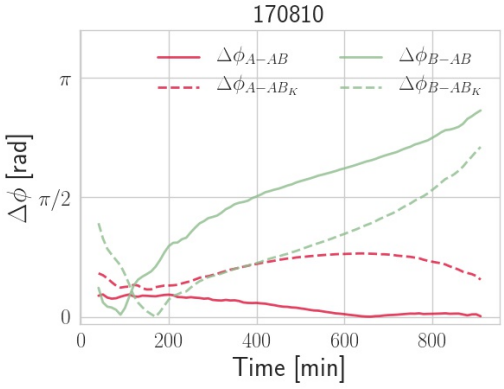

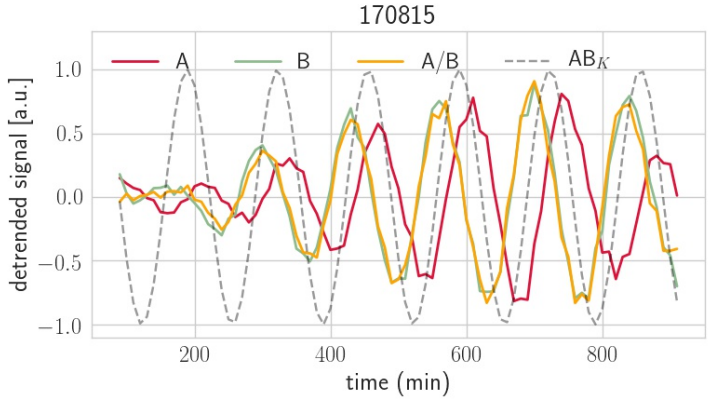
170815
A
B
A/B
AB_K
detrended signal [a.u.]
time (min)

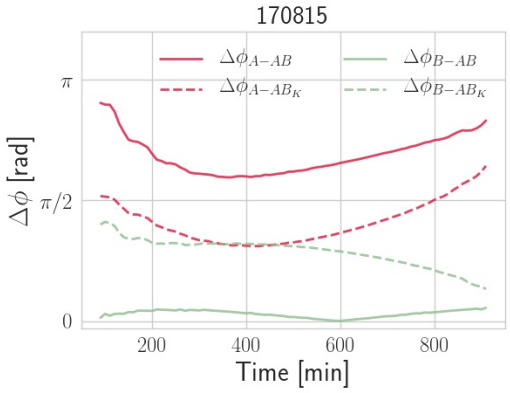
170815
$\Delta\phi_{A-AB}$
$\Delta\phi_{A-AB_K}$
$\Delta\phi_{B-AB}$
$\Delta\phi_{B-AB_K}$
$\Delta\phi$ [rad]
Time [min]

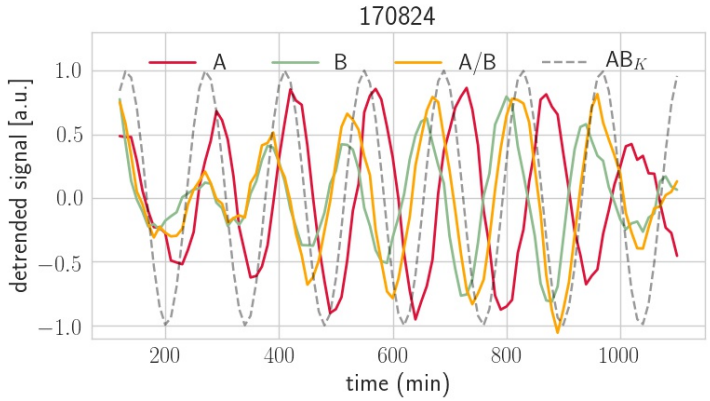
170824
A
B
A/B
AB_K
detrended signal [a.u.]
time (min)

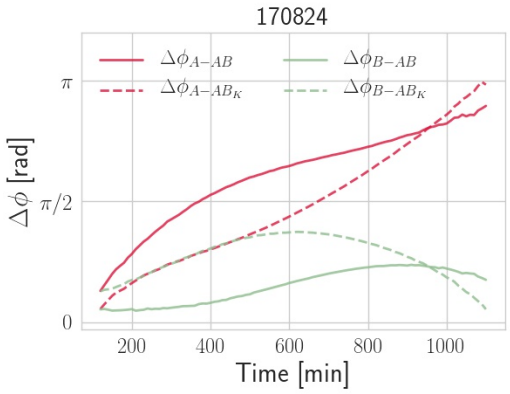
170824
$\Delta\phi_{A-AB}$
$\Delta\phi_{A-AB_K}$
$\Delta\phi_{B-AB}$
$\Delta\phi_{B-AB_K}$
$\Delta\phi$ [rad]
Time [min]

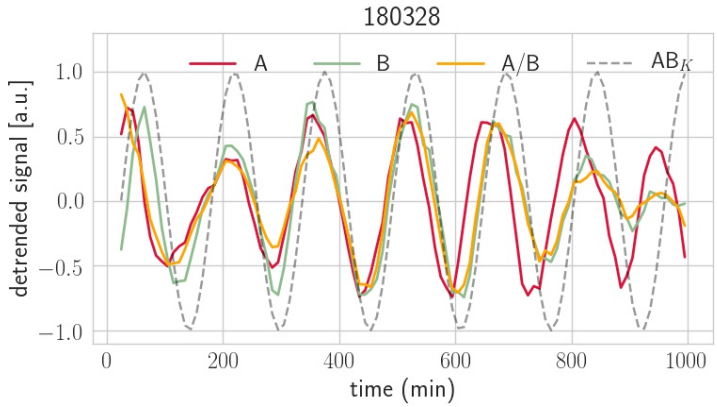
180328
A
B
A/B
AB_K
detrended signal [a.u.]
time (min)

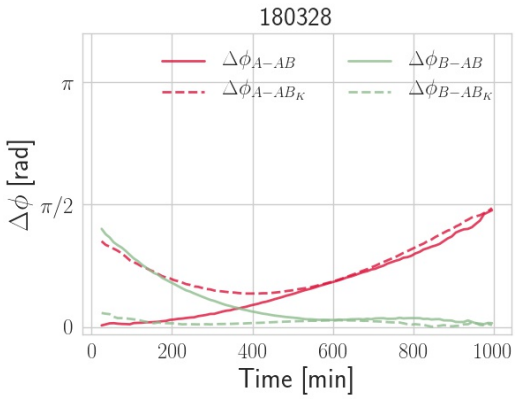
180328
$\Delta\phi_{A-AB}$
$\Delta\phi_{A-AB_K}$
$\Delta\phi_{B-AB}$
$\Delta\phi_{B-AB_K}$
$\Delta\phi$ [rad]
Time [min]

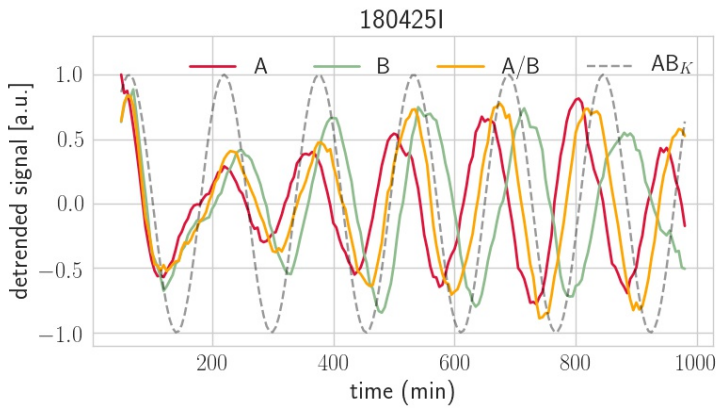
180425I
A
B
A/B
AB_K
detrended signal [a.u.]
time (min)

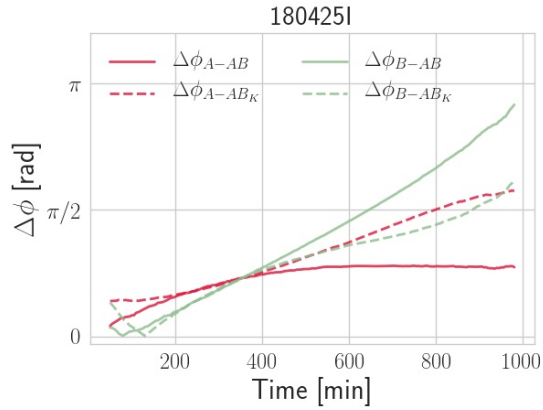
180425I
$\Delta\phi_{A-AB}$
$\Delta\phi_{A-AB_K}$
$\Delta\phi_{B-AB}$
$\Delta\phi_{B-AB_K}$
$\Delta\phi$ [rad]
Time [min]

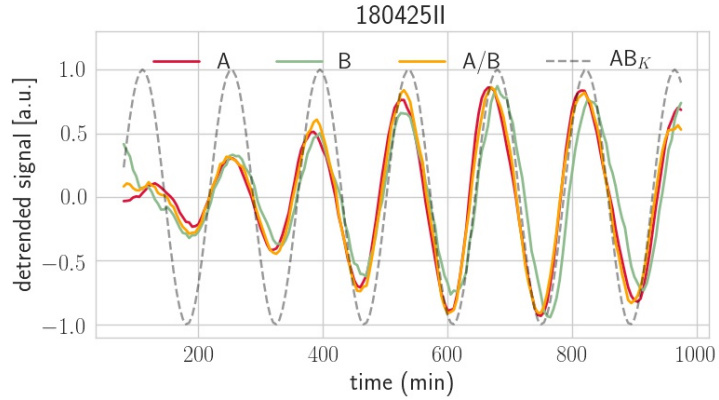
180425II
A
B
A/B
AB$_K$
detrended signal [a.u.]
time (min)

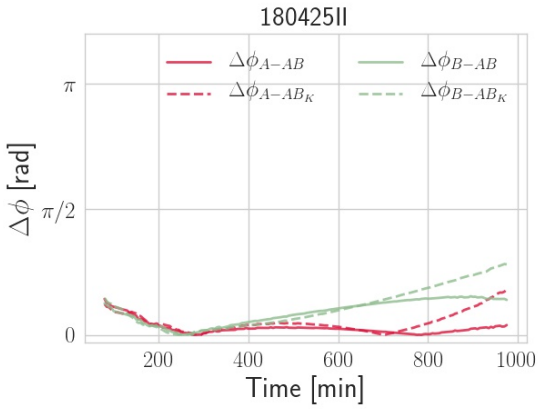
180425II
$\Delta\phi_{A-AB}$
$\Delta\phi_{A-AB_K}$
$\Delta\phi_{B-AB}$
$\Delta\phi_{B-AB_K}$
$\Delta\phi$ [rad]
Time [min]

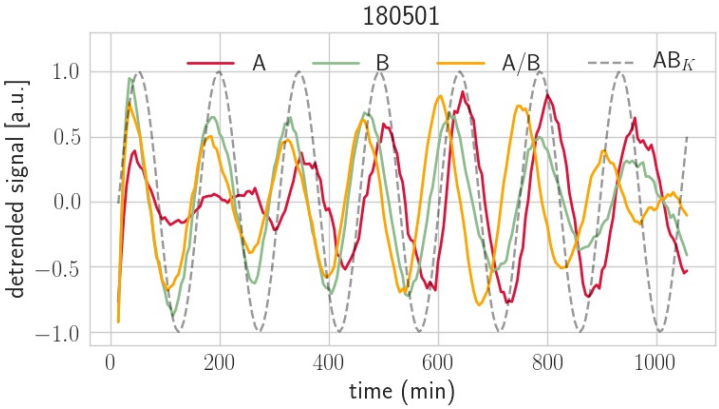
180501
A
B
A/B
AB$_K$
detrended signal [a.u.]
time (min)

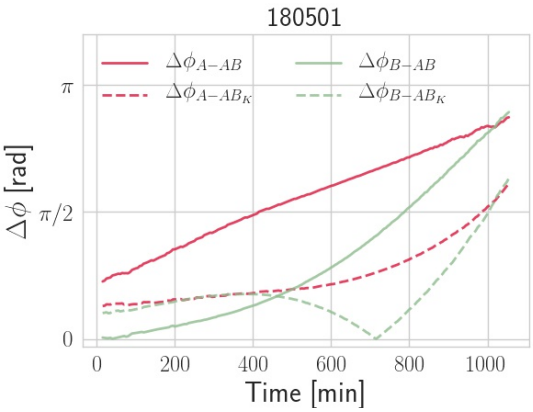
180501
$\Delta\phi_{A-AB}$
$\Delta\phi_{A-AB_K}$
$\Delta\phi_{B-AB}$
$\Delta\phi_{B-AB_K}$
$\Delta\phi$ [rad]
Time [min]

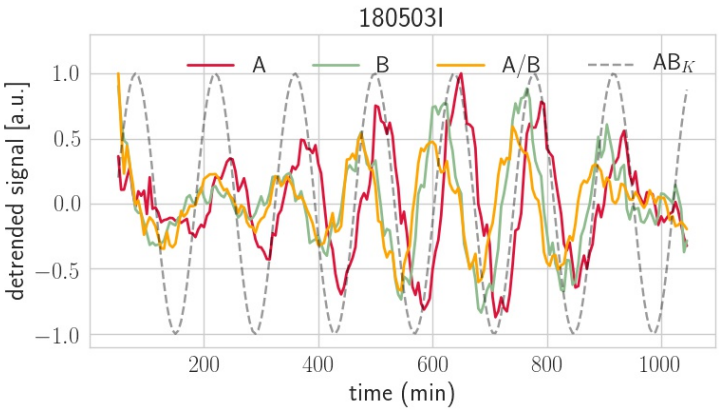
180503I
A
B
A/B
AB$_K$
detrended signal [a.u.]
time (min)

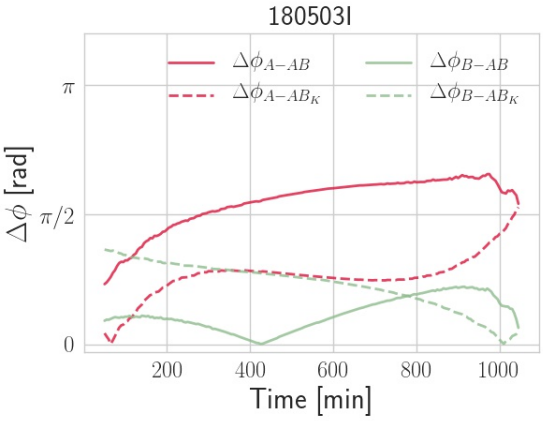
180503I
$\Delta\phi_{A-AB}$
$\Delta\phi_{A-AB_K}$
$\Delta\phi_{B-AB}$
$\Delta\phi_{B-AB_K}$
$\Delta\phi$ [rad]
Time [min]

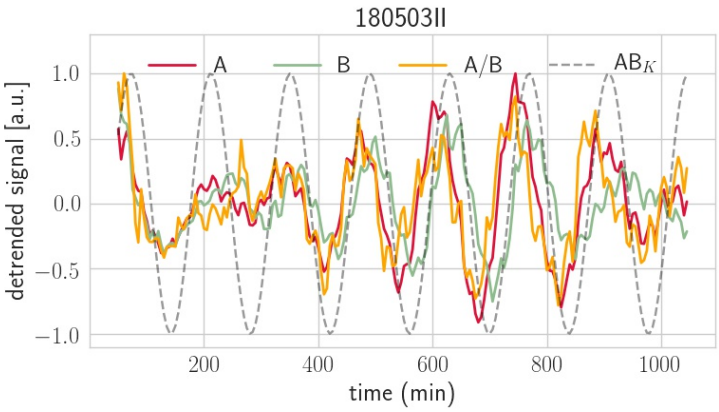
180503II
A
B
A/B
AB$_K$
detrended signal [a.u.]
time (min)

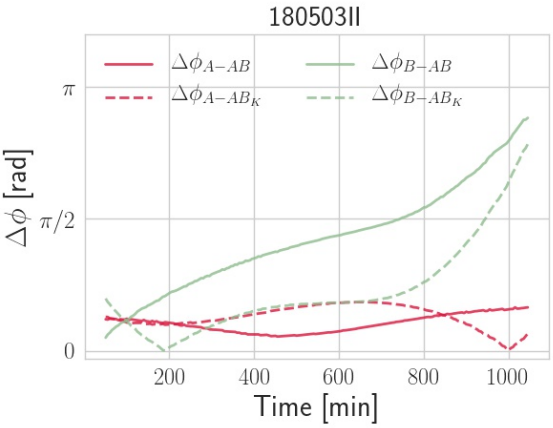
180503II
$\Delta\phi_{A-AB}$
$\Delta\phi_{A-AB_K}$
$\Delta\phi_{B-AB}$
$\Delta\phi_{B-AB_K}$
$\Delta\phi$ [rad]
Time [min]

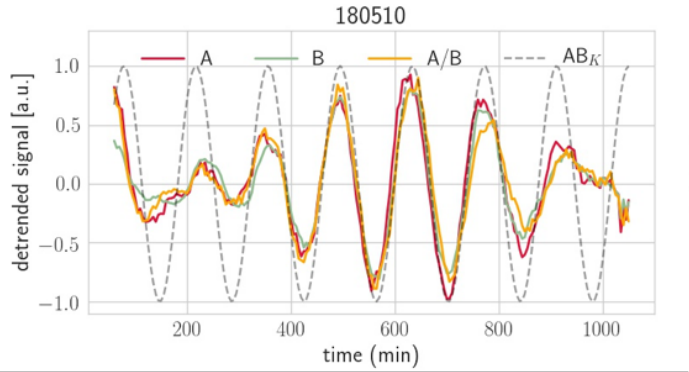
180510
A
B
A/B
AB$_K$
detrended signal [a.u.]
time (min)

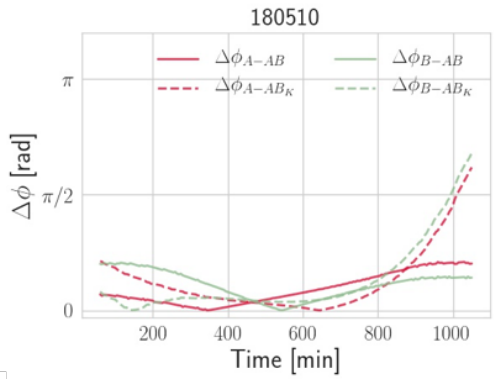
180510
$\Delta\phi_{A-AB}$
$\Delta\phi_{B-AB}$
$\Delta\phi_{A-AB_K}$
$\Delta\phi_{B-AB_K}$
$\Delta\phi$ [rad]
Time [min]

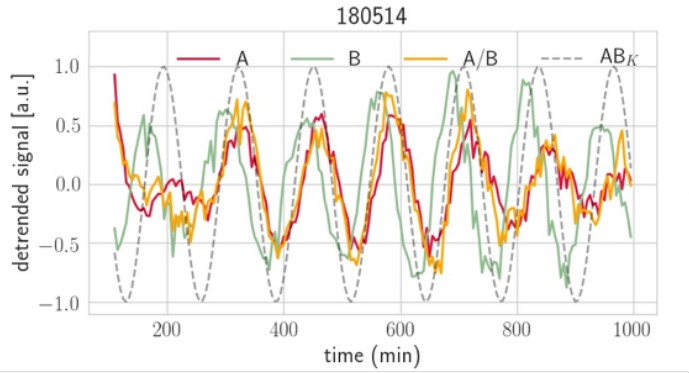
180514
A
B
A/B
AB$_K$
detrended signal [a.u.]
time (min)

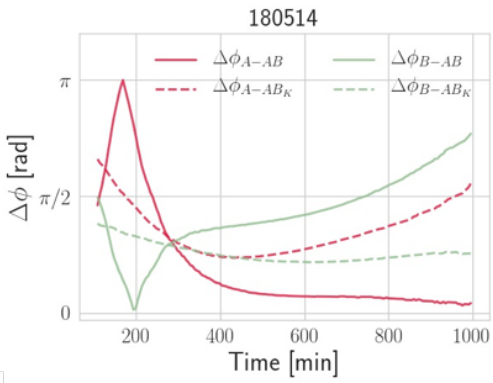
180514
$\Delta\phi_{A-AB}$
$\Delta\phi_{B-AB}$
$\Delta\phi_{A-AB_K}$
$\Delta\phi_{B-AB_K}$
$\Delta\phi$ [rad]
Time [min]

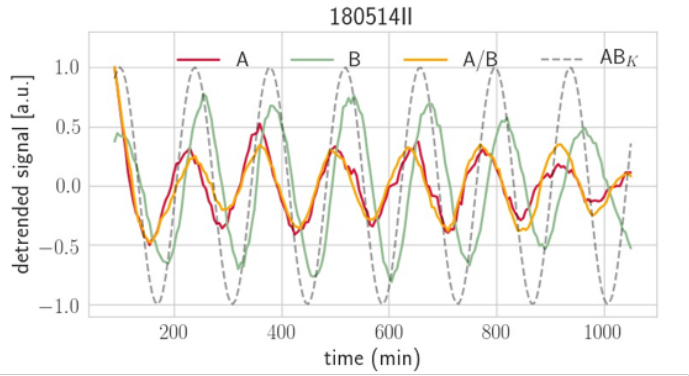
180514II
A
B
A/B
AB$_K$
detrended signal [a.u.]
time (min)

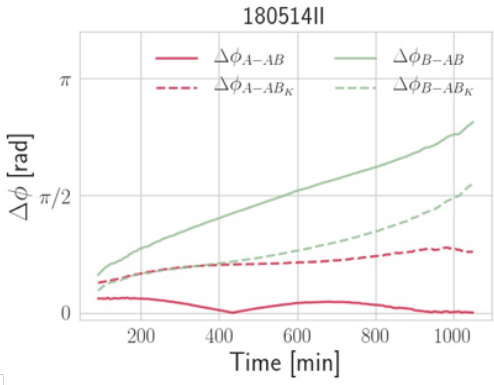
180514II
$\Delta\phi_{A-AB}$
$\Delta\phi_{B-AB}$
$\Delta\phi_{A-AB_K}$
$\Delta\phi_{B-AB_K}$
$\Delta\phi$ [rad]
Time [min]

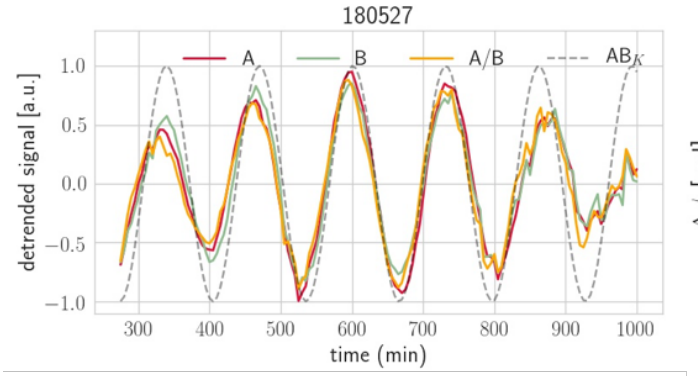
180527
A
B
A/B
AB$_K$
detrended signal [a.u.]
time (min)

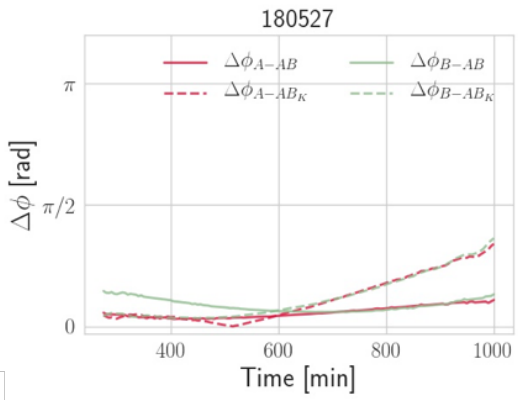
180527
$\Delta\phi_{A-AB}$
$\Delta\phi_{B-AB}$
$\Delta\phi_{A-AB_K}$
$\Delta\phi_{B-AB_K}$
$\Delta\phi$ [rad]
Time [min]

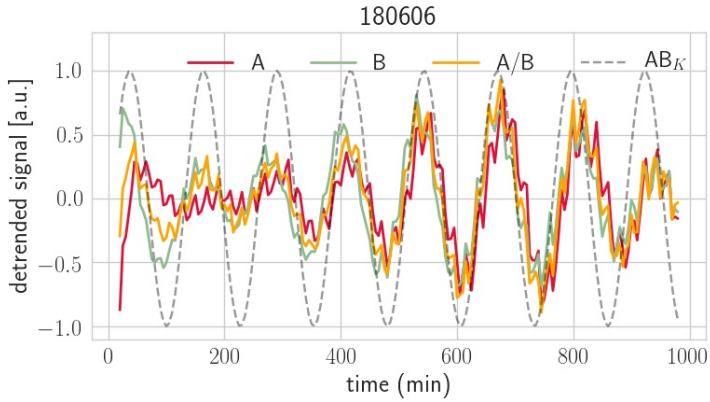
180606
A
B
A/B
AB_K
detrended signal [a.u.]
time (min)

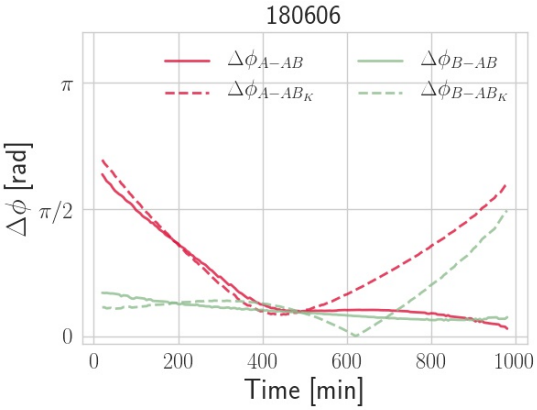
180606
$\Delta\phi_{A-AB}$
$\Delta\phi_{B-AB}$
$\Delta\phi_{A-AB_K}$
$\Delta\phi_{B-AB_K}$
$\Delta\phi$ [rad]
Time [min]

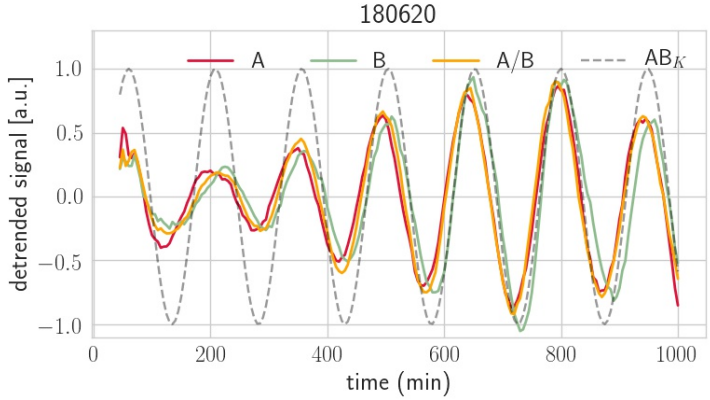
180620
A
B
A/B
AB_K
detrended signal [a.u.]
time (min)

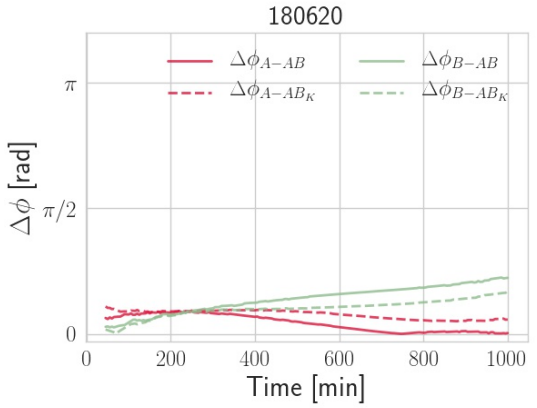
180620
$\Delta\phi_{A-AB}$
$\Delta\phi_{B-AB}$
$\Delta\phi_{A-AB_K}$
$\Delta\phi_{B-AB_K}$
$\Delta\phi$ [rad]
Time [min]

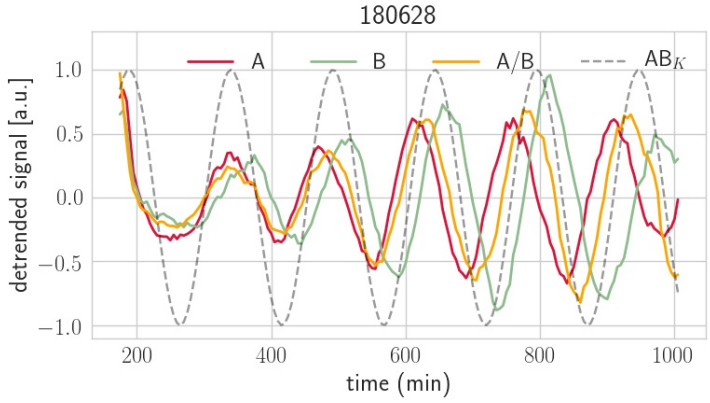
180628
A
B
A/B
AB_K
detrended signal [a.u.]
time (min)

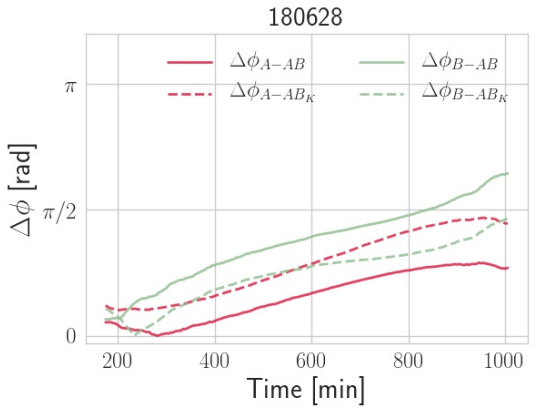
180628
$\Delta\phi_{A-AB}$
$\Delta\phi_{B-AB}$
$\Delta\phi_{A-AB_K}$
$\Delta\phi_{B-AB_K}$
$\Delta\phi$ [rad]
Time [min]

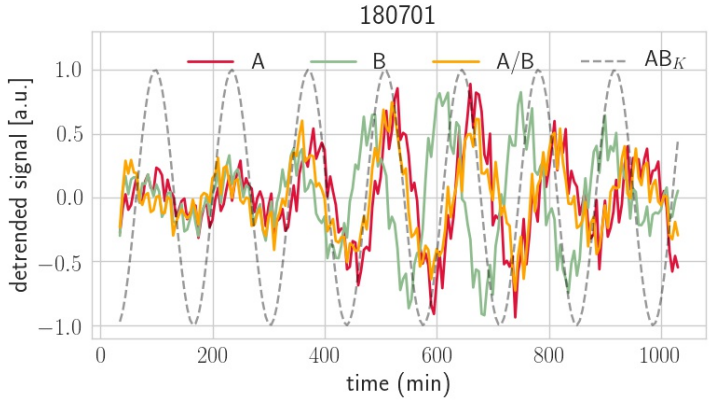
180701
A
B
A/B
AB_K
detrended signal [a.u.]
time (min)

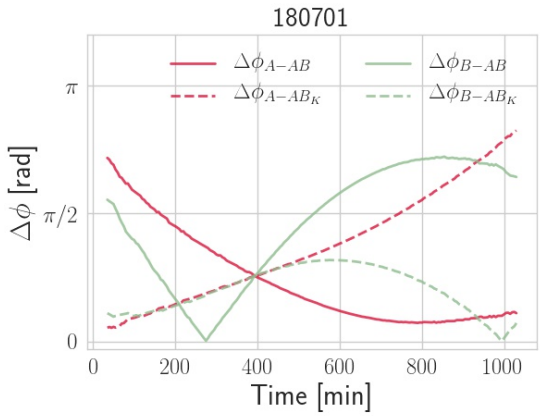
180701
$\Delta\phi_{A-AB}$
$\Delta\phi_{B-AB}$
$\Delta\phi_{A-AB_K}$
$\Delta\phi_{B-AB_K}$
$\Delta\phi$ [rad]
Time [min]

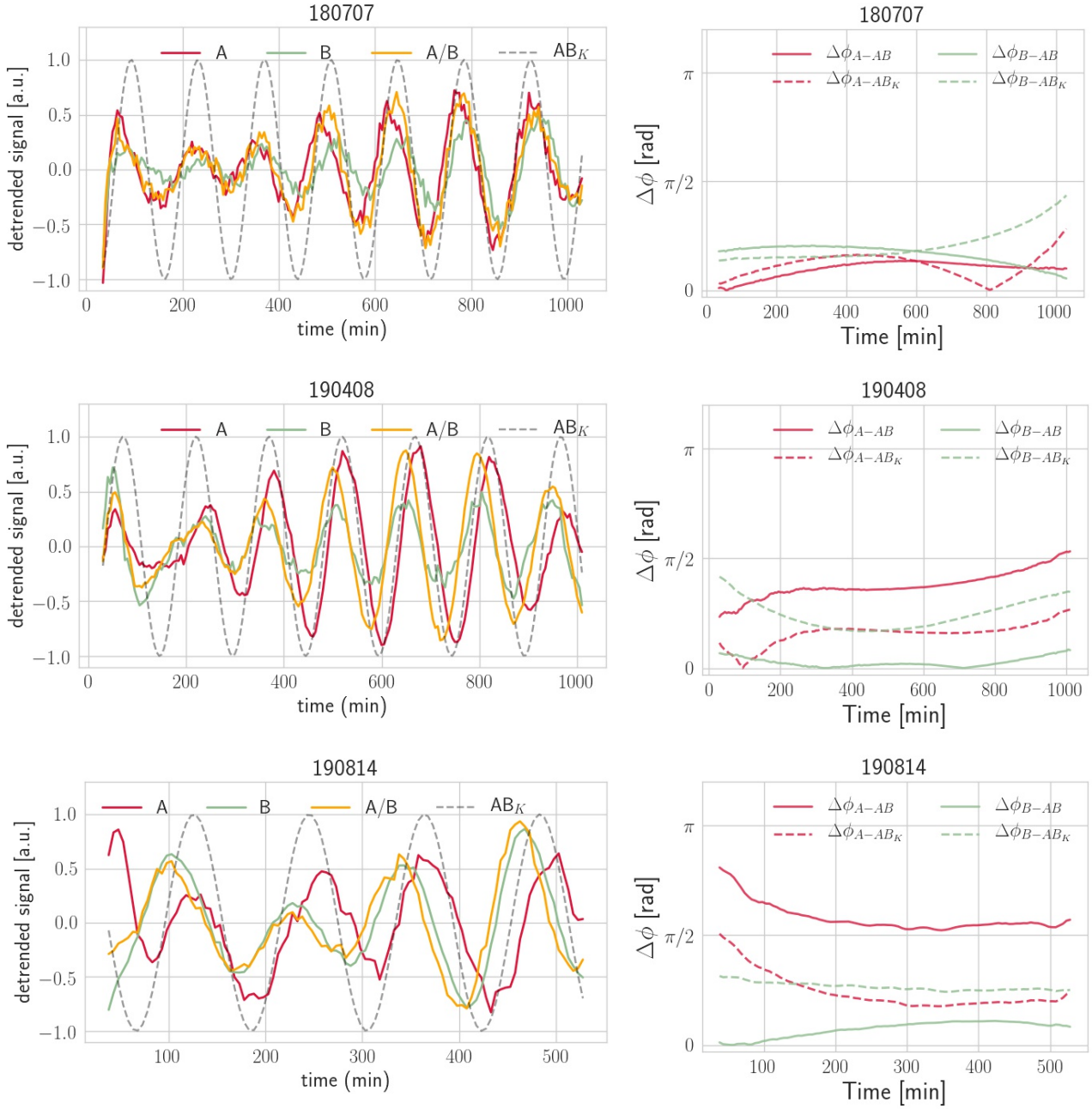

Supplementary data: For all the following figures: (Left panel): detrended signals for LuVelu intensity for each population A, B and AB. Dash line is the theoretical phase averaging according to Kuramoto model. (Right panel): Quantification of phase differences between each population. Dash lines are theoretical phase differences between each population in Kuramoto model.

References

Aulehla, A., Herrmann, B.G., 2004. Segmentation in vertebrates: clock and gradient finally joined. Genes Dev. 18, 2060–2067. https://doi.org/10.1101/gad.1217404

Aulehla, A., Pourquie, O., 2010. Signaling Gradients during Paraxial Mesoderm Development. Cold Spring Harb. Perspect. Biol. 2, a000869–a000869. https://doi.org/10.1101/cshperspect.a000869

Aulehla, A., Wehrle, C., Brand-Saberi, B., Kemler, R., Gossler, A., Kanzler, B., Herrmann, B.G., 2003. Wnt3a Plays a Major Role in the Segmentation Clock Controlling Somitogenesis. Dev. Cell 4, 395–406. https://doi.org/10.1016/S1534-5807(03)00055-8

Aulehla, A., Wiegraebe, W., Baubet, V., Wahl, M.B., Deng, C., Taketo, M., Lewandoski, M., Pourquié, O., 2008. A β-catenin gradient links the clock and wavefront systems in mouse embryo segmentation. Nat. Cell Biol. 10, 186–193. https://doi.org/10.1038/ncb1679

Baker, R.E., Schnell, S., Maini, P.K., 2006. A clock and wavefront mechanism for somite formation. Dev. Biol. 293, 116–126. https://doi.org/10.1016/j.ydbio.2006.01.018

Bettenhausen, B., Hrabě de Angelis, M., Simon, D., Guénet, J.L., Gossler, A., 1995. Transient and restricted expression during mouse embryogenesis of Dll1, a murine gene closely related to Drosophila Delta. Dev. Camb. Engl. 121, 2407–2418.

Bone, R.A., Bailey, C.S.L., Wiedermann, G., Ferjentsik, Z., Appleton, P.L., Murray, P.J., Maroto, M., Dale, J.K., 2014. Spatiotemporal oscillations of Notch1, Dll1 and NICD are coordinated across the mouse PSM. Dev. Camb. Engl. 141, 4806–4816. https://doi.org/10.1242/dev.115535

Bray, S., Bernard, F., 2010. Chapter Eight - Notch Targets and Their Regulation, in: Kopan, R. (Ed.), Current Topics in Developmental Biology, Notch Signaling. Academic Press, pp. 253–275. https://doi.org/10.1016/S0070-2153(10)92008-5

Brou, C., Logeat, F., Gupta, N., Bessia, C., LeBail, O., Doedens, J.R., Cumano, A., Roux, P., Black, R.A., Israël, A., 2000. A novel proteolytic cleavage involved in Notch signaling: the role of the disintegrin-metalloprotease TACE. Mol. Cell 5, 207–216.

BUCK, J., BUCK, E., n.d. Biology of Synchronous Flashing of Fireflies [WWW Document]. Nature. https://doi.org/10.1038/211562a0

Cabrera, C.V., 1990. Lateral inhibition and cell fate during neurogenesis in Drosophila: the interactions between scute, Notch and Delta. Dev. Camb. Engl. 110, 733–742.

Camazine, S., Franks, N.R., Sneyd, J., Bonabeau, E., Deneubourg, J.-L., Theraula, G., 2001. Self-Organization in Biological Systems. Princeton University Press, Princeton, NJ, USA.

Chal, J., Oginuma, M., Al Tanoury, Z., Gobert, B., Sumara, O., Hick, A., Bousson, F., Zidouni, Y., Mursch, C., Moncuquet, P., Tassy, O., Vincent, S., Miyanari, A., Bera, A., Garnier, J.-M., Guevara, G., Hestin, M., Kennedy, L., Hayashi, S., Drayton, B., Cherrier, T., Gayraud-Morel, B., Gussoni, E., Relaix, F., Tajbakhsh, S., Pourquié, O., 2015. Differentiation of pluripotent stem cells to muscle fiber to model Duchenne muscular dystrophy. Nat. Biotechnol. 33, 962–969. https://doi.org/10.1038/nbt.3297

Conlon, R.A., Reaume, A.G., Rossant, J., 1995. Notch1 is required for the coordinate segmentation of somites. Dev. Camb. Engl. 121, 1533–1545.

Cooke, J., Zeeman, E.C., 1976. A clock and wavefront model for control of the number of repeated structures during animal morphogenesis. J. Theor. Biol. 58, 455–476.
Dale, J.K., Malapert, P., Chal, J., Vilhais-Neto, G., Maroto, M., Johnson, T., Jayasinghe, S., Trainor, P., Herrmann, B., Pourquié, O., 2006. Oscillations of the Snail Genes in the Presomitic Mesoderm Coordinate Segmental Patterning and Morphogenesis in Vertebrate Somitogenesis. Dev. Cell 10, 355–366. https://doi.org/10.1016/j.devcel.2006.02.011
Dale, J.K., Maroto, M., Dequeant, M.-L., Malapert, P., McGrew, M., Pourquie, O., 2003. Periodic Notch inhibition by Lunatic Fringe underlies the chick segmentation clock. Nature 421, 275–278. https://doi.org/10.1038/nature01244
De, J.F.C., Bray, S., 1997. Feed-back mechanisms affecting Notch activation at the dorsoventral boundary in the Drosophila wing. Development 124, 3241–3251.
Delaune, E.A., François, P., Shih, N.P., Amacher, S.L., 2012. Single-Cell-Resolution Imaging of the Impact of Notch Signaling and Mitosis on Segmentation Clock Dynamics. Dev. Cell 23, 995–1005. https://doi.org/10.1016/j.devcel.2012.09.009
Dequeant, M.-L., Glynn, E., Gaudenz, K., Wahl, M., Chen, J., Mushegian, A., Pourquie, O., 2006. A Complex Oscillating Network of Signaling Genes Underlies the Mouse Segmentation Clock. Science 314, 1595–1598. https://doi.org/10.1126/science.1133141
Diaz-Cuadros, M., Wagner, D.E., Budjan, C., Hubaud, A., Touboul, J., Michaut, A., Tanoury, Z.A., Yoshioka-Kobayashi, K., Niino, Y., Kageyama, R., Miyawaki, A., Pourquié, O., 2018. In vitro characterization of the human segmentation clock. bioRxiv 461822. https://doi.org/10.1101/461822
Diez del Corral, R., Olivera-Martinez, I., Goriely, A., Gale, E., Maden, M., Storey, K., 2003. Opposing FGF and retinoid pathways control ventral neural pattern, neuronal differentiation, and segmentation during body axis extension. Neuron 40, 65–79.
Dubrulle, J., McGrew, M.J., Pourquié, O., 2001. FGF signaling controls somite boundary position and regulates segmentation clock control of spatiotemporal Hox gene activation. Cell 106, 219–232. https://doi.org/10.1016/s0092-8674(01)00437-8
Dubrulle, J., Pourquié, O., 2004. fgf8 mRNA decay establishes a gradient that couples axial elongation to patterning in the vertebrate embryo. Nature 427, 419–422. https://doi.org/10.1038/nature02216
Ermentrout, G.B., 1985. Synchronization in a pool of mutually coupled oscillators with random frequencies. J. Math. Biol. 22, 1–9. https://doi.org/10.1007/BF00276542
Evrard, Y.A., Lun, Y., Aulehla, A., Gan, L., Johnson, R.L., 1998. lunatic fringe is an essential mediator of somite segmentation and patterning. Nature 394, 377–381. https://doi.org/10.1038/28632
Fehon, R.G., Johansen, K., Rebay, I., Artavanis-Tsakonas, S., 1991. Complex cellular and subcellular regulation of notch expression during embryonic and imaginal development of Drosophila: implications for notch function. J. Cell Biol. 113, 657–669. https://doi.org/10.1083/jcb.113.3.657
Giudicelli, F., Özbudak, E.M., Wright, G.J., Lewis, J., 2007. Setting the Tempo in Development: An Investigation of the Zebrafish Somite Clock Mechanism. PLOS Biol. 5, e150. https://doi.org/10.1371/journal.pbio.0050150
Goel, P., Ermentrout, B., 2002. Synchrony, stability, and firing patterns in pulse-coupled oscillators. Phys. Nonlinear Phenom. 163, 191–216. https://doi.org/10.1016/S0167-2789(01)00374-8

Goldbeter, A., Pourquié, O., 2008. Modeling the segmentation clock as a network of coupled oscillations in the Notch, Wnt and FGF signaling pathways. J. Theor. Biol. 252, 574–585. https://doi.org/10.1016/j.jtbi.2008.01.006
Gomez, C., Ozbudak, E.M., Wunderlich, J., Baumann, D., Lewis, J., Pourquié, O., 2008. Control of segment number in vertebrate embryos. Nature 454, 335–339. https://doi.org/10.1038/nature07020
Gray, R.A., Chattipakorn, N., 2005. Termination of spiral waves during cardiac fibrillation via shock-induced phase resetting. Proc. Natl. Acad. Sci. 102, 4672–4677. https://doi.org/10.1073/pnas.0407860102
Guruharsha, K.G., Kankel, M.W., Artavanis-Tsakonas, S., 2012. The Notch signalling system: recent insights into the complexity of a conserved pathway. Nat. Rev. Genet. 13, 654–666. https://doi.org/10.1038/nrg3272
Harada, N., Tamai, Y., Ishikawa, T., Sauer, B., Takaku, K., Oshima, M., Taketo, M.M., 1999. Intestinal polyposis in mice with a dominant stable mutation of the beta-catenin gene. EMBO J. 18, 5931–5942. https://doi.org/10.1093/emboj/18.21.5931
Henry, C.A., Urban, M.K., Dill, K.K., Merlie, J.P., Page, M.F., Kimmel, C.B., Amacher, S.L., 2002. Two linked hairy/Enhancer of split-related zebrafish genes, her1 and her7, function together to refine alternating somite boundaries. Dev. Camb. Engl. 129, 3693–3704.
Holley, S.A., Jülich, D., Rauch, G.-J., Geisler, R., Nüsslein-Volhard, C., 2002. her1 and the notch pathway function within the oscillator mechanism that regulates zebrafish somitogenesis. Dev. Camb. Engl. 129, 1175–1183.
Hori, K., Sen, A., Artavanis-Tsakonas, S., 2013. Notch signaling at a glance. J. Cell Sci. 126, 2135–2140. https://doi.org/10.1242/jcs.127308
Horikawa, K., Ishimatsu, K., Yoshimoto, E., Kondo, S., Takeda, H., 2006. Noise-resistant and synchronized oscillation of the segmentation clock. Nature 441, 719–723. https://doi.org/10.1038/nature04861
Jho, E., Zhang, T., Domon, C., Joo, C.-K., Freund, J.-N., Costantini, F., 2002. Wnt/β-Catenin/Tcf Signaling Induces the Transcription of Axin2, a Negative Regulator of the Signaling Pathway. Mol. Cell. Biol. 22, 1172–1183. https://doi.org/10.1128/MCB.22.4.1172-1183.2002
Jiang, Y.J., Aerne, B.L., Smithers, L., Haddon, C., Ish-Horowicz, D., Lewis, J., 2000. Notch signalling and the synchronization of the somite segmentation clock. Nature 408, 475–479. https://doi.org/10.1038/35044091
Kopan, R., Ilagan, M.X.G., 2009. The canonical Notch signaling pathway: unfolding the activation mechanism. Cell 137, 216–233. https://doi.org/10.1016/j.cell.2009.03.045
Kuramoto, Y., 1984. Chemical Oscillations, Waves, and Turbulence. Springer, Berlin, Heidelberg usw.
Kusumi, K., May, C.M., Eckalbar, W.L., 2013. A large-scale view of the evolution of amniote development: insights from somitogenesis in reptiles. Curr. Opin. Genet. Dev., Developmental mechanisms, patterning and evolution 23, 491–497. https://doi.org/10.1016/j.gde.2013.02.011
Lauschke, V.M., Tsiairis, C.D., François, P., Aulehla, A., 2013. Scaling of embryonic patterning based on phase-gradient encoding. Nature 493, 101–105. https://doi.org/10.1038/nature11804
Lewis, J., 2003. Autoinhibition with transcriptional delay: a simple mechanism for the zebrafish somitogenesis oscillator. Curr. Biol. CB 13, 1398–1408.

Liao, B.-K., Oates, A.C., 2017. Delta-Notch signalling in segmentation. Arthropod Struct. Dev. 46, 429–447. https://doi.org/10.1016/j.asd.2016.11.007
Lustig, B., Jerchow, B., Sachs, M., Weiler, S., Pietsch, T., Karsten, U., Wetering, M. van de, Clevers, H., Schlag, P.M., Birchmeier, W., Behrens, J., 2002. Negative Feedback Loop of Wnt Signaling through Upregulation of Conductin/Axin2 in Colorectal and Liver Tumors. Mol. Cell. Biol. 22, 1184–1193. https://doi.org/10.1128/MCB.22.4.1184-1193.2002
Masamizu, Y., Ohtsuka, T., Takashima, Y., Nagahara, H., Takenaka, Y., Yoshikawa, K., Okamura, H., Kageyama, R., 2006. Real-time imaging of the somite segmentation clock: revelation of unstable oscillators in the individual presomitic mesoderm cells. Proc. Natl. Acad. Sci. U. S. A. 103, 1313–1318. https://doi.org/10.1073/pnas.0508658103
Micchelli, C.A., Rulifson, E.J., Blair, S.S., 1997. The function and regulation of cut expression on the wing margin of Drosophila: Notch, Wingless and a dominant negative role for Delta and Serrate. Dev. Camb. Engl. 124, 1485–1495.
Mirollo, R.E., Strogatz, S.H., 1990. Synchronization of Pulse-Coupled Biological Oscillators. SIAM J. Appl. Math. 50, 1645–1662.
Morelli, L.G., Ares, S., Herrgen, L., Schröter, C., Jülicher, F., Oates, A.C., 2009. Delayed coupling theory of vertebrate segmentation. HFSP J. 3, 55–66. https://doi.org/10.2976/1.3027088
Moreno, T.A., Kintner, C., 2004. Regulation of segmental patterning by retinoic acid signaling during Xenopus somitogenesis. Dev. Cell 6, 205–218.
Murray, P.J., Maini, P.K., Baker, R.E., 2013. Modelling Delta-Notch perturbations during zebrafish somitogenesis. Dev. Biol. 373, 407–421. https://doi.org/10.1016/j.ydbio.2012.10.014
Niwa, Y., Masamizu, Y., Liu, T., Nakayama, R., Deng, C.-X., Kageyama, R., 2007. The Initiation and Propagation of Hes7 Oscillation Are Cooperatively Regulated by Fgf and Notch Signaling in the Somite Segmentation Clock. Dev. Cell 13, 298–304. https://doi.org/10.1016/j.devcel.2007.07.013
O'Keeffe, K.P., Krapivsky, P.L., Strogatz, S.H., 2015. Synchronization as Aggregation: Cluster Kinetics of Pulse-Coupled Oscillators. Phys. Rev. Lett. 115, 064101. https://doi.org/10.1103/PhysRevLett.115.064101
Okubo, Y., Sugawara, T., Abe-Koduka, N., Kanno, J., Kimura, A., Saga, Y., 2012. Lfng regulates the synchronized oscillation of the mouse segmentation clock via *trans*-repression of Notch signalling. Nat. Commun. 3, 1141. https://doi.org/10.1038/ncomms2133
Palmeirim, I., Henrique, D., Ish-Horowicz, D., Pourquié, O., 1997. Avian hairy gene expression identifies a molecular clock linked to vertebrate segmentation and somitogenesis. Cell 91, 639–648.
Peña Ramirez, J., Olvera, L.A., Nijmeijer, H., Alvarez, J., 2016. The sympathy of two pendulum clocks: beyond Huygens' observations. Sci. Rep. 6, 23580. https://doi.org/10.1038/srep23580
Penton, A.L., Leonard, L.D., Spinner, N.B., 2012. Notch signaling in human development and disease. Semin. Cell Dev. Biol. 23, 450–457. https://doi.org/10.1016/j.semcdb.2012.01.010
Pikovsky, A., Rosenblum, M., Kurths, J., n.d. Synchronization: A universal concept in nonlinear sciences 433.
Potts, W.K., 1984. The chorus-line hypothesis of manoeuvre coordination in avian flocks. Nature 309, 344. https://doi.org/10.1038/309344a0

Pourquié, O., 2007. Building the spine: the vertebrate segmentation clock. Cold Spring Harb. Symp. Quant. Biol. 72, 445–449. https://doi.org/10.1101/sqb.2007.72.016
Riedel-Kruse, I.H., Müller, C., Oates, A.C., 2007. Synchrony dynamics during initiation, failure, and rescue of the segmentation clock. Science 317, 1911–1915. https://doi.org/10.1126/science.1142538
Sawada, A., Shinya, M., Jiang, Y.J., Kawakami, A., Kuroiwa, A., Takeda, H., 2001. Fgf/MAPK signalling is a crucial positional cue in somite boundary formation. Dev. Camb. Engl. 128, 4873–4880.
Schindelin, J., Arganda-Carreras, I., Frise, E., Kaynig, V., Longair, M., Pietzsch, T., Preibisch, S., Rueden, C., Saalfeld, S., Schmid, B., Tinevez, J.-Y., White, D.J., Hartenstein, V., Eliceiri, K., Tomancak, P., Cardona, A., 2012. Fiji: an open-source platform for biological-image analysis. Nat. Methods 9, 676–682. https://doi.org/10.1038/nmeth.2019
Serth, K., Schuster-Gossler, K., Cordes, R., Gossler, A., 2003. Transcriptional oscillation of Lunatic fringe is essential for somitogenesis. Genes Dev. 17, 912–925. https://doi.org/10.1101/gad.250603
Shaya, O., Binshtok, U., Hersch, M., Rivkin, D., Weinreb, S., Amir-Zilberstein, L., Khamaisi, B., Oppenheim, O., Desai, R.A., Goodyear, R.J., Richardson, G.P., Chen, C.S., Sprinzak, D., 2017. Cell-Cell Contact Area Affects Notch Signaling and Notch-Dependent Patterning. Dev. Cell 40, 505-511.e6. https://doi.org/10.1016/j.devcel.2017.02.009
Shimojo, H., Isomura, A., Ohtsuka, T., Kori, H., Miyachi, H., Kageyama, R., 2016. Oscillatory control of Delta-like1 in cell interactions regulates dynamic gene expression and tissue morphogenesis. Genes Dev. 30, 102–116. https://doi.org/10.1101/gad.270785.115
Sommer, C., Straehle, C., Köthe, U., Hamprecht, F.A., 2011. Ilastik: Interactive learning and segmentation toolkit, in: 2011 IEEE International Symposium on Biomedical Imaging: From Nano to Macro. Presented at the 2011 IEEE International Symposium on Biomedical Imaging: From Nano to Macro, pp. 230–233. https://doi.org/10.1109/ISBI.2011.5872394
Sonnen, K.F., Lauschke, V.M., Uraji, J., Falk, H.J., Petersen, Y., Funk, M.C., Beaupeux, M., François, P., Merten, C.A., Aulehla, A., 2018. Modulation of Phase Shift between Wnt and Notch Signaling Oscillations Controls Mesoderm Segmentation. Cell 172, 1079-1090.e12. https://doi.org/10.1016/j.cell.2018.01.026
Sprinzak, D., Lakhanpal, A., LeBon, L., Garcia-Ojalvo, J., Elowitz, M.B., 2011. Mutual Inactivation of Notch Receptors and Ligands Facilitates Developmental Patterning. PLOS Comput. Biol. 7, e1002069. https://doi.org/10.1371/journal.pcbi.1002069
Sprinzak, D., Lakhanpal, A., LeBon, L., Santat, L.A., Fontes, M.E., Anderson, G.A., Garcia-Ojalvo, J., Elowitz, M.B., 2010. Cis Interactions between Notch and Delta Generate Mutually Exclusive Signaling States. Nature 465, 86–90. https://doi.org/10.1038/nature08959
Strogatz, S., 2003. Sync: How Order Emerges from Chaos in the Universe, Nature, and Daily Life. Hachette Books.
Strogatz, S.H., Abrams, D.M., McRobie, A., Eckhardt, B., Ott, E., 2005. Crowd synchrony on the Millennium Bridge. Nature 438, 43. https://doi.org/10.1038/438043a
Struhl, G., Greenwald, I., 1999. Presenilin is required for activity and nuclear access of Notch in Drosophila. Nature 398, 522–525. https://doi.org/10.1038/19091

Szymczak, A.L., Workman, C.J., Wang, Y., Vignali, K.M., Dilioglou, S., Vanin, E.F., Vignali, D.A.A., 2004. Correction of multi-gene deficiency in vivo using a single "self-cleaving" 2A peptide–based retroviral vector. Nat. Biotechnol. 22, 589. https://doi.org/10.1038/nbt957

Tam, P.P., Tan, S.S., 1992. The somitogenetic potential of cells in the primitive streak and the tail bud of the organogenesis-stage mouse embryo. Dev. Camb. Engl. 115, 703–715.

Tsiairis, C.D., Aulehla, A., 2016. Self-Organization of Embryonic Genetic Oscillators into Spatiotemporal Wave Patterns. Cell 164, 656–667. https://doi.org/10.1016/j.cell.2016.01.028

Vermot, J., Pourquié, O., 2005. Retinoic acid coordinates somitogenesis and left-right patterning in vertebrate embryos. Nature 435, 215–220. https://doi.org/10.1038/nature03488

Wahi, K., Bochter, M.S., Cole, S.E., 2016. The many roles of Notch signaling during vertebrate somitogenesis. Semin. Cell Dev. Biol., Bone development and disease 49, 68–75. https://doi.org/10.1016/j.semcdb.2014.11.010

Webb, A.B., Lengyel, I.M., Jörg, D.J., Valentin, G., Jülicher, F., Morelli, L.G., Oates, A.C., n.d. Persistence, period and precision of autonomous cellular oscillators from the zebrafish segmentation clock. eLife 5. https://doi.org/10.7554/eLife.08438

Willms Allan R., Kitanov Petko M., Langford William F., n.d. Huygens' clocks revisited. R. Soc. Open Sci. 4, 170777. https://doi.org/10.1098/rsos.170777

Winfree, A.T., 1967. Biological rhythms and the behavior of populations of coupled oscillators. J. Theor. Biol. 16, 15–42. https://doi.org/10.1016/0022-5193(67)90051-3

Wolff, C., Tinevez, J.-Y., Pietzsch, T., Stamataki, E., Harich, B., Guignard, L., Preibisch, S., Shorte, S., Keller, P.J., Tomancak, P., Pavlopoulos, A., 2018. Multi-view light-sheet imaging and tracking with the MaMuT software reveals the cell lineage of a direct developing arthropod limb. eLife 7, e34410. https://doi.org/10.7554/eLife.34410

Yang, Y., Wu, M., 2018. Rhythmicity and waves in the cortex of single cells. Philos. Trans. R. Soc. B Biol. Sci. 373. https://doi.org/10.1098/rstb.2017.0116

Zhang, N., Gridley, T., 1998. Defects in somite formation in lunatic fringe-deficient mice. Nature 394, 374–377. https://doi.org/10.1038/28625

Acknowledgements